Technical Report No. 20

HYDROLOGICAL DROUGHT CHARACTERISTICS OF THE NEDOŽERY SUB CATCHMENT, UPPER NITRA, SLOVAKIA, BASED ON HBV MODELING

Author names: Jacob Oosterwijk, Anne F. van Loon, Andrej Machlica, Oliver Horvát, Henny A.J. van Lanen & Miriam Fendeková

Date: December 2009

WATCH is an Integrated Project Funded by the European Commission under the Sixth Framework Programme, Global Change and Ecosystems Thematic Priority Area (contract number: 036946).
The WACH project started 01/02/2007 and will continue for 4 years.

Title:	Hydrological drought characteristics of the Nedožery sub catchment, Upper Nitra, Slovakia, based on HBV modelling
Authors:	Jacob Oosterwijk, Anne F. van Loon, Andrej Machlica, Oliver Horvát, Henny A.J. van Lanen & Miriam Fendeková
Organisations:	Wageningen University, Wageningen, the Netherlands Comenius University, Bratislava, Slovakia
Submission date:	December 2009
Function:	This report is an output from Work Block 4 Extremes: frequency, severity and scale, and will contribute to Task 4.1.1 Investigate processes controlling the propagation of drought, Task 4.1.2 Spatial and temporal scales and severity of droughts in 20th century, and Task 4.3.1 Frequency, severity and extent of droughts in 21st century.
Deliverable	The report contributes to WATCH deliverable D.4.1.4 Report on the increased understanding of the propagation of drought in different hydro-climatological regions, physical catchment structures and different scales.

Preface

This study is based on research done by Jacob Oosterwijk for his MSc thesis Hydrology and Quantitative Water Management (HWM-80436) at the Wageningen University, the Netherlands to obtain a MSc degree of Hydrology and Water Quality. He received input from his supervisors Anne F. van Loon, Andrej Machlica, Oliver Horvát, Henny A.J. van Lanen and Miriam Fendeková. In the context of his MSc research, the first author spent about one month at the Comenius University. This stay was partially supported by the EU-FP6 project WATCH (WATer and global Change). The authors visited the River Upper-Nitra Basin early 2009 to discuss preliminary outcome from the different hydrological models that are being developed and applied to study hydrological drought in the Upper-Nitra (WATCH test basin). The field trip and associated workshop were supported by the WATCH project. We thank Jan Seibert (University of Zurich, Switzerland) for providing HBV light, including the automatic calibration module.

Henny A.J. van Lanen, Wageningen, December 2009.

Contents

Summary

Drought reflects below average water availability. Drought typically is long-lasting and regionally extensive. In this study hydrological drought in the Nedožery sub catchment (Upper-Nitra catchment, Slovakia) is investigated using the hydrological model HBV. The hydrological regime of the catchment shows a clear pattern in which seasonal snow plays an important role. Based on climatic and catchment input data the conceptual, semi-distributed, rainfall-runoff model HBV simulates time series of actual evapotranspiration, soil moisture, groundwater and discharge for the period 1974-2006. Calibration on the Nash–Sutcliffe using the logarithm of discharge (to give more weight to low flows) resulted in an efficiency of 0.68. The use of groundwater observations in calibration did not improve simulation of low flows. Trend analysis on the input data showed downward trends in the observed discharge and upward trends in the observed precipitation and the annual number of snow days. The simulated discharge shows, similar to the observed precipitation (input data), but in contradiction with the observed discharge, upward trends. This results in an over- (1974-1990) and underestimation (1991-2006) of the observed discharge. Results were compared with results from the lumped, conceptual hydrological model BILAN and the distributed, physically-based hydrological model FRIER. Both models show the same over- and underestimation of discharge as HBV. Drought analysis is carried out using a monthly threshold of 80% smoothed by a moving average. Hydrological droughts (both winter and summer) in Nedožery develop due to above average temperatures combined with below average precipitation. In winter this leads to a below average snow cover (resulting in lower spring discharges) and the occurrence of above average evapotranspiration. In winter, hydrological drought can also be caused by below average temperature, because water is stored on the surface as snow for a longer period. Such a winter drought does not continue into summer, because it ends by above average snowmelt in spring. Droughts start in soil moisture and discharge (only a few days difference) followed by groundwater (after a week or more). Groundwater droughts are the most persistent droughts. Drought analysis using the output from the BILAN model gives a lower number of droughts which are longer as compared with HBV. Recession curves simulated with BILAN are long and response on precipitation events during the recession is almost invisible. FRIER output shows more, but shorter droughts which indicates FRIER reacts faster to precipitation than HBV and BILAN.

Keywords: HBV model, drought, drought propagation, threshold analysis, model comparison, trends, FRIER, BILAN

1. Introduction

A decrease in water availability can cause severe problems in sectors or places that depend on water. People use water for domestic purposes, agriculture and industry; and ecosystems are dependent on water availability. Both water quantity and quality play a role for people and ecosystems (UNDP, 2006; Kabat et al., 2002).

When a below average water availability persists and becomes regionally extensive it is called a drought. Drought can be characterized by a prolonged deviation from normal conditions of variables, such as precipitation, streamflow, groundwater and soil moisture (Tallaksen & Van Lanen, 2004b). Drought can be seen as a slow onset natural hazard, which is regionally persistent and produces a complex web of impacts (Demuth & Stahl, 2002; Wilhite et al., 2007). A lack of precipitation over a large area and for an extensive period of time (meteorological drought) has widespread impacts on different parts of the hydrological cycle (Tallaksen & Van Lanen, 2004b). Lack of precipitation can lead to soil water deficiency, which causes a soil moisture drought. An above average potential evapotranspiration can enhance the drought. If the drought period lasts long enough groundwater heads will fall because of a lack of groundwater recharge, and a groundwater drought will occur. Decreasing discharge leads to a streamflow drought. The order of occurrence of the different droughts depends on the characteristics of the catchment.

Drought in one or more parts of the hydrological cycle has an impact on society, economy and environment. The terms agricultural drought, socio-economic drought and ecological drought are used in the case that agriculture, society and economy, and ecosystems respectively, are affected by drought. The impacts of drought are dependent on its duration, severity, time of occurrence and spatial extent, which are the key aspects of drought characterization (Tallaksen & Van Lanen, 2004b). Impacts are an interplay between the natural event and the demand placed on water (vulnerability). Limited access to (clean) water caused by drought results in socio-economic and environmental problems (Wilhite et al., 2007; UNDP, 2006).

An important aspect not mentioned yet is climate change. Due to a likely warmer future climate changes in the hydrological cycle will occur. Reports from the Intergovernmental Panel on Climate Change (IPCC) give some closely linked trends which are likely to occur in a warmer future climate (Meehl et al., 2007; Kundzewicz et al., 2007; Bates et al., 2008): a concentration of precipitation into more intense events with longer periods of little precipitation in between; an increased evaporative demand; an increased risk of more intense, more frequent and longer-lasting heat waves; and an increased summer dryness and winter wetness in most parts of the northern middle and high latitudes. Frequency, severity and geographical location of droughts are likely to change due to climate change (Kabat et al., 2002). There is a general agreement among scientists that climate change will result in an intensification of the global hydrological cycle causing a higher occurrence of extremes (Hisdal et al., 2001).

Variability of river flows in time is high: almost everywhere on earth a strong seasonal variability in river regimes is visible (Kabat et al., 2002). The trends identified by IPCC will

have an impact on this seasonality. Higher peak flows and either lower flows during the low flow season or extended dry periods are expected. In regions where much precipitation in winter falls as snow earlier snowmelt leads to a shift in the timing of river flow. In regions with no snowfall the change in river flow is more dependent on change in precipitation than on change in temperature (Bates et al., 2008).

The occurring and predicted trends in the hydrological cycle, the complexity of the propagation of drought through the hydrological cycle and the impacts drought has on society, economy and environment show the importance of further research. Understanding and modeling of changes related to the hydrological cycle is needed at scales relevant to decision making (Bates et al., 2008). Focus needs to be on predictability of extremes and description of its characteristics (Kundewicz et al., 2007; Kabat et al., 2002).

The Integrated Project Water and Global Change (WATCH) is a project funded under the EU FP6 which has taken up the challenge of global change. WATCH "will bring together the hydrological, water resources and climate communities to analyze, quantify and predict the components of the current and future global water cycles and related water resources states; evaluate their uncertainties and clarify the overall vulnerability of global water resources related to the main societal and economic sectors" (eu-watch.org). The project is divided in seven interdependent work blocks. The fourth work block has as main objective "to advance our knowledge of the impact of global change on hydrological extremes, including spatial and temporal patterns of droughts and large-scale floods" (eu-watch.org: WorkBlock 4 - Extremes: Frequency, Severity and Scale).

Research objectives

This research investigates the characteristics of the Nedožery sub catchment of the Upper-Nitra catchment in Slovakia and its drought propagation, by developing the hydrological model HBV (Bergström and Forsman, 1973; Seibert, 2005) for that catchment. Observed and simulated time series of hydro meteorological variables are studied to characterize drought.

Main research question is:

What are, based on rainfall-runoff modeling with HBV, characteristics of hydrological drought in the Nedožery sub catchment of the Upper-Nitra catchment, Slovakia?

Sub questions needed to answer the main question are:

- How to model hydrological drought in the catchment using the semi-distributed conceptual rainfall-runoff model HBV?
- What are the characteristics of drought events in the catchment?
- What are differences between HBV results and results from other models for the same catchment?

These questions are answered using HBV modeling of soil moisture, groundwater and discharge of the Nedožery sub catchment of the Upper-Nitra catchment in Slovakia and analysis of observed and modeled time series of the catchment.

In the next chapter the catchment and available data will be described (Chapter 2). The methodology including the HBV model will be described in Chapter 3. Chapter 4 deals with the data quality including trends in the data. HBV results are discussed in Chapter 5, followed by Chapter 6 in which the drought analysis is described. Chapter 7 deals with the model comparison between HBV, BILAN and FRIER. The last chapters give conclusions, discussion points and recommendations for further research.

2. General description

2.1 The catchment

2.1.1 Location

The Nedožery sub catchment is part of the Upper Nitra catchment, which is located in the Prievidza district of Slovakia. Slovakia is located in Central Europe (Figure 2.1). The discharge gauging station for the Nedožery sub catchment is located at Nedožery-Brezany, which is the outlet of the catchment. The Nedožery catchment has an area of 181 km^2. Within the Nedožery catchment, several sub-catchments can be distinguished. Three of them are gauged, from west to east: Chvojnica, Tužina and Kľačno (Figure 2.4).

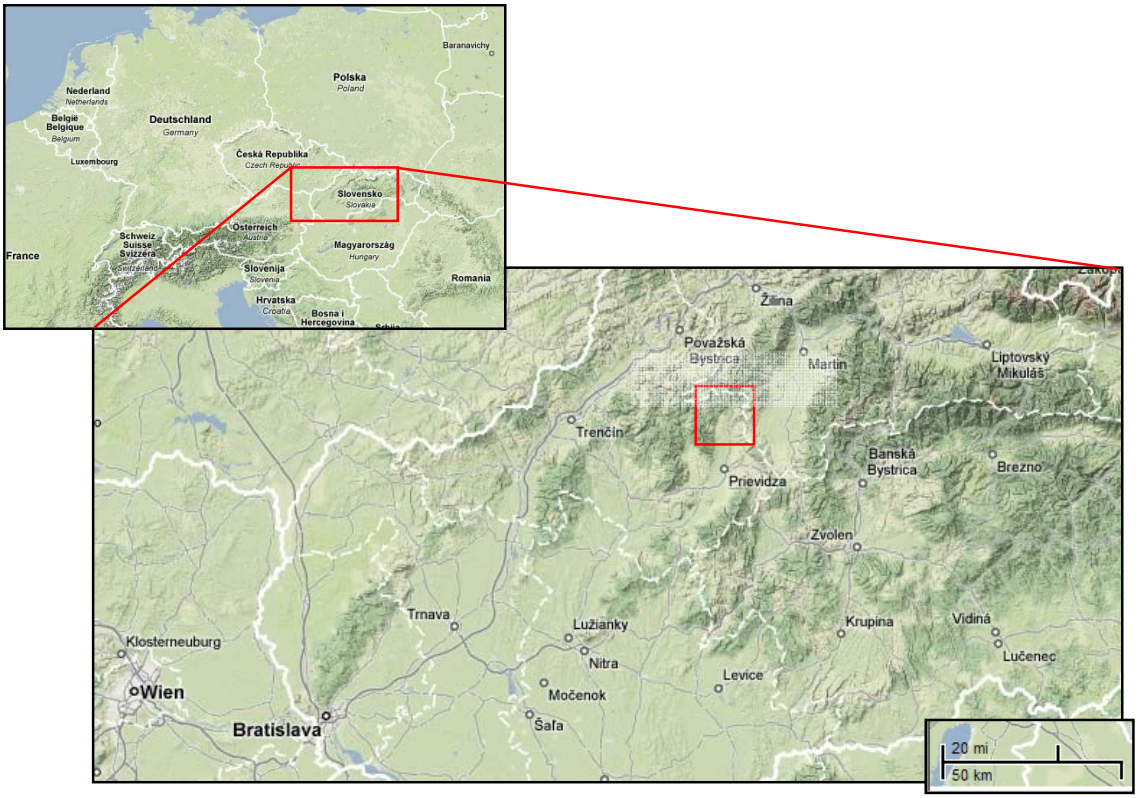

Figure 2.1 The location of the catchment (maps.google.com).

2.1.2 Climate

The upper Nitra region belongs to a moderately warm, humid climatic region, with a mean annual precipitation of 800-900 mm and a mean annual air temperature of 7-8 ^{o}C (based on observation period 1961-1999) (Machlica & Stojkovová, 2008).

The hydrological regime of the Nedožery catchment can be characterized as seasonal. There is a clear distinction between winter and summer periods. Maximum discharges occur in spring, minimum discharges occur in summer and autumn (Machlica & Stojkovová, 2008). The discharge of the three tributaries shows the same seasonal pattern as Nedožery (Figure

2.2). A detailed description of the hydrological regime in the Nedožery catchment, based on data and modeling, can be found in Section 5.

2.1.3 Altitude

The average altitude of the catchment is 573 m a.s.l., with the lowest point in the southern part of the catchment at 288 m a.s.l. (Nedožery-Brezany) and the highest point at 1172 m a.s.l. (Figure 2.4 a). The Nedožery catchment is an asymmetric valley, with the lowest parts in the east and most of the highest parts in the west.

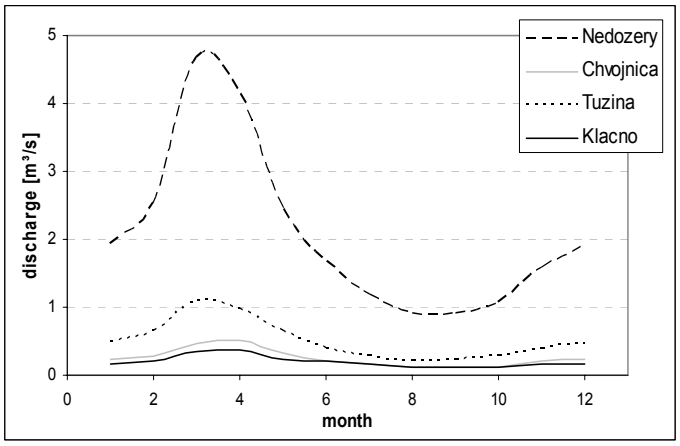

Figure 2.2 Mean monthly discharge in m^3/s for the different (sub)catchments (based on period 1973-2006).

2.1.4 Geo(hydro)logy

The largest part of the Nedožery catchment consists of Mesozoic rocks of the Inner Carpathians (IC). These rocks are located in the northern, eastern and western parts of the catchment, and form together more than 50% of the total area (Figure 2.4 b; Figure 2.3). The valley is a neogene tectonic basin filled with sediments (15% of the catchment). In the southwestern and southeastern part of the catchment magmatic rocks and rocks of the early Paleozoic – Proterozoic can be found, which cover together more than 30% of the total area.

The three tributaries (Section 2.1.1) are situated in different geological conditions. From west to east the contribution of Mesozoic rocks increases, while the amount of crystalline (magmatic) rocks decreases. This means that in general from west to east the contribution of groundwater increases and the influence of fast components decreases [1]. Downstream of the gauging stations the three tributaries unite and flow through the neogene tectonic basin.

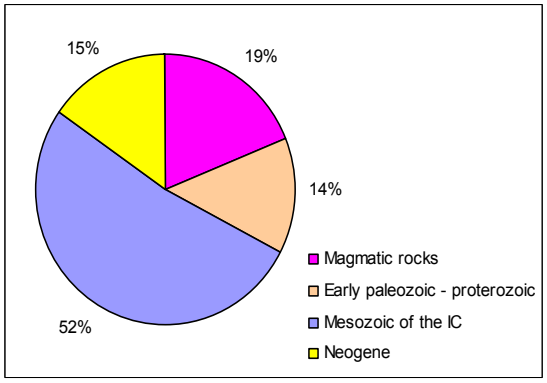

Figure 2.3 Geology in the Nedožery catchment.

[1] During a fieldtrip in the snowmelt period (31-03-2009), EC-measurements confirmed this hypothesis. A detailed description of the measurements (electro conductivity and temperature) in the three sub-catchments can be found in Annex 1.

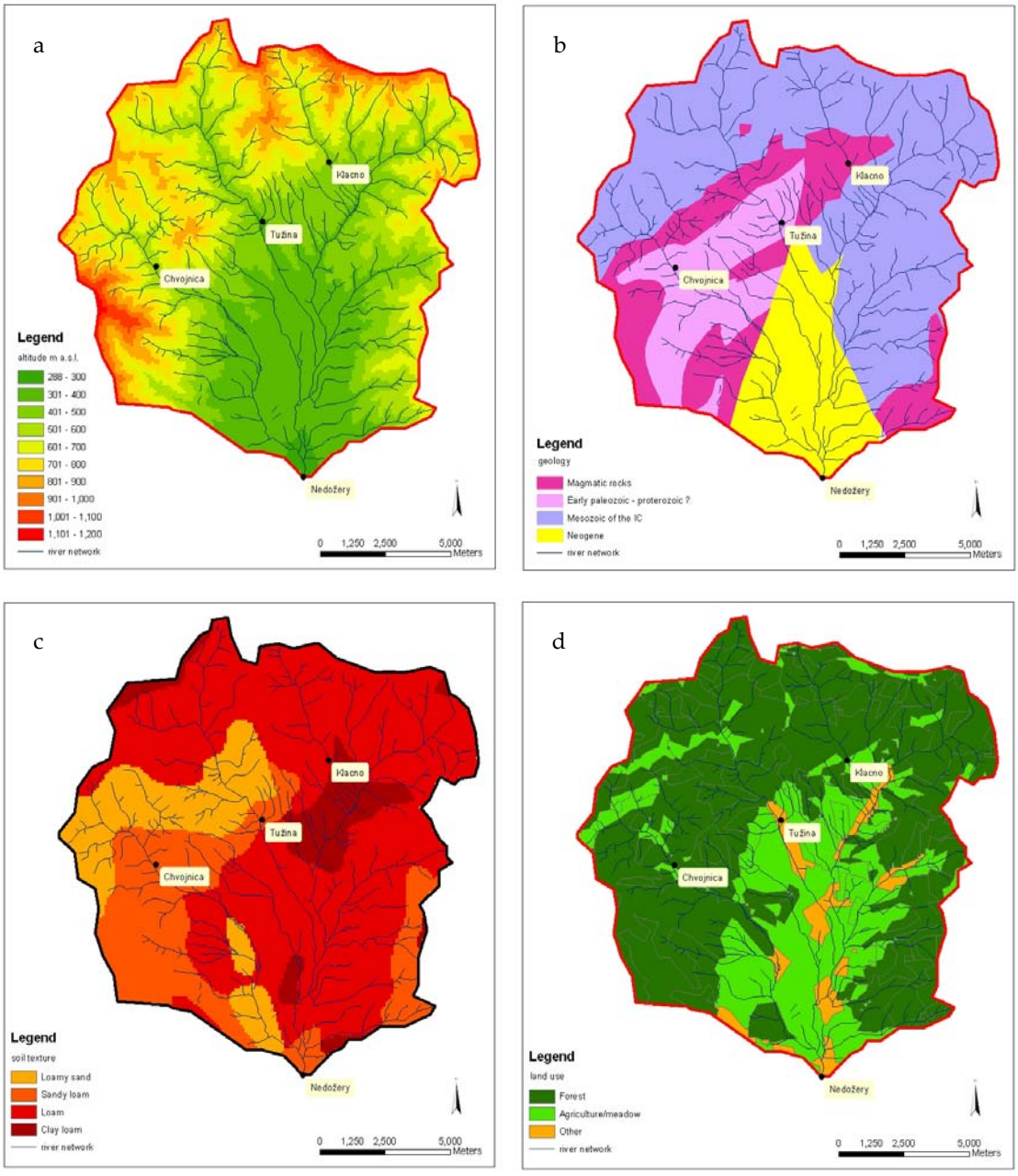

Figure 2.4 The Nedožery catchment: **a)** altitude, **b)** geology, **c)** soil texture and **d)** land use.

2.1.5 Soil texture

A soil map using the USDA soil texture classification was available for the Nedožery catchment (Figure 2.4 c; Figure 2.5). Soils in the area vary from loamy sand to clay loam. Almost sixty percent of the area consists of loam, mainly located in the northern and eastern part of the catchment. In the southwestern part of the catchment mainly loamy sand and sandy loam can be found (together more than thirty percent of the total area). Clay loam can be found in parts of the valley and in the highest parts in the northwest of the area.

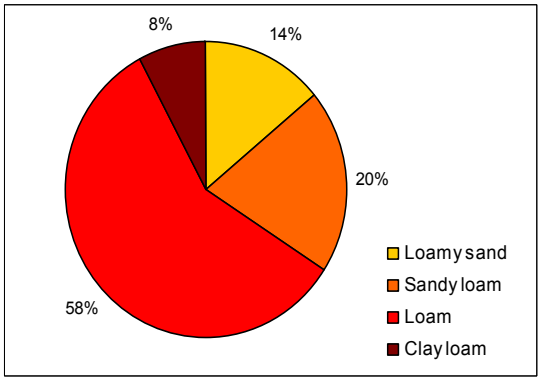

Figure 2.5 Soil texture in the Nedožery catchment, based on USDA classification.

2.1.6 Land use

Two third of the Nedožery catchment is covered by forest. Agriculture covers 23% percent of the catchment and 6% of the catchment is natural meadow. Together this makes up almost 30% of the total area. Artificial (built-up) surface covers 5% of the catchment. Roughly agricultural areas and meadows are in the lower parts of the catchment, while forests are present on the higher parts (Figure 2.4 d; Figure 2.6).

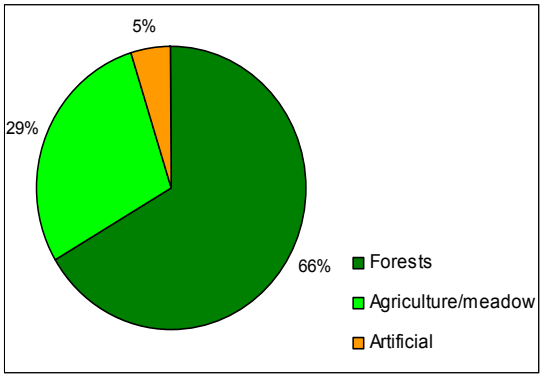

2.2 Available data

Data of the Nedožery catchment was received from Comenius University in Bratislava. Daily time series were obtained from various meteo-rological stations in the region. The stations are located at different altitudes. Most stations are located outside the Nedožery catchment. Not all time series are without gaps. The most representative and complete meteorological station for Nedožery is located in Prievidza. For Prievidza station all variables except minimum and maximum temperature are available without gaps. For a complete overview of the data, altitude of the stations and length of the time series see Annex 2. Data preprocessing is described in Section 3.2, data quality is described in Chapter 4.

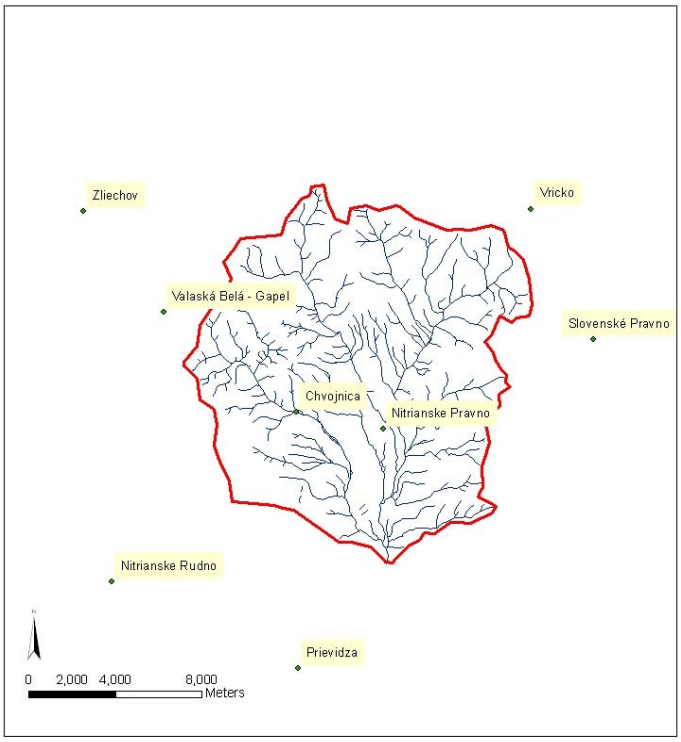

Figure 2.7 Precipitation stations in and around Nedožery.

Daily precipitation data is available from ten stations (Table 2.1; Figure 2.7). The longest available time series is that of Prievidza starting July 1972. Starting in 1981 daily time series of seven additional stations are available. Only two time series for precipitation are available in the catchment itself (Nitrianske Pravno and Chvojnica, 1980-2007).

Daily time series for air temperature are available from ten stations (Table 2.2). The longest time series without gaps is again that of Prievidza (1972-2007).

Table 2.1 Precipitation stations and their altitude

Station	Altitude [m a.s.l.]
Nitrianske Pravno	351
Chvojnica	435
Vrícko	603
Valaská Belá - Gápel	490
Slovenské Pravno	500
Prievidza	260
Bojnice	325
Kláštor pod Znievom	480
Nitrianske Rudno	312
Zliechov	598

Table 2.2 Temperature stations and their altitude

Station	Altitude [m a.s.l.]
Prievidza	260
Turčianske Teplice	510
Banská Bystrica	427
Banská Štiavnica	575
Kremnické Bane	758
Krížna	1570
Lom nad Rimavicou	1018
Topoľčany	192
Trenčianske Teplice	306
Trenčín - Biskupice	209

Daily discharge data is available for the Nedožery catchment starting in 1940. Daily discharge data is also available for three sub-catchments Chvojnica (1974-2006), Tužina (1969-2006) and Kl'ačno (1975-2006) (location in Figure 2.4) and for a downstream gauging station Chalmová (1930-2006).

3. Methods

3.1 Description of hydrological model HBV

3.1.1 General description

The HBV model is a conceptual, semi-distributed, rainfall-runoff model which is developed by Bergström at the Swedish Meteorological and Hydrological Institute (SMHI) (Bergström & Forsman, 1973). Seibert (2005) developed a new version called HBV *light*, which is an easy to use Windows version for research and education. Seibert (2005) and Hohenrainer (2008) describe the model as follows: daily discharge is simulated by HBV using daily rainfall, temperature and potential evaporation as input. The simulated catchment can be divided in several elevation (max. 10) and vegetation (max. 3) zones. It is not necessary to set initial conditions, the model has a 'warming-up' period in which an initial state is reached.

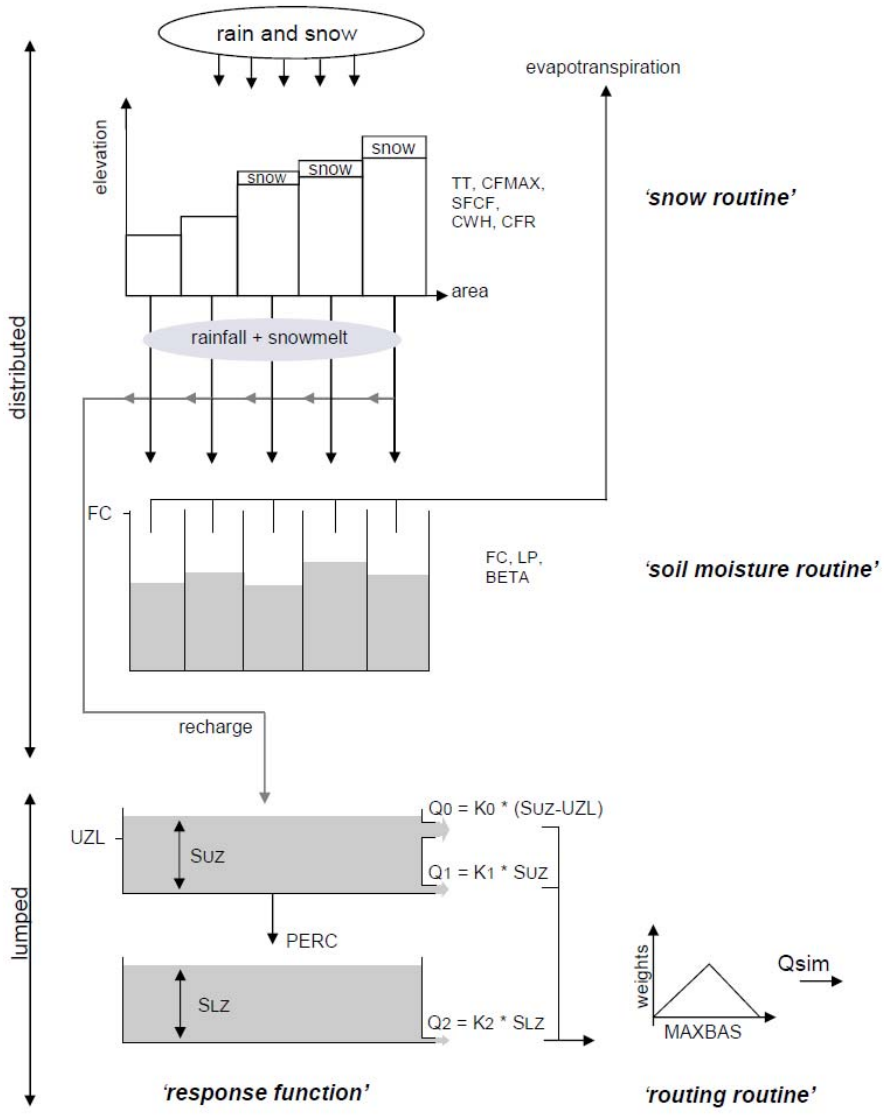

Figure 3.1 Schematic structure of the standard version of the HBV *light* model (after Seibert, 2005).

3.1.2 Routines

The standard version of the HBV *light* model consists of several (sub)routines (Figure 3.1): a snow routine simulating snow accumulation, melting and freezing; a soil moisture routine simulating storage, evapotranspiration and recharge; a response function consisting of two groundwater boxes (an upper box with two outflows with different recession coefficients, and a lower box with one outflow that receives water from the upper box by percolation); and a river routing routine distributing the calculated discharge for one day onto the next days. The snow routine and the soil routine are spatially distributed, the response function is lumped over the whole catchment.

Snow routine Precipitation accumulates as snow if the temperature (T) is below a certain threshold temperature (TT), snow melt starts if T > TT. All precipitation that falls as snow is multiplied with a snowfall correction factor (SFCF). This factor corrects for undercatch due to wind and evaporation losses from snow. Snow melt is calculated with a degree-day method and meltwater and rain are retained in the snowpack until they exceed a certain portion (CWH, the water holding capacity of the snowpack). Meltwater refreezes if T < TT, but at a lower efficiency. All water that can not be retained in the snowpack is passed on to the soil moisture routine. Computation is done for each elevation-vegetation zone separately.

Daily input data: precipitation [mm/d], temperature [°C].
Daily output data: snow water equivalent [mm], snow melt [mm/d].

Soil moisture routine Rainfall (P) and snowmelt are divided into a part going to the soil (moisture) storage and a part to the groundwater (recharge to the response function). Thus recharge is only generated in case of rainfall or snowmelt. The fraction of water going to the response function (Figure 3.1) is depending on the relation between water content of the soil moisture routine (SM) and the maximum soil moisture storage (FC) (Figure 3.2; equation 3.1).

$$\text{recharge} = \left(\frac{SM(t)}{FC}\right)^{BETA} \cdot P(t) \qquad \textit{equation 3.1}$$

FC is a model parameter and is not necessarily equal to the real field capacity. Water is removed from the soil storage only by evapotranspiration. The actual evapotranspiration (ET_{act}) is dependent on potential evapotranspiration (ET_{pot}) and the actual soil moisture content (by using a threshold value for soil moisture (LP) above which ET_{act} reaches ET_{pot}[2]). ET_{act} is computed as a fraction of ET_{pot}.

Evapotranspiration can be simulated when there is a snow cover.

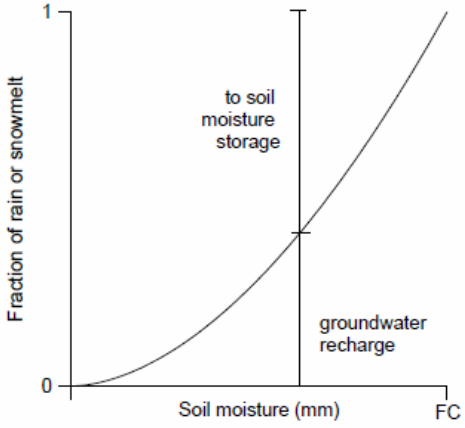

Figure 3.2 Contribution from rainfall or snowmelt to the soil routine and the upper groundwater box (Seibert, 2005).

Computation is done for each elevation-vegetation zone separately. Note that there is no surface runoff, the fast component is modeled through the response routine.

[2] ET_{act} reaches ET_{pot} when SM = FC * LP

Daily input data: potential evaporation [mm/d], precipitation [mm/d], snowmelt [mm/d].
Daily output data: actual evapotranspiration [mm/d], soil moisture [mm], groundwater recharge [mm/d].

Response function The groundwater is simulated by linear reservoirs. The standard version of HBV *light* consists of two groundwater boxes placed in series. The output from the soil routine is the input for the uppermost groundwater box. Water can leave the upper groundwater box by percolation to the lower box or by generating discharge. The upper box is divided in two parts: a slow component (Q1: intermediate flow) generating runoff proportional to the amount of storage in the upper box (SUZ), and a part generating runoff at strong precipitation events (Q0: peak flow) when the amount of incoming water exceeds the fixed percolation value (PERC) and the amount of water in the upper groundwater box exceeds the threshold (UZL). Water can leave the lower box by generating runoff (Q2: base flow) or by evaporation from a lake. The lower groundwater box has the smallest recession coefficient. For lakes (as a fraction of the total catchment area) precipitation is added directly to the lower groundwater box and evaporation is subtracted directly from the lower groundwater box. The reason for this is the constant water availability in this box.

Total discharge is computed as the sum of Q0, Q1 and Q2. Computation is done lumped for the whole catchment.

Daily input data: groundwater recharge [mm/d].
Daily output data: discharge [mm/d], groundwater level [mm]

Routing routine The total discharge of the response routine for one time step is distributed over the next days using the parameter MAXBAS. This parameter is the base of a equilateral triangular weighting function.
Daily input data: discharge [mm/d]
Daily output data: simulated discharge [mm/d]

3.1.3 Parameters

The routines described in the previous section make use of parameters, which are listed in Table 3.1.

Table 3.1 Parameters needed for HBV *light* (Seibert, 2005)

Parameter	Explanation	Unit
Snow routine		
TT	threshold temperature	^{o}C
CFMAX	degree-day factor	mm $^{o}C^{-1}$ d^{-1}
SFCF	snowfall correction factor	-
CWH	water holding capacity snowpack	-
CFR	refreezing coefficient	-
Soil routine		
FC	largest value for SM (soil moisture)	mm
LP	threshold for reduction of evaporation	-
BETA	shape coefficient	-
Response routine		
K_0	recession coefficient (upper storage)	d^{-1}
K_1	recession coefficient (upper storage)	d^{-1}
K_2	recession coefficient (lower storage)	d^{-1}
UZL	threshold for Q_0 outflow	mm
S_{UZ}	storage in upper zone *1	mm
S_{LZ}	storage in lower zone *2	mm
PERC	maximum flow from upper to lower box	mm d^{-1}
River routing routine		
MAXBAS	triangular weighting function	d

*1 S_{UZ} has no upper limit

*2 S_{LZ} can never exceed PERC/K_2

3.1.4 Calibration

For calibration and optimization of the model a visual inspection of simulated and observed hydrographs gives the best judgment. Besides visual inspection an objective and quantitative evaluation of the model performance is needed (Saelthun, 1996). The HBV model provides a number of objective functions, which makes it possible to do automatic calibration.

The sum of squares of errors and the Nash-Sutcliffe efficiency criterion (R_{eff}) are very sensitive to high flow events. To give more weight to the low flow events the Nash-Sutcliffe efficiency criterion based on the logarithm of observed and simulated discharge ($\ln R_{eff}$) can be used (equation 3.5) (Saelthun, 1996; Seibert, 2005).

$$\ln R_{eff} = 1 - \frac{\sum \left(\ln Q_{obs} - \ln Q_{sim}\right)^2}{\sum \left(\ln Q_{obs} - \overline{\ln Q_{obs}}\right)^2} \qquad \textit{equation 3.5}$$

The focus on modeling low flow will cause the simulated water balance to deviate from reality because the peaks are likely to be underestimated.

Usually, calibration and validation of a conceptual hydrological model is limited to comparing simulated and observed discharge at the catchment outlet (Seibert, 2000). If there is sufficient data on groundwater heads and soil moisture, this data can be used additionally (multi-criteria calibration). In HBV maximum 1000 groundwater observations are possible as input. In the current HBV light structure it is not possible to calibrate both on $\ln R_{eff}$ and on groundwater (r^2 (GW)). Calibration on r^2 (GW) is only possible in combination with calibration on R_{eff}.

GAP optimization

Using a genetic algorithm the GAP optimization method generates parameter sets which are used to generate new parameter sets. The chance for a generated parameter set to be used in generation of the new parameter sets is dependent on the value of the used objective function. Parameter sets with a high fit get a higher probability to be used. The genetic algorithm is described in more detail by Seibert (2000).

For the GAP optimization a minimum and maximum can be set for each parameter. For parameters of the snow and soil routines it can be defined whether the value of the parameter must increase or decrease with vegetation zone, be the same for all vegetation zones or be random for each vegetation zone.

3.1.5 Model setup

In this research the period of modeling was 1974-2006. The period July 1972 to December 1973 was used as 'warming-up' period.

Parameter ranges for calibration were used according to Seibert (2000). For the snow and soil routines the option 'random' was chosen for the difference in parameter values between the three vegetation zones.

The GAP optimization method was used. The number of model runs was set to 3500. The number of runs for local optimization was set to 1200. The number of parameter sets was 50 with 4 populations.

Calibration was done on lnR_{eff} and on a combination of (R_{eff}) and the coefficient of determination between simulated and observed groundwater heads (r^2). In this study more than 1000 groundwater observations were available, therefore the monthly mean was used as a value for the 15^{th} day of the particular month.

Calibration output are four files with parameters (the ones with the highest efficiency of each population). These parameter files are used as input for HBV. The four resulting runs are compared and the best run is chosen after visual inspection of the simulation and taking into account lnR_{eff}.

In the statistical program R (r-project.org) the simulated precipitation[3] is calculated as a rest term of the water balance for the upper distributed boxes (snow and soil routine) (pers. comm. Van Loon, 2009).

[3] The catchment average precipitation calculated and used (but not provided as output) by HBV.

3.2 Data preprocessing and calculations

For HBV input one time series is needed for each variable (precipitation, temperature, potential evapotranspiration). For each variable an average time series needed to be calculated from the data of various stations. Because the stations are on a different altitude, the values needed to be corrected to one altitude before calculating the average.

3.2.1 Calculation of altitude gradients

Based on available data an altitude gradient was calculated for each variable.

Precipitation gradient

The precipitation gradient is calculated using eight precipitation stations (Table 2.1 except Bojnice and Kláštor pod Znievom). Before calculating the precipitation gradient, all days on which one or more of the eight stations showed a precipitation value equal to or lower than 0.1 mm (dry days), or a NA value (no data), were removed. Only the days on which all stations had a value for precipitation that was higher than 0.1 mm were used. For each of these days a precipitation gradient was calculated (in mm precipitation / m altitude) with linear regression using the altitude of the station and the precipitation amount for each station (Figure 3.3). The average precipitation gradient was 0.0071 mm/m. Next the average precipitation gradient (based on the daily values) was calculated for each month (Annex 3). Other gradients (Table 3.2) were calculated in the same way as the precipitation gradient, except for the removal of dry days which is not relevant for other variables.

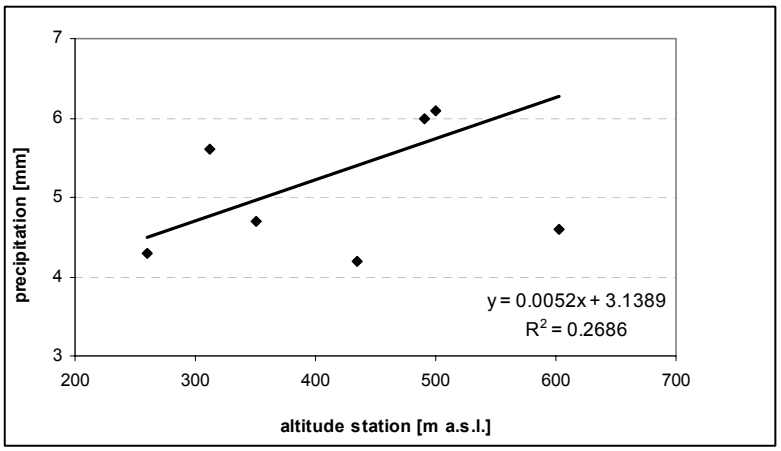

Figure 3.3 Example calculation of the precipitation gradient (3-2-1981) using eight stations on different altitudes with different precipitation amount, resulting in a gradient of 0.0052 mm/m for that day.

Table 3.2 Average altitude gradients

Variable	Altitude gradient	Unit
Cloudiness	0.0000	[-/m]
Wind speed	0.0020	[m/s/m]
Relative air humidity	0.0068	[%/m]
T_{air}	-0.0054	[°C/m]
T_{min}	-0.0041	[°C/m]
T_{max}	-0.0070	[°C/m]
Precipitation	0.0071	[mm/m]

3.2.2 Altitude correction

Correction was done towards a reference altitude, the average altitude of the Nedožery catchment (573 m a.s.l.). The measured value of a certain station is corrected towards the reference altitude using the gradient for that variable (equation 3.6).

$$V_{corrected} = V_{station} + (\Delta_{altitude} \cdot dV / dh) \qquad \textit{equation 3.6}$$

$V_{corrected}$	corrected value of variable V
$V_{station}$	measured value of variable V at station
$\Delta_{altitude}$	altitude reference station – altitude station
dV/dh	altitude gradient of variable V

For some variables correction towards the reference altitude led to negative values; while variables like cloudiness, wind speed, relative humidity and precipitation can not be negative. For these variables, values that were below zero were set to zero.

3.2.3 Calculation of precipitation and temperature gradients as input for HBV

In HBV the input data for temperature and precipitation are corrected for altitude in each elevation zone. A file with daily or monthly values for the correction factor is used. Both gradients were calculated from the data as described in Section 3.2.1. For the precipitation gradient percentages were used in stead of amounts. These percentages were calculated from the gradient [mm/m] and a precipitation value [mm]. Using an average of the stations resulted in an average precipitation gradient of 12.73 % / 100 meter altitude (Annex 3). The precipitation gradients for each month de not show a clear pattern (Figure 3.4). However a clear pattern is visible for the temperature gradient, with lowest gradients in winter months (Figure 3.5). This can be explained by the frequent occurrence of inverse temperature gradients in winter (Hohenrainer, 2008).

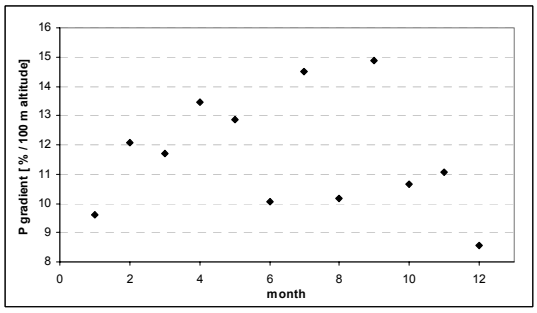

Figure 3.4 Monthly precipitation gradient.

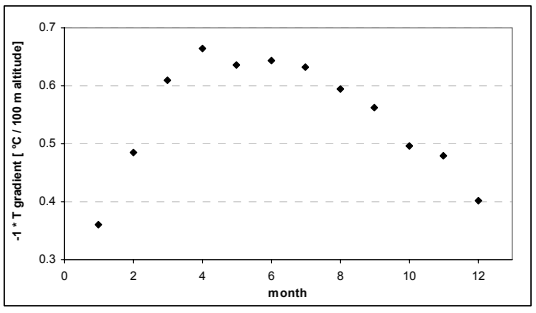

Figure 3.5 Monthly temperature gradient.

3.2.4 Weighted average of stations

The weighted average of the time series for each variable was computed using Thiessen polygons, calculated with ArcGIS. For the calculation of the average minimum temperature, average maximum temperature, average air temperature (Figure 3.6), average wind speed, and average cloudiness, time series of two stations were used. For the days with no data in one of the time series, only one series was used. For the calculation of the average precipitation, time series of five stations were used (Figure 3.7). For days with no data for one or more of these five stations the value of Prievidza was used in stead of a weighted average. For snow cover only one time series was used, which meant no averaging was needed. For an overview of all available data and the used Thiessen factors see Annex 2 and Section 2.2. Table 3.3 gives an overview of the data that were used.

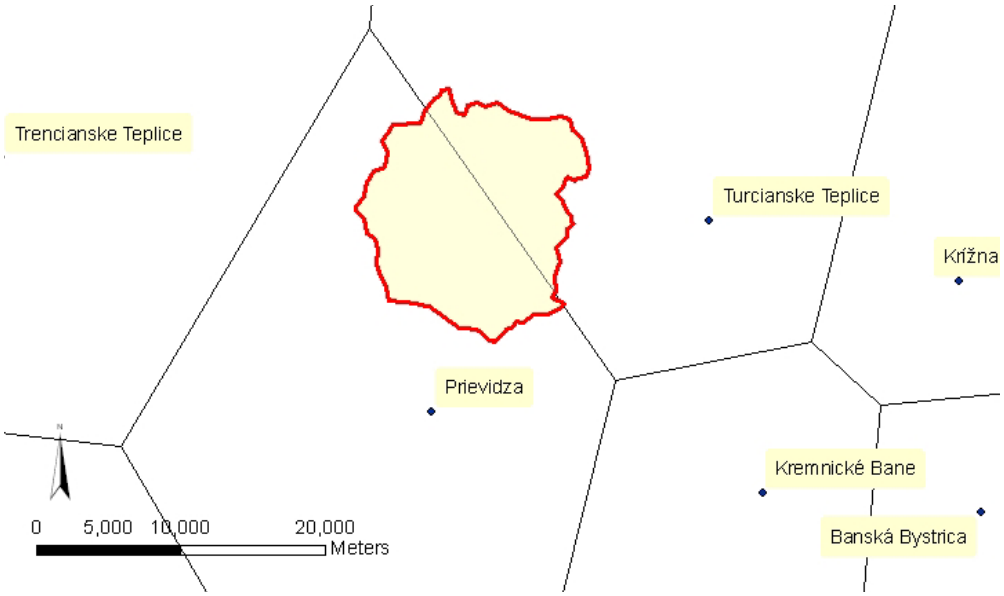

Figure 3.6 Temperature stations around the Nedožery sub catchment (including used Thiessen polygons) (for a more detailed description see Annex 2).

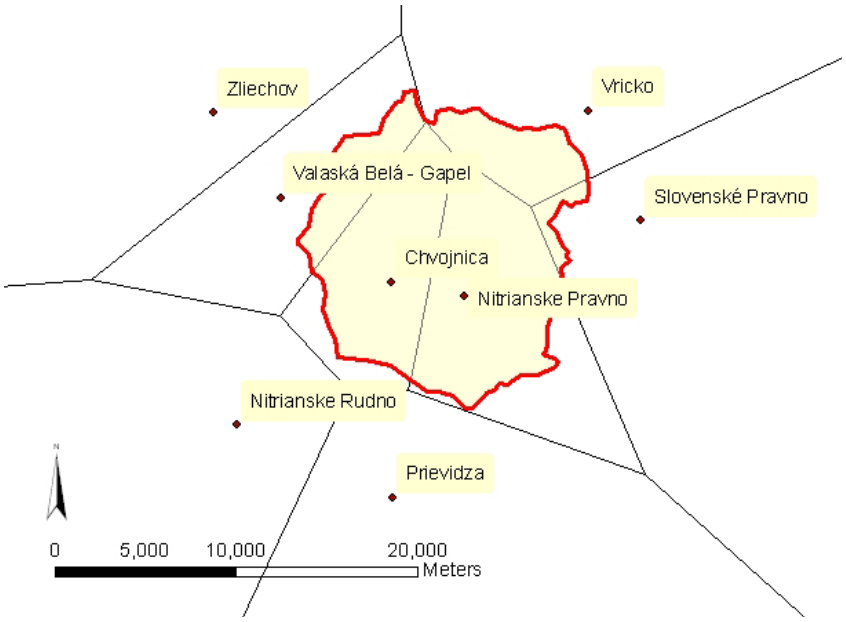

Figure 3.7 Precipitation stations in and around the Nedožery sub catchment (including used Thiessen polygons) (for a more detailed description see Annex 2).

Table 3.3 Used data

Action	Used data
calculation potential evapotranspiration	minimum temperature
	maximum temperature
	wind speed
	cloudiness
	relative air humidity
HBV input	precipitation
	air temperature
	potential evapotranspiration
HBV calibration	discharge
	groundwater
validation HBV model results	snow cover

3.2.5 Calculation of potential evapotranspiration

The potential evapotranspiration was calculated using Penman-Monteith as proposed by the FAO in Allen et al. (1998) (equation 3.7).

$$ET_0 = \frac{0.408\Delta(R_n - G) + \gamma \frac{900}{T+273} u_2 (e_s - e_a)}{\Delta + \gamma(1 + 0.34u_2)} \qquad \textit{equation 3.7}$$

ET_0	reference evapotranspiration [mm/day]
R_n	net radiation at the crop surface [MJ/m²/day]
G	soil heat flux density [MJ/m²/day]
T	air temperature at 2 m height [°C]
u_2	wind speed at 2 m height [m/s]
e_s	saturation vapour pressure [kPa]
e_a	actual vapour pressure [kPa]
$e_s - e_a$	saturation vapour pressure deficit [kPa]
Δ	slope vapour pressure curve [kPa/°C]
γ	psychometric constant [kPa/°C]

Shortwave radiation was calculated from extraterrestrial radiation by using cloudiness. Daily cloudiness data was available on a 1 to 10 scale. Using a lookup table in FAO paper 24 (Doorenbos & Pruitt, 1975) the cloudiness data were converted to a form which could be used in the computation of the daily shortwave radiation. A description of the calculations can be found in FAO paper 56 (Allen et al., 1998).

In a few cases, the calculation of reference evapotranspiration (eq. 3.7) led to negative values (< 0.5% of daily time series 1972-2006), which were set to zero.

3.2.6 Elevation-vegetation zones

Based on land use and elevation data (Section 2.1), 10 elevation zones and 3 land use classes were intersected in GIS. An input file containing the percentage of the total area of the Nedožery catchment for each land use-elevation combination was created. Also a soil texture-elevation input file and a geology-elevation input file were created (Section 2.1; Annex 4). HBV was calibrated with each of this input files and differences between the resulting simulations were analyzed.

3.3 Trend analysis

Some input and output data showed trends and these were investigated looking at annual sums or averages. For some variables also monthly sums were investigated to see whether there are different trends throughout the year.

The slope of a trend in the annual sums or means was calculated using equation 3.8. In this equation the x-values are years (e.g. 1975 – 2006) and the y-values are the annual sums or averages. The percentage slope was calculated using equation 3.9.

$$slope = \frac{\sum (x - \bar{x})(y - \bar{y})}{\sum (x - \bar{x})^2} \qquad \textit{equation 3.8}$$

$$slope\% = \frac{slope}{\bar{y}} \cdot 100\% \qquad \textit{equation 3.9}$$

$\bar{y}$ = average of variable over whole time series

A Mann-Kendall test was carried out in to give the statistical significance of the trends (Stahl et al., 2008). This Mann-Kendall (MK) test is a non-parametric test which identifies trends in a time series by comparing successive values.

For a sample (x_1, …, x_n) with size n the MK statistic S is calculated according to equation 3.10.

$$S = \sum_{i=1}^{n-1} \sum_{j=i+1}^{n} sign(x_j - x_i) \qquad \textit{equation 3.10}$$

Under the null hypothesis that there is no trend in the time series, the expected value for S is zero with a variance $Var(S) = n(n-1)(2n+5)/18$. The test statistic is the standardized value which is calculated according to equation 3.11.

$$Z = \begin{cases} \dfrac{S-1}{\sqrt{Var(S)}} & \text{if } S > 0 \\ 0 & \text{if } S = 0 \\ \dfrac{S+1}{\sqrt{Var(S)}} & \text{if } S < 0 \end{cases} \qquad \textit{equation 3.11}$$

The outcome of this |Z| statistic has a certain probability (p-value). For a two sided test with a significance of 5% this means the null hypothesis of no trend is rejected if the p-value < 0.025. This means the outcome has a low probability under the assumption there is no trend. Therefore the null hypothesis (no trend) has to be rejected. The test was carried out with the statistical program R using the function *MannKendall* (r-project.org). Auto-correlation was not taken into account, but this can have effect on the results.

3.4 Threshold method

For drought definition the threshold level method was used which was described first by Yevjevich (1967). Tallaksen et al. (1997) and Hisdal et al. (2004) describe the threshold method in detail. The threshold method is the most frequently applied quantitative method in drought

analysis. The period that the values of a certain variable (e.g. daily discharge) are below the threshold level is defined as a drought period. In that period a deficit builds up. The onset and end of a drought can be defined. The drought duration (d_i) is the time that the variable is below the threshold, the deficit volume (s_i) is the volume below the threshold (Figure 3.8). The drought intensity is the ratio between drought deficit volume and drought duration.

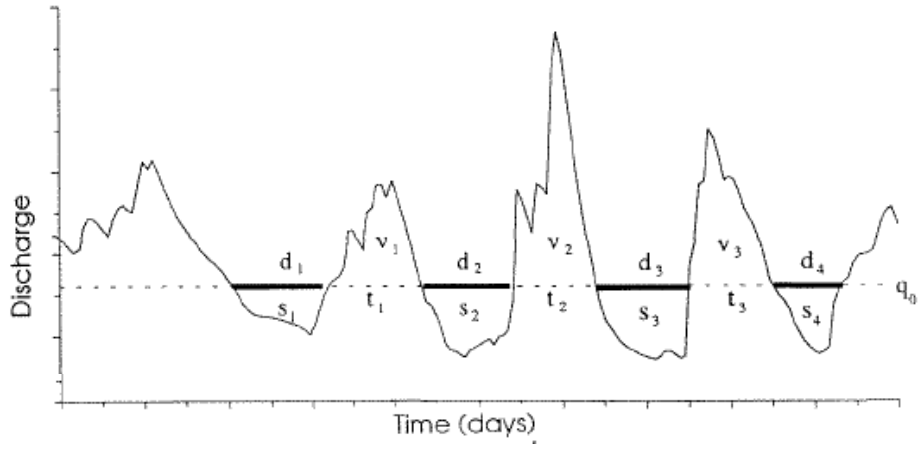

Figure 3.8 The threshold level method (modified after Tallaksen et al.,1997).
Legend: q_0 = threshold level, d_i = duration, s_i = deficit volume, t_i = inter-event time, v_i = inter-event volume.

For state variables (like soil moisture and groundwater) defining a deficit volume using the threshold method does not make sense. Therefore, the maximum difference between the threshold level and the value of the state variable is used as an indicator.

The selection of the threshold can depend on certain needs in the area (e.g. minimum ecological flow, minimal reservoir flow) but in this case a percentage of the flow duration curve is used. A threshold level between 70 and 95% percent is considered reasonable for drought research (Hisdal et al., 2004). The choice for a high or low threshold has influence on the calculated occurrence of drought. The outcome of calculation with two different threshold percentages (80% and 90%) was investigated.

Because of the seasonality in the catchment (Section 2.1.2), a yearly threshold will every year result in a summer drought. Therefore Van Lanen (2006) proposes the use of a monthly threshold. To prevent steps in the threshold (resulting in artificial droughts), a moving average of 30 days was used so that a smooth line for the threshold was obtained.

To improve the drought analysis, a minimum drought duration can be set. Droughts shorter than this minimum duration will be ignored in the analysis. The outcome of drought analysis using two minimal drought duration settings (3 days and 5 days) was investigated.

Drought analysis was carried out both on observed variables (30-day moving average of precipitation, discharge) and HBV outputs (soil moisture, groundwater and discharge).

4. Data quality

The HBV *light* model needs meteorological data as input (Section 3.1). A critical assessment of the data showed irregularities for the discharge data and trends in almost all datasets. In this Chapter, first discharge and precipitation data source and quality (Section 4.1) and then trends will be discussed (Section 4.2).

4.1 Source and quality

Discharge

Daily discharge data is available for the Nedožery catchment starting in 1940. The gauging station was always located at Nedožery-Brezany (Figure 4.1), although during the period of measurement the location has displaced somewhat within Nedožery-Brezany. Because of possible changes in the river bed at the measuring point and differences between summer and winter period, the rating curve of the gauging station is updated regularly. Usually, six to eight measurements a year are done to check and adjust the rating curve. Water level measurements are done automatically. Before 2002, a floating gauge was used and measurements were monitored graphically. Starting in 2002, pressure sensors were used and data was recorded digitally (pers. comm. Blaškovičová, 2009).

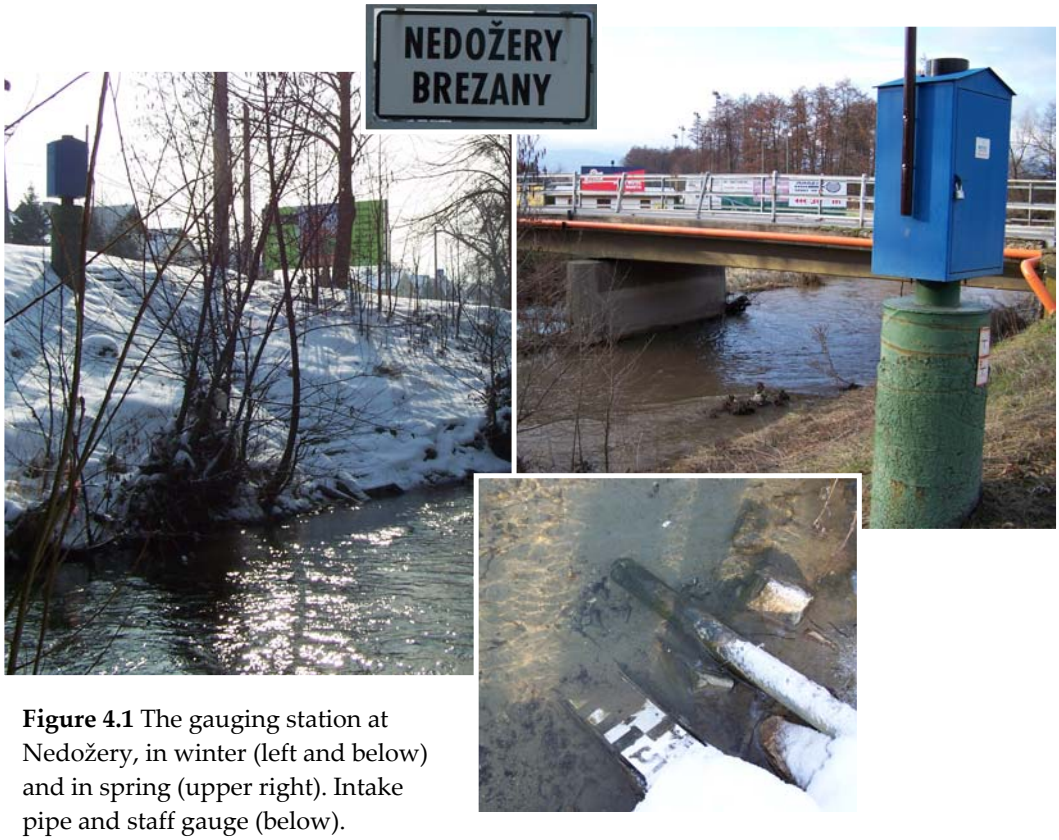

Figure 4.1 The gauging station at Nedožery, in winter (left and below) and in spring (upper right). Intake pipe and staff gauge (below).

In some years the observed discharge showed some strange patterns (Figure 4.2). For a few days the observed discharge remained constant. In 1977 a rainfall event did not lead to a peak in discharge (peak 1 in Figure 4.2), while later rainfall events show a clear response in the discharge (peak 2 in Figure 4.2.).

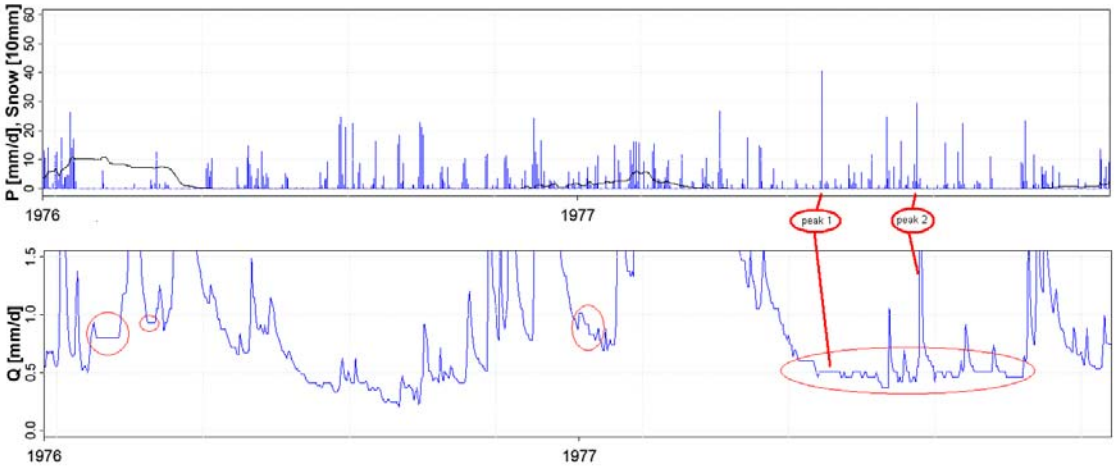

Figure 4.2 Precipitation and strange patterns in observed discharge at Nedožery.

A possible explanation of these constant values is that mud in the intake pipe closes the connection between the river and the stilling well. Especially downstream this can be a problem. Usually, a high flow will clean up the entrance again. Another explanation might be that in low flow situations the water level is below the entrance of the stilling well (pers. comm. Blaškovičová, 2009). The above listed irregularities occur only in a few years and were not expected to have a significant influence. Thus no correction was done.

Precipitation

The Prievidza precipitation time series is the only precipitation dataset without gaps. The meteorological station Prievidza (Figure 2.7; Figure 4.3) is located on the airport of Prievidza. Nowadays measurements in Prievidza are automatic and the rain gauge is heated to measure snow also.

Figure 4.3 Meteorological station Prievidza.

4.2 Trends in the data

Assessment of the data showed a trend in almost all input datasets for the period of modeling. It is important whether the trend is significant[4] and what its impact on the modeling is (Section 5.4). Significance of the trends was investigated using a Mann-Kendall test as described in Section 3.3.

4.3.1 Discharge

Annual sums of observed discharge show downward trends for all gauging stations (Table 4.1; Figure 4.4). Only the trend in the annual sums for Chalmová is not significant. Also the annual minimum flow (based on a moving average of seven days) shows a downward tendency (Figure 4.5).

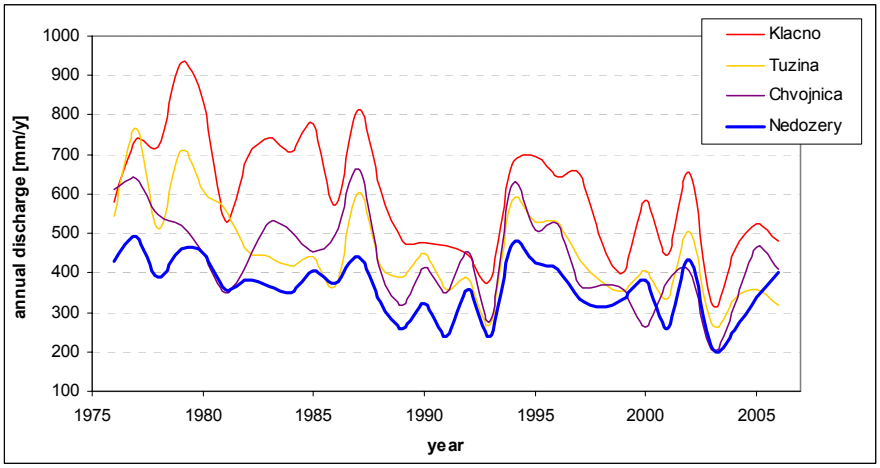

Figure 4.4 Annual discharge sums [mm/y] for the Nedožery (sub)catchments (1976-2006).

Table 4.1 Trends in annual sum of discharge for the gauging stations in the catchment (over period 1976-2006)

	Sum [mm]	Slope [mm/y]	Slope [%/y]	P-value*1
Kľačno	597	-9.79	-1.64%	**0.001**
Tužina	452	-8.46	-1.87%	**0.000**
Chvojnica	439	-6.69	-1.53%	**0.004**
Nedožery	361	-3.58	-0.99%	**0.013**
Chalmová	301	-1.83	-0.61%	0.089

*1 significant trend printed in bold.

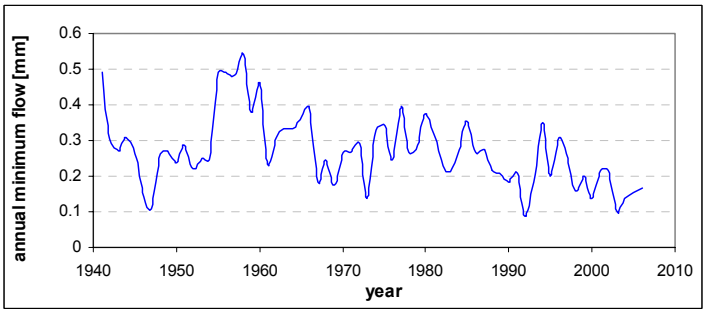

Figure 4.5. Annual minimum flow for Nedožery based on moving average of 7 days.

When looking at each month separately for the observed monthly discharge at Nedožery (Table 4.2), all months except March and April show a downward tendency. The upward tendency in

[4] If not significant, a trend is called tendency throughout this report

March and April have a high p-value compared to the downward tendencies in the other months. The lowest p-values occur in the summer months.

Table 4.2 Trends in the monthly and yearly discharge sums for Nedožery based on the modeling period (1974-2006)

	Sum [mm]	Slope [mm/y]	Slope [%/y]	P-value
January	28.19	-0.30	-1.08%	0.178
February	33.46	-0.36	-1.09%	0.198
March	64.47	0.24	0.37%	0.840
April	55.70	0.14	0.26%	0.768
May	33.78	-0.30	-0.88%	0.345
June	22.98	-0.27	-1.17%	0.150
July	17.31	-0.16	-0.92%	0.029
August	13.10	-0.19	-1.46%	0.046
September	12.47	-0.09	-0.76%	0.091
October	18.28	-0.64	-3.48%	**0.010**
November	22.47	-0.20	-0.89%	0.345
December	29.97	-1.28	-4.29%	0.029
Year	352.2	-3.42	-0.97%	**0.014**

4.3.2 Precipitation

Annual precipitation sums show upward tendencies for all stations. The lowest p-value occurs for Vrícko and Zliechov, the two stations located at the highest altitude (Table 4.3). The tendencies are between 0.2 and 0.8% of the annual sum except for Zliechov (1.7% of the annual sum).

Table 4.3 Trends in the annual precipitation sums for the various stations (see also Annex 6a)

Precipitation station	Altitude station [m a.s.l.]	Period	Sum [mm]	Slope [mm/y]	Slope [%/y]	P-value
Chvojnica	435	1981-2006	898	3.97	0.44%	0.355
Nitrianske Pravno	351	1981-2006	734	1.77	0.24%	0.724
Nitrianske Rudno	312	1981-2006	754	5.67	0.75%	0.064
Prievidza	260	1973-2006	642	1.22	0.19%	0.836
Slovenské Pravno	500	1981-2006	797	1.43	0.18%	0.659
Valaská Belá - Gápel	490	1981-2006	886	6.64	0.75%	0.086
Vrícko	603	1981-2006	1050	8.20	0.78%	**0.017**
Zliechov	598	1981-2006	867	14.91	1.72%	**0.006**
Weighted average	573 *1	1974-2006	873	5.66	0.65%	**0.007**

*1 Reference altitude: mean altitude of catchment (Section 2.1.3).

In some months each station shows an upward tendency (February, April, July, August, November) and two months show a downward tendency for all stations (June, December) (Figure 4.6).

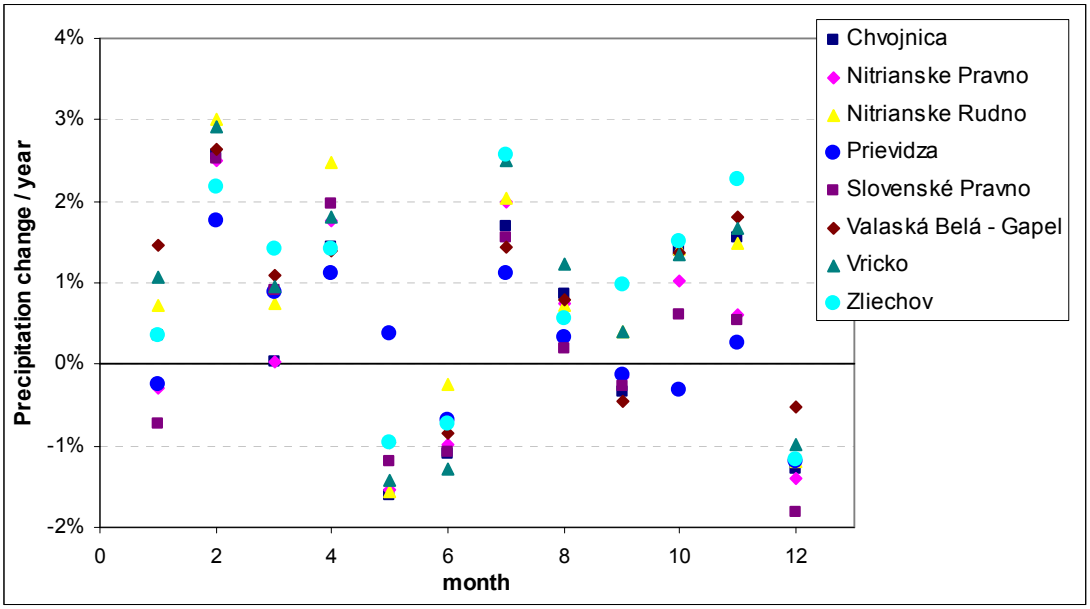

Figure 4.6 Trends in the monthly precipitation data (based on period 1981-2006).

The calculated weighted average of five stations (Section 3.2.4) which is used as input for HBV (Figure 4.7) shows an upward trend (Table 4.5). Most tendencies are upward, except for June and December. Only the trends in February and April are significant.

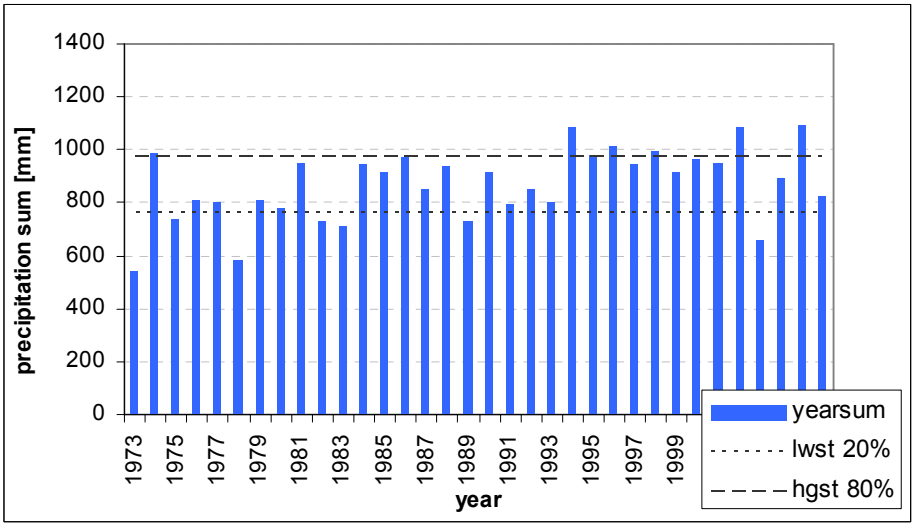

Figure 4.7 Annual precipitation sums for the period 1973-2006 based on the weighted average of 5 stations compared to the 20 and 80% threshold for precipitation.

Table 4.5. Trends in the monthly and yearly precipitation sums (of the weighted average) for the modeling period (1974-2006)

	Sum [mm]	Slope [mm/y]	Slope [%/y]	P-value
January	62.7	0.4	0.60%	0.466
February	52.3	1.4	2.63%	**0.007**
March	58.2	0.9	1.49%	0.198
April	63.2	1.1	1.78%	**0.012**
May	82.0	0.3	0.40%	0.664
June	96.0	-0.9	-0.96%	0.299
July	86.7	1.1	1.23%	0.233
August	83.5	0.1	0.08%	0.631
September	72.7	0.3	0.42%	0.963
October	67.4	0.2	0.35%	0.448
November	73.4	1.1	1.49%	0.150
December	75.6	-0.2	-0.33%	0.687
Year	874	5.7	0.65%	**0.007**

4.3.3 Snow cover

Annual total number of snow days (observed at Prievidza) shows a significant upward trend (Figure 4.8. and Table 4.6).

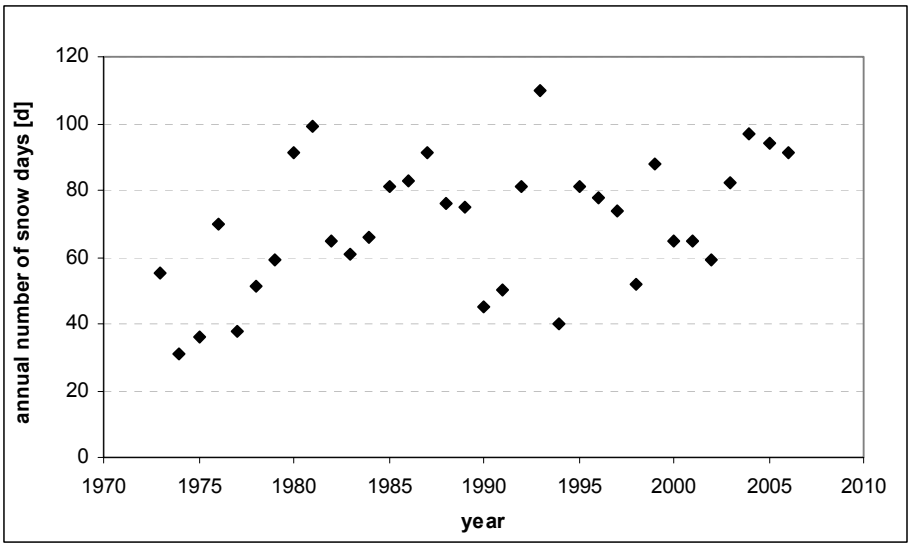

Figure 4.8 Annual total number of snow days for Prievidza for the period 1973-2006.

The monthly number of snow days for February and March shows a significant upward trend.

Table 4.6 Trends in the monthly and yearly number of snow days for Prievidza for the modeling period (1974-2006)

	Mean nr. of days	Slope [d/y]	Slope [%/y]	P-value
January	23	0.06	0.26%	0.254
February	19	0.39	2.07%	**0.021**
March	7	0.36	5.15%	**0.005**
April	1	0.04	6.86%	0.253
October	0	0.00	-1.30%	0.810
November	5	0.01	0.16%	0.891
December	16	-0.01	-0.07%	0.941
Year	70	0.85	1.21%	**0.015**

4.3.4 Temperature

Annual mean, minimum and maximum temperature show an upward tendency for almost all stations (Annex 6b). The weighted average of the annual mean air temperature shows an upward but not significant trend (Table 4.7). The winter months (December to March) show downward tendencies while April to November show upward tendencies. The upward tendencies from April to August have the lowest p-value. The downward tendency for the temperature in the winter months explains the upward tendency in the number of snow days in those months (Table 4.6).

Table 4.7 Trends in the monthly and yearly mean air temperature (of the weighted average) for the modeling period (1974-2006)

	Mean temperature [°C]	Slope [°C/y]	P-value
January	-2.84	-0.02	0.486
February	-1.43	-0.02	0.546
March	2.48	-0.05	0.209
April	7.55	0.08	**0.003**
May	12.93	0.06	0.061
June	15.72	0.07	**0.008**
July	17.54	0.08	**0.013**
August	17.14	0.06	**0.014**
September	12.86	0.01	0.816
October	8.06	0.02	0.828
November	2.52	0.05	0.299
December	-1.52	-0.02	0.525
Year	7.58	0.03	0.046

4.3.5 Potential evapotranspiration

Annual sums of the potential evapotranspiration show a significant upward trend (Table 4.8). In general, a distinction between winter months (December till March) with a downward tendency and summer months with an upward tendency can be made. The months April to August have the lowest p-value.

Table 4.8 Trends in the monthly and yearly potential evapotranspiration sum (of the weighted average) for the modeling period (1974-2006)

	Mean [mm]	Slope [mm/y]	Slope [%/y]	P-value
January	49.47	-0.10	-0.21%	0.505
February	53.63	-0.10	-0.20%	0.631
March	75.12	-0.32	-0.43%	0.168
April	93.64	0.84	0.90%	**0.003**
May	114.84	0.68	0.59%	0.070
June	120.58	0.83	0.69%	**0.009**
July	127.34	1.07	0.84%	**0.013**
August	112.89	0.69	0.61%	**0.010**
September	77.42	0.05	0.07%	0.914
October	59.29	0.13	0.22%	0.840
November	49.16	0.24	0.48%	0.271
December	47.64	-0.09	-0.19%	0.631
Year	981.01	3.90	0.40%	**0.001**

The upward trend for the potential evapotranspiration in the summer months can be explained by the upward trend in the temperature for those months (Table 4.7). Also in winter a relation between temperature and evapotranspiration trends is clear.

No further analysis on trends in cloudiness, wind speed and relative humidity is done because the evapotranspiration trend analysis implicitly accounts for this.

4.3.6 'Conflicting' trends

Because of the relation between precipitation and discharge, it is expected that an upward trend in precipitation will result in an upward trend for discharge. For Nedožery this is not the case. Bates et al. (2008) found the same: "trends in runoff are not always consistent with changes in precipitation". An upward trend in the (potential) evapotranspiration could be (part of) the explanation. The summer months show an upward trend in potential evapotranspiration, which could decrease the discharge. However, the downward trend in discharge is not only in summer. Other explanations for the conflicting trend of precipitation and discharge can be land use changes (which is a potential source of uncertainty (Das et al. 2008)) or groundwater extractions. The above listed possible explanations are underlined by Bates et al. (2008) who state that conflicting trends may be due to data limitations, the effect of human interventions or the competing effects of changes in precipitation and temperature.

5. HBV results

HBV simulates parts of the hydrological cycle which play a role in drought propagation (but from which no data is available) and thus can be an useful instrument in drought analysis. The model results give insight in the hydrological regime and the variability within the hydrological cycle. This Chapter describes different approaches used in improving the HBV simulation of Nedožery (Section 5.1), the sensitivity of the model to some parameters (Section 5.2), the hydrological regime (Section 5.3) and trends in the HBV outputs (Section 5.4).

5.1 Improving the simulation

The simulations resulting from use of groundwater observations, three input files for zonation and two methods for calculating potential evapotranspiration were compared. The best simulation was chosen for drought analysis. An overview of all runs can be found in table 5.1.

Table 5.1 Overview all runs

Name	Input zonation file	Potential evapotranspiration	Calibration
Z1_Var1_lnQ	soil texture - elevation	HBV approach (PET_M)	lnR_{eff}
Z1_Var1_Q&GW	soil texture - elevation	HBV approach (PET_M)	R_{eff} and r^2 (GW)
Z1_Var2_lnQ	soil texture - elevation	daily values	lnR_{eff}
Z2_Var1_lnQ	geology - elevation	HBV approach (PET_M)	lnR_{eff}
Z3_Var1_lnQ	land use - elevation	HBV approach (PET_M)	lnR_{eff}

5.1.1 Use of groundwater observations

Both calibration using a combination of observed discharge and groundwater heads, and calibration using the logarithm of the observed discharge was done. The obtained parameter sets were used to run HBV and results were compared.

Table 5.2 Results of calibration without and with considering groundwater

Calibrated on	LnR_{eff}	R_{eff}	r^2 (GW)
LnR_{eff}	0.68	0.64	0.42
R_{eff} & r^2 (GW)	0.52	0.67	0.65

From Table 5.2 it follows that calibration on both discharge and groundwater improves the efficiency of the discharge simulation (R_{eff}) and groundwater simulation (r^2 (GW)). However the efficiency of modeling of low flows (LnR_{eff}) decreases.

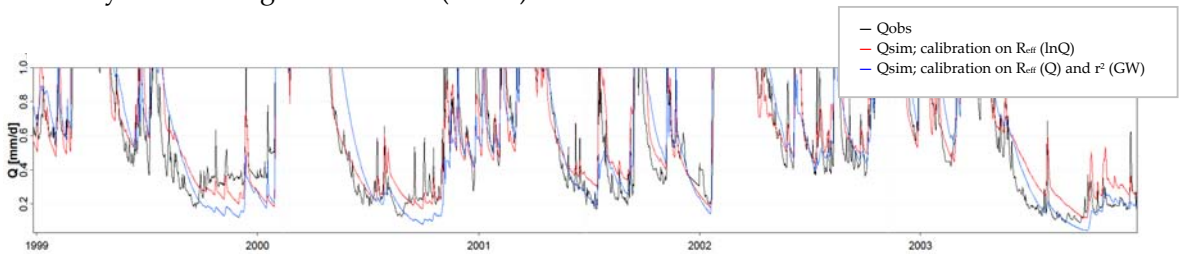

Figure 5.1 Observed (Q_{obs}) and simulated (Q_{sim}) discharge, calibrated on lnR_{eff} and on r^2 (GW) and R_{eff}.

Visual inspection shows (Figure 5.1) that simulated discharge resulting from calibration on r^2 (GW) and R_{eff} is too low in autumn of 1999 and 2000. But the modeling of the recession curve of the 2003 drought seems to be better for the calibration on r^2 (GW) and R_{eff}. For the whole time series, it happens frequently that simulated recession curves (resulting from calibration on r^2 (GW) and R_{eff}) are underestimating the observed discharge (Annex 7).

When comparing simulated and observed groundwater heads (Annex 8), it becomes clear that calibration on lnR_{eff}, results in low efficiency for the groundwater simulations (r^2 = 0.42). Calibration on R_{eff} and r^2 (GW) heads results in a higher efficiency for the simulation of groundwater (r^2 = 0.65). Only the modeling of the high groundwater levels improves, for the low groundwater levels there is no improvement when calibrating on r^2 (GW) and R_{eff}.

In general, both the efficiency and visual inspection of the time series leads to the conclusion that using groundwater observations in the calibration not results in a higher lnR_{eff}. For the simulation of recession curves and low flows the use of groundwater heads for calibration is not advantageous, so in the rest of this research HBV is calibrated on lnR_{eff}.

5.1.2 Zonation

Calibration was carried out first with land use-elevation classes as an input, later also geology-elevation and soil texture-elevation classes were used. Differences between simulations resulting from calibration using the three input files were minimal (Table 5.3). Because the use of soil texture-elevation classes fits in the HBV model structure, this classification was used in HBV (soil texture is likely to influence processes in the soil routine, which is distributed in HBV; while geology is likely to have more influence on the groundwater which is part of the lumped response function in HBV).

Table 5.3 Differences between simulations resulting from the three zonation files

	Elevation soil texture	Elevation land use	Elevation geology
Reff	0.648	0.617	0.643
lnReff	0.677	0.676	0.682
Sum Qsim [mm]	346	346	346
Sum Qobs [mm]	352	352	352
Contribution of Q2	0.544	0.537	0.527
Contribution of Q1	0.365	0.369	0.374

5.1.3 Use of different potential evaporation

In HBV there are two possibilities for using evaporation data that are evaluated by two model variants, both calibrated on lnReff. The first variant uses the HBV approach: correcting the long term mean of potential evaporation (PETM) for a certain month of the year to its value at day t by using the deviation of the temperature (T(t)) from its long term mean (TM) and a correction factor CET (Seibert, 2005). The second variant uses a daily time series for potential evaporation as input. The modeling of discharge does not differ that much and efficiency is almost the same (Table 5.4). The example of 2003 shows the general pattern (Figure 5.2). Variant 1 is chosen.

Table 5.4 Differences between the two variants

	1	2	Unit
lnReff	0.68	0.66	
Reff	0.64	0.63	
sum ETpot	980	975	mm/year
sum ETact	556	552	mm/year
sum Qsim	345	346	mm/year
sum Qobs	352	352	mm/year
contribution of Q1	0.386	0.356	
contribution of Q2	0.505	0.565	

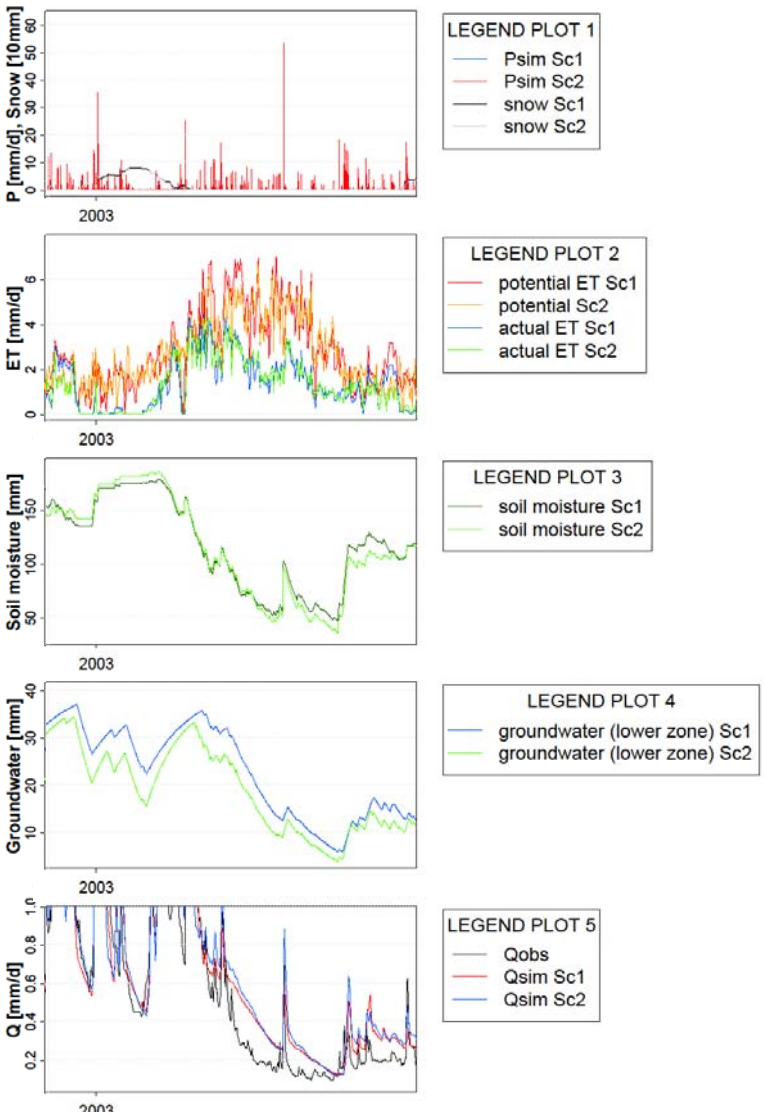

Figure 5.2 Different HBV output for variants 1 (Sc1) and 2 (Sc2) for a sample year (2003).

5.2 Parameter sensitivity

Some parameters (Section 3.1.3) varied a lot, some had the same value almost every calibration round (Figure 5.3; Annex 9).

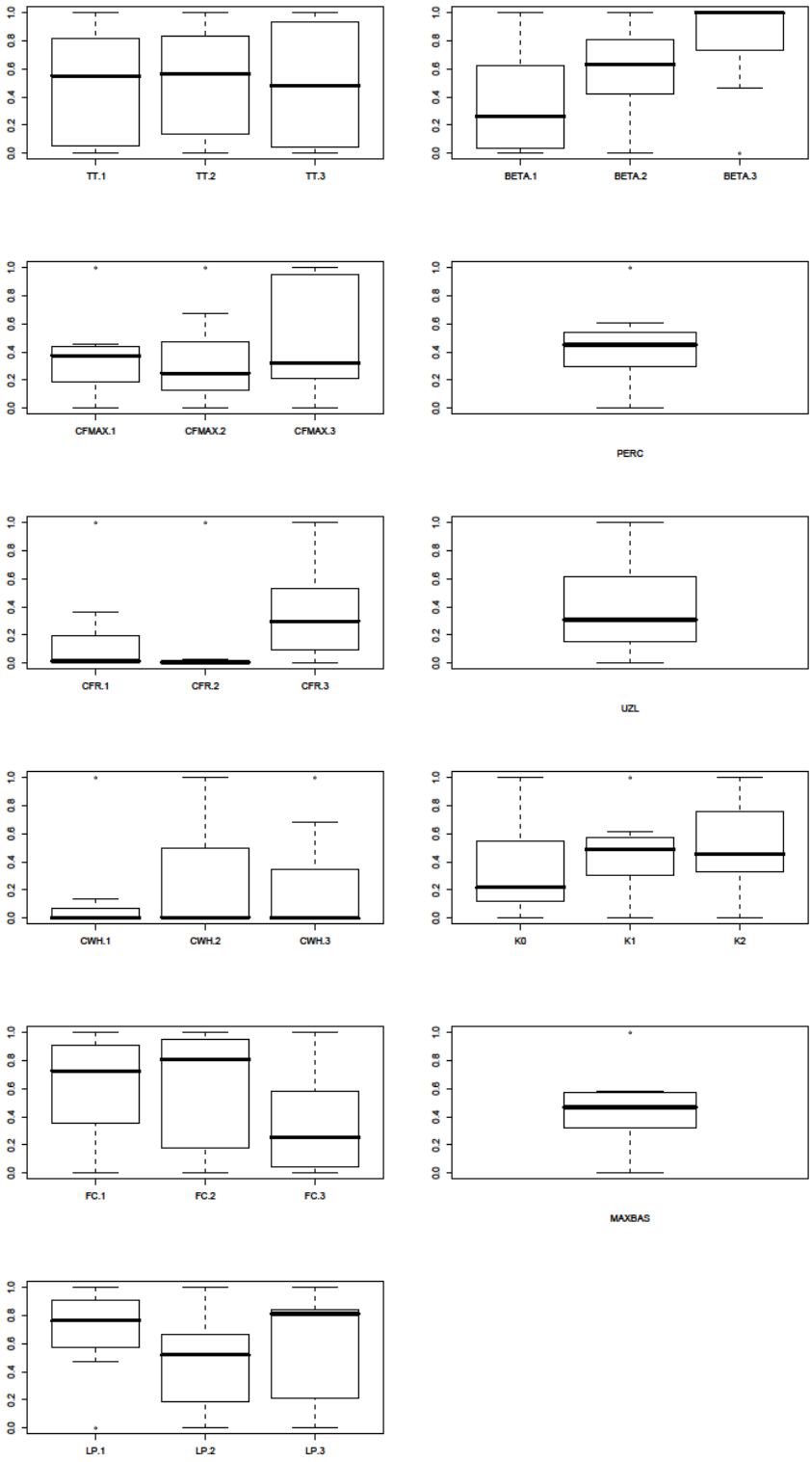

Figure 5.3 Standardized parameter values resulting from calibration (soil texture zones indicated with 1,2,3).

The sensitivity of HBV was investigated changing only one parameter, while all others were kept the same. The outcomes were compared by looking at efficiency, the contribution (as a fraction of the total discharge) of discharge from the upper (Q1) and the lower (Q2) groundwater box, and other outputs that show a difference.

UZL

A higher threshold for Q0-outflow (UZL) means that more storage is possible in the upper zone, so that less fast discharge is expected. HBV was ran with two different values for the threshold for Q0-outflow (UZL = 22 and UZL = 15) (Table 5.4). The simulated discharge for both runs did not differ, but the contribution of discharge from the upper groundwater box is higher for a higher threshold. This can be explained by the higher storage in the upper groundwater box which decreases peak flow (Q_K0) and leaves more water for intermediate flow (Q_K1). The higher storage capacity results in a higher amount of water in the upper groundwater box (SUZ). The efficiency does not change.

Table 5.4 HBV results: efficiency, fraction upper (Q1) and lower (Q2) groundwater box, other outputs (mean values) for UZL = 15 and UZL = 22

UZL	R_{eff} (ln Q)	Contribution of Q1	Contribution of Q2	SUZ [mm]	SLZ [mm]	Q_K0 [mm/d]	Q_K1 [mm/d]	Q_K2 [mm/d]
15	0.6773	0.369	0.503	3.62	23.83	0.12	0.35	0.47
22	0.6741	0.411	0.506	4.09	24.00	0.08	0.39	0.48

PERC

A higher maximum flow from upper to lower box (PERC) will increase percolation and base flow. HBV was ran with two different values for the maximum flow from upper to lower groundwater box (PERC = 0.4 and PERC = 2) (Table 5.5). The contribution of the lower groundwater box is higher for a higher PERC. The increased percolation results in a lower fast discharge (Q_K0) and intermediate flow (Q_K1), and an increased base flow (Q_K2). Recession curves are higher and thus a too high percolation value results in overestimation of low flows.

Table 5.5 HBV results: efficiency, fraction upper (Q1) and lower (Q2) groundwater box, other outputs (mean values) for PERC = 0.4 and PERC = 2

PERC	R_{eff} (ln Q)	Contribution of Q1	Contribution of Q2	SUZ [mm]	SLZ [mm]	Q_K0 [mm/d]	Q_K1 [mm/d]	Q_K2 [mm/d]
0.4	0.6336	0.538	0.320	5.32	15.15	0.13	0.51	0.31
2.0	0.5623	0.187	0.754	1.84	35.74	0.06	0.18	0.71

TT

Increasing the threshold temperature (below which precipitation falls as snow) will increase the amount of snow. HBV was ran with different values for the threshold temperature (TT) (Table 5.6). A higher TT leads to an increase in discharge both for the upper (Q_K0, Q_K1) and the lower (Q_K2) groundwater box. Increase in the upper groundwater box is relatively higher than for the lower groundwater box. This is the reason that the contribution of the higher groundwater box to the total flow increases. Actual evapotranspiration decreases with a higher threshold temperature. The snow water equivalent and the number of snow days are higher for a higher threshold temperature.

Table 5.6 HBV results: efficiency, fraction upper (Q1) and lower (Q2) groundwater box, other outputs (mean values) for 4 different values for $TT_{1,2,3}$

		1	2	3	4
TT 1	[°C]	-1.7	-1.5	-1.3	-1.0
TT 2	[°C]	0.9	1.1	1.3	1.6
TT 3	[°C]	1.6	1.8	2.1	2.4
Reff (ln Q)		0.644	0.647	0.644	0.626
contribution Q1		0.244	0.249	0.256	0.265
contribution Q2		0.741	0.733	0.724	0.711
annual sum Qsim	[mm]	332	338	344	353
annual sum act.ET	[mm]	568	564	559	552
mean snow water eq.	[mm]	13.60	15.03	16.86	19.33
annual snow days	[d]	141	144	148	152
mean SM	[mm]	109.0	109.5	110.0	110.6
mean recharge	[mm/d]	0.908	0.924	0.941	0.965
mean SUZ	[mm]	1.13	1.17	1.23	1.30
mean SLZ	[mm]	19.15	19.28	19.39	19.53
mean Q_K0	[mm/d]	0.014	0.016	0.019	0.023
mean Q_K1	[mm/d]	0.221	0.230	0.241	0.256
mean Q_K2	[mm/d]	0.674	0.678	0.682	0.687

K0

Increasing the recession coefficient the peak flow will speed up discharge Q0 in case the maximum storage for the upper groundwater box (determined by UZL) is reached. HBV was ran with two different values for the recession coefficient (K0 = 0.05 and K0 = 0.4) (Table 5.7). Only minimal changes occur in HBV outputs. The amount of water in the upper groundwater box is lower for the higher recession coefficient, because (when UZL is reached) more water goes to the routing routine. This is also the reason that peak flow (Q_K0) increases while the intermediate flow (Q_K1) slightly decreases. Efficiency does not change.

Table 5.7 HBV results: efficiency, fraction upper (Q1) and lower (Q2) groundwater box, other outputs (mean values) for K0 = 0.05 and K0 = 0.40

K0	R_{eff} (ln Q)	Contribution of Q1	Contribution of Q2	SUZ [mm]	SLZ [mm]	Q_K0 [mm/d]	Q_K1 [mm/d]	Q_K2 [mm/d]
0.05	0.6455	0.266	0.728	1.28	19.35	0.01	0.25	0.68
0.40	0.6469	0.248	0.727	1.18	19.33	0.02	0.23	0.68

K1

Increasing the recession coefficient for intermediate flow will speed up the discharge from the upper groundwater box (the part below the threshold UZL). HBV was ran with two different values for the recession coefficient (K1 = 0.10 and K1 = 0.25) (Table 5.8). The amount of water in the upper groundwater box (SUZ) is lower for a higher K1 and, because of less percolation, also the amount of water in the lower groundwater box (SLZ) is lower. The contribution of the upper groundwater box to total discharge (Q1) is higher for a higher K1 and peak flow decreases because the threshold for peak flow (UZL) is reached less. The efficiency shows a minor change.

Table 5.8 HBV results: efficiency, fraction upper (Q1) and lower (Q2) groundwater box, other outputs (mean values) for K1 = 0.10 and K1 = 0.25

K1	R_{eff} (ln Q)	Contribution of Q1	Contribution of Q2	SUZ [mm]	SLZ [mm]	Q_K0 [mm/d]	Q_K1 [mm/d]	Q_K2 [mm/d]
0.10	0.6309	0.201	0.764	1.66	20.31	0.03	0.19	0.71
0.25	0.6425	0.299	0.692	0.83	18.39	0.01	0.28	0.65

K2

Increasing the recession coefficient for base flow will speed up the discharge from the lower groundwater box. HBV was ran with two different values for the recession coefficient (K2 = 0.015 and K2 = 0.045) (Table 5.9). The storage in the lower groundwater box is lower for the higher K2. Other variables do not show a clear pattern or do not show any change at all. A visual inspection of the discharge graphs shows that a higher K2 results in a better fit with the observed recession curve, while the run with the lower K2 is overestimating recessions. This is also visible in the higher efficiency for the run with the higher K2. The difference in storage in the lower zone (SLZ) between the two K2 values can be explained by a different initial state. The reason for this difference is not found.

Table 5.9 HBV results: efficiency, fraction upper (Q1) and lower (Q2) groundwater box, other outputs (mean values) for K2 = 0.015 and K2 = 0.045

K2	R_{eff} (ln Q)	Contribution of Q1	Contribution of Q2	SUZ [mm]	SLZ [mm]	Q_K0 [mm/d]	Q_K1 [mm/d]	Q_K2 [mm/d]
0.015	0.5592	0.254	0.727	1.21	44.63	0.02	0.24	0.68
0.045	0.6212	0.253	0.727	1.21	14.44	0.02	0.24	0.68

Conclusion

The parameters that deal with the lower groundwater box have the most significant effect on efficiency.

5.3 Hydrological regime

The general pattern of the HBV simulation will be described using monthly averages. Figures 5.4 to 5.8 show the monthly (smoothed) averages of some HBV outputs for the hydrological year (November – October). The discharge shows a clear seasonal pattern: high discharges occur during snowmelt (February – April) (Figure 5.4). Highest groundwater level and discharge occur at the end of snowmelt (March) (Figure 5.6). August and September have the lowest discharge. HBV simulates this pattern quite well. some underestimation in winter and some overestimation in summer is visible. Highest recharge to the response function occurs during snowmelt (Figure 5.5). The precipitation peak in June is hardly visible in the recharge. Lowest recharge occurs in August. In winter the simulated precipitation (Figure 5.7) is higher than the observed precipitation (input). Simulated precipitation is computed from the water balance of the snow and soil routine (Section 3.1.5). Potential and actual evapotranspiration are strongly correlated with temperature (Figure 5.8). The peaks of actual (June) and potential (July) evapotranspiration do not coincide. This can be explained by the reduction of soil moisture in summer (Figure 5.9), which is reducing actual evapotranspiration. Also in winter actual evapotranspiration does not reach its potential level. The reason is that in HBV evapotranspiration is at its potential level only when the amount of soil moisture reaches a certain threshold and this threshold is calibrated at a very high level (Section 3.1.2). The negative relation between soil moisture and temperature (Figure 5.9) indicates the effect of evapotranspiration on the soil moisture content. It is also visible that soil moisture is at its maximum at maximum snow water equivalent (February).

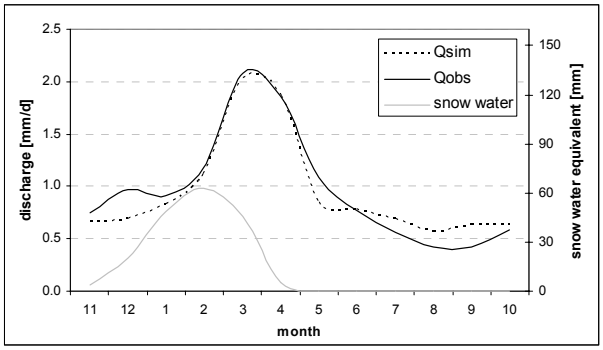

Figure 5.4 Monthly average discharge in mm/d and snow water equivalent in mm (based on period 1973-2006).

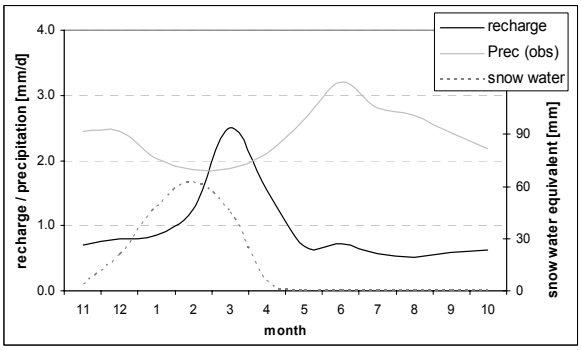

Figure 5.5 Monthly average recharge and precipitation in mm/d and snow water equivalent in mm (based on period 1973-2006).

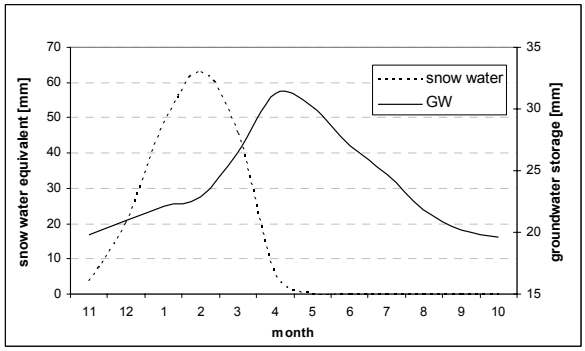

Figure 5.6 Monthly average snow water equivalent and groundwater storage in mm (based on period 1973-2006).

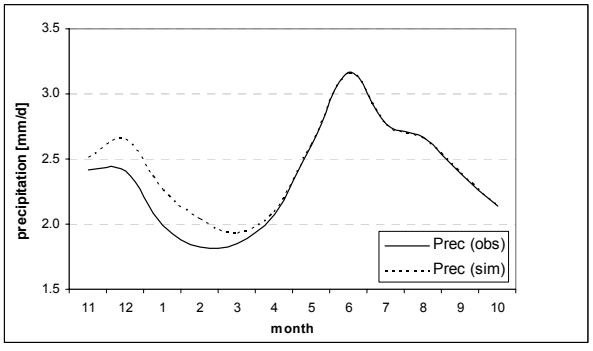

Figure 5.7 Monthly average observed and simulated precipitation in mm/d (based on period 1973-2006).

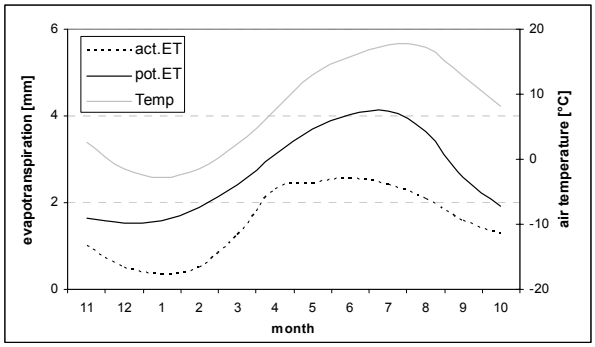

Figure 5.8 Monthly average actual and potential evapotranspiration in mm/d and temperature in °C (based on period 1973-2006).

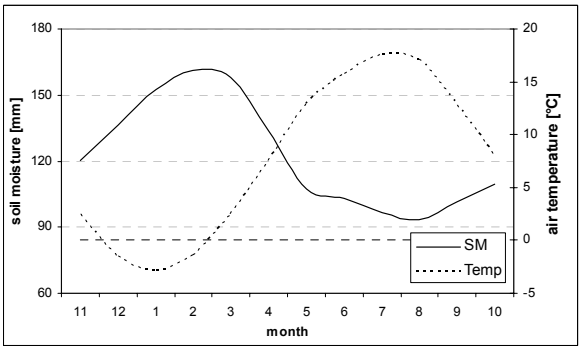

Figure 5.9 Monthly average soil moisture content in mm and temperature in °C (based on period 1973-2006).

When temperature starts to rise above zero soil moisture goes down. At that moment also evaporation rises and snow melt starts. Soil moisture rises during the increase of snow water equivalent (snow growth period from December to end of January) (Figure 5.5 and 5.9). This can be explained by the fact that, although the mean temperature for those months is below zero, some days have temperatures above zero causing some snow melt. This is different from the situation in Nordic countries were temperatures stay below zero during snow cover. Recharge (Figure 5.5) shows only a minor increase during the time of snow growth (compared to the increase in February due to snow melt) which indicates that in case of snow melt in December and January most of the melt water goes to the soil moisture routine.

From the monthly averages can be concluded that besides precipitation, temperature is an important factor for the hydrological regime in Nedožery. In winter, temperature is important both for the amount of storage in snow and for the release from storage (snow melt) (Figure 5.5). In summer, temperature is important for evapotranspiration (Figure 5.8).

5.4 Trends in the HBV output

Because of trends in the input data (Section 4.3), also the HBV output file was investigated on trend behavior. Table 5.10 shows trends in annual averages, some trends will be discussed in more detail in the Sections below.

Table 5.10 Tendencies in the annual means of the HBV output[*1]

	Mean [unit]	Slope [unit/y]	Slope [%/y]	P-value
Qsim [mm/d]	0.94	0.01	1.31%	**0.011**
Qobs [mm/d]	0.96	-0.01	-0.97%	**0.013**
Pobs [mm/d]	2.39	0.02	0.65%	**0.008**
Temp [°C]	7.63	0.03	0.35%	0.039
act.ET [mm/d]	1.52	0.01	0.38%	**0.018**
pot.ET [mm/d]	2.69	0.01	0.40%	**0.002**
Snow water eq. [mm]	15.3	0.26	1.71%	0.198
Soil moisture [mm]	122.6	0.12	0.10%	0.361
Recharge [mm/d]	0.94	0.01	1.28%	**0.013**
SUZ [mm]	3.81	0.06	1.63%	**0.012**
SLZ [mm]	23.9	0.04	0.18%	0.745
Q_K0 [mm/d]	0.10	0.01	5.02%	**0.012**
Q_K1 [mm/d]	0.36	0.01	1.72%	**0.011**
Q_K2 [mm/d]	0.48	0.00	0.18%	0.722

[*1] Significant trends printed in bold.

5.4.1 Discharge

The yearly averages of the simulated discharge show an upward trend (1.3%) (Table 5.10), while the yearly averages of the observed discharge show a downward trend (-1.0%) (Section 4.3.1). This conflicting trend results in an underestimation of observed annual discharge in the first half of the simulated time series and an overestimation of observed annual discharge in the second half of the simulated time series (Figure 5.10).

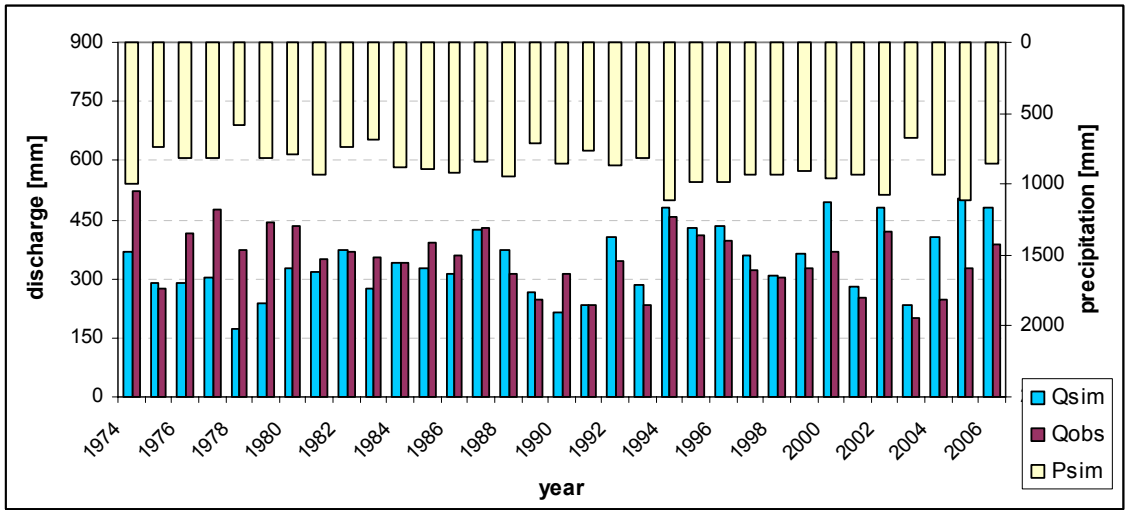

Figure 5.10 Observed discharge and simulated discharge and precipitation.

The effect of the opposing trend for observed and simulated discharge is also visible in the individual recession curves: in the first half of the time series observed recession curves are

underestimated, and in the second half observed recession curves are overestimated by the simulation (Annex 10). For the 7-day annual minimum flow the same over- and underestimation occurs (Figure 5.11).

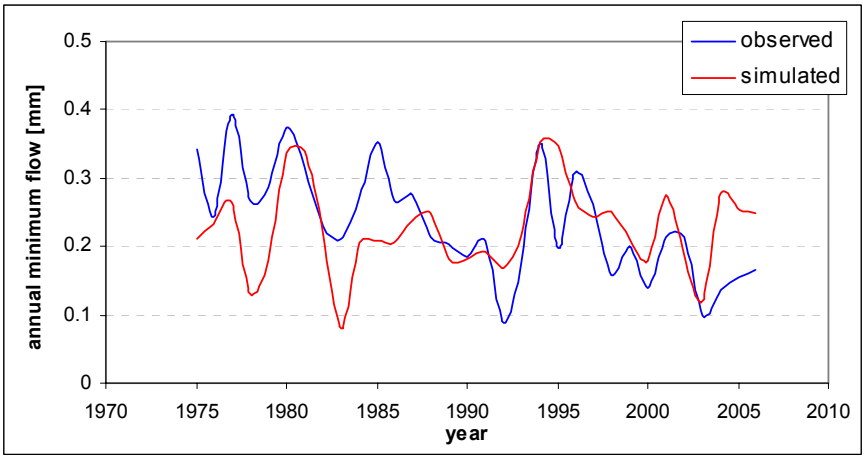

Figure 5.11 Annual minimum flow for observed and simulated discharge, based on moving average of 7 days.

When looking at monthly simulated discharge sums, March and April show an upward tendency with a low p-value (Table 5.11). For observed discharge all months, except March and April, show downward tendencies (Section 4.3.1). This is not reflected in the simulation.

Table 5.11 Tendencies in monthly and yearly sums of simulated discharge

	Mean [mm]	Slope [mm/y]	Slope [%/y]	P-value
January	25.61	0.15	0.57%	0.429
February	31.66	0.46	1.46%	0.566
March	62.93	1.67	2.65%	0.027
April	55.96	1.58	2.83%	0.042
May	26.42	0.25	0.93%	0.329
June	23.62	-0.03	-0.11%	0.963
July	21.25	0.10	0.48%	0.865
August	17.84	-0.01	-0.06%	0.698
September	18.75	0.12	0.66%	0.889
October	19.61	-0.20	-1.04%	0.889
November	19.86	0.36	1.82%	0.178
December	21.42	0.05	0.24%	0.486
Year	344.9	4.50	1.31%	**0.012**

HBV provides the discharge from the separate groundwater boxes, which gives more insight in the processes that play a role. The annual mean peak flow (Q_K0) shows a significant upward trend of 5% (Table 5.10). February, March and April show a low p-value for the upward tendency in the monthly sums of peak flow (5 - 6%) (Annex 11a). The increase of peak flow in the months just after snowmelt indicates that snowmelt is an important factor in explaining occurring tendencies. The significant upward trend in the monthly number of observed snow days for February and March (Table 4.6) underlines the relation of the trend in peak flow with snowmelt. The effect of snowmelt is also visible in the monthly sums of intermediate flow (Q_K1) which show upward trends (with a

low p-value) for March (2.3%) and April (3.2%)(Annex 11b). In the monthly sums of base flow no significant trends are visible (Annex 11c).

5.4.2 Actual evapotranspiration

Both potential (Section 4.3.5) and actual evapotranspiration show a significant upward trend in the annual averages (0.4%). The months April to July show the lowest p-value, this months have upward tendencies of between 0.5 and 1.3% (Annex 12c).

5.4.3 Snow

Comparison between simulated and observed snow cover makes clear that HBV is able to simulate snow in the right period: differences are only a few days in some cases (Annex 13). The observed and simulated annual number of snow days show an upward tendency (Table 5.12 and Figure 5.12).

Table 5.12 Tendencies in the observed and simulated annual number of snow days

	Mean [days]	Slope [d/y]	Slope [%/y]	P-value
observed (Prievidza)	64	0.84	1.30%	**0.019**
simulated (HBV elev.zone 1)	55	0.53	0.97%	0.069

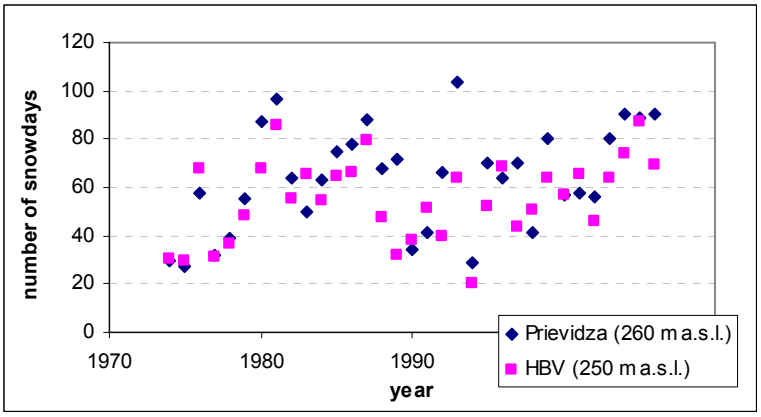

Figure 5.12 Observed (Prievidza) and simulated (HBV elevation zone 1) annual number of snow days.

5.4.4 Conclusion

The effect of conflicting trends is visible in the HBV output. An underestimation of observed discharge in the first half of the modeling period and an overestimation of observed discharge in the second half of the period is the result (Figure 5.10 and 5.11). The upward trend in the shallow groundwater storage (upper groundwater box) in the first three months of the year and the upward trend in snow cover show that (part of) the trend in simulated discharge is caused by (increasing) snowmelt peaks. The effect of increasing evapotranspiration is reflected in the observed discharge, but simulated discharge does not show a clear pattern.

6. Drought analysis

HBV simulates time series of soil moisture, groundwater and discharge and thus gives insight in drought occurrence and propagation. In this Chapter the results of drought analysis on the HBV outputs are presented. The use of different threshold levels and minimum duration will be discussed in Section 6.1. In Section 6.2 the occurrence of drought will be discussed in general and examples of two winter droughts and a summer drought will be discussed in more detail in Section 6.3.

6.1 Influence of threshold on occurrence of drought

The use of a 30-day moving average of the monthly threshold takes into account seasonality (Annex 5; Section 3.3).

The difference between the use of an 80% and a 90% threshold was investigated (threshold values are given in Annex 5). Also the difference between a minimum drought duration of 3 and 5 days was investigated.

Changing the threshold from 80% to 90% of the FDC means lowering the threshold value leading to less droughts. Droughts are shorter and have a lower deficit and intensity (Table 6.1). Changing the minimum drought duration from 3 to 5 days decreases the number of droughts, but the average drought is longer, has a higher deficit and is more intense.

Table 6.1 Changes in drought characteristics due to changing threshold (min. duration = 3 days)

	Threshold	80 → 90%
Psim	nr of droughts	-36%
	mean nr. of days	-23%
	mean deficit	-45%
	mean intensity	-30%
SM	nr of droughts	-41%
	mean nr. of days	-22%
GW	nr of droughts	-32%
	mean nr. of days	-28%
Qsim	nr of droughts	-42%
	mean nr. of days	-16%
	mean deficit	-41%
	mean intensity	-33%
Qobs	nr of droughts	-43%
	mean nr. of days	-16%
	mean deficit	-47%
	mean intensity	-29%

The change in the monthly threshold value as a result of the changing percentile is dependent on the flow duration curve for a certain month. This means that changing the threshold from 80 to 90% does not mean that the magnitude of the threshold will change by 10%. The change of the threshold value varies depending on the flow duration curve of the variable (see Annex 5 for the monthly threshold values).

For the following drought analysis the monthly 80% threshold values are used.

6.2 Occurrence of drought

The occurrence of drought is not the same in all parts of the hydrological cycle (Table 6.2). Because of the trends (Section 4.2.) there is also a difference between droughts in observed and simulated discharge. Simulated discharge has 36% less droughts than observed discharge, but droughts in simulated discharge are longer and have a higher deficit. The difference between observed and simulated discharge indicates that the simulation has less variability than the observed discharge. This can be explained by the fact that simulated discharge is the result of an average catchment precipitation, while the observed discharge is the result of real precipitation, which varies over the catchment (effect of local showers) (Bergström and Forsman, 1973). It is likely that local showers have effect on drought occurrence and especially recovery, but this effect is unknown and was not investigated in this study.

The high number of short droughts in precipitation indicates a high variability over time. This is different for soil moisture and groundwater that react slow and therefore have less but longer droughts.

The total number of drought days (number of droughts times mean number of days) for simulated discharge (2400 days) is higher than for observed discharge drought (2244 days) (Table 6.2). Whether there is an effect from the conflicting trends and what that effect is, can not easily be concluded. The total number of droughts is the sum of summer and winter droughts and occurring trends differ between winter/spring (more snowmelt) and summer (more evapotranspiration) (Section 4.3 and 5.4). Therefore, a more detailed study on the separate months and the occurrence of summer and winter droughts is needed.

Table 6.2 Drought characteristics using a 80% monthly threshold (moving average) and a minimum drought duration of 3 days for the modeled time series (1974-2006)

Variable	Nr of droughts	Mean nr of days	Mean max. diff.	Mean deficit	Mean intensity
Simulated precipitation	150	15	-	6.7	0.33
Soil moisture	108	20	13.6	-	-
Groundwater	68	35	4.0	-	-
Simulated discharge	120	20	-	1.7	0.06
Observed discharge	187	12	-	1.2	0.07

6.3 Case studies

Three droughts that are typical for the catchment are analyzed in more detail: the 1989-1990 (winter) drought, the 2001-2002 (winter) drought and the 2003 (summer) drought.

6.3.1 The 1989-1990 drought

An above average temperature and a below average precipitation in winter, caused a below average amount of snow from January to April 1990 and an above average actual evapotranspiration (Table 6.3). The effect on groundwater, soil moisture and discharge is visible: a drought developed in all parts of the hydrological cycle (Figure 6.1 and Figure 6.2). The drought can be divided in two parts which are separated by peaks due to a combination of snowmelt and rain (half December). The first part of the drought was caused by a combination of below average precipitation and temperature, while the second part of the drought was caused by above average temperature.

Onset first part
In October and November 1989 a series of shorter droughts (Figure 6.1) occurred in groundwater, soil moisture and discharge. Below average precipitation caused a discharge drought to start 18 October, followed by a groundwater drought and a soil moisture drought (Table 6.4). Precipitation in the first days of November rose the values of discharge, soil moisture and groundwater above the threshold for a few days. Starting half November temperatures were below zero causing soil moisture to remain at one level and groundwater to go down. 16 November a discharge drought started, followed by a groundwater drought and a soil moisture drought.

End first part In December temperatures were above zero (with a temperature above 5°C for eight consecutive days, with a maximum of 9.4°C) and some rain occurred (Figure 6.2). This caused soil moisture drought to end on 12 December, followed by the end of discharge drought on 13 December. Groundwater drought ended 21 December.

Onset second part
From 25 December temperatures were below zero again, but because of the low precipitation (precipitation drought started 10 December) only a below average snow cover developed. Soil moisture was below the threshold from 27 December. Also a discharge drought (starting from 30 December) and a groundwater drought (starting from 4 January) developed. Values dropped below the threshold because the threshold was rising according to 'normal' situations (because of expected snowmelt and precipitation).

The value of soil moisture stayed the same during below zero temperatures (but below the threshold because the threshold was going up). When temperatures rose above zero again (20 January to 10 February) soil moisture went down because of evapotranspiration (Figure 6.2) (the only way out from the soil routine is by evapotranspiration, Section 3.1.2). In this winter drought, evapotranspiration enhanced the soil moisture drought.

Table 6.3. Actual and mean (1973-2006) observed snow days, air temperature, sum of evapotranspiration and recharge sum for November 1989 to April 1990

	Snow days [d]		Temperature [oC]		Act. ET [mm]		Recharge [mm]	
	act.	mean	act.	mean	act.	mean	act.	mean
November	8	5	1.4	2.4	23.1	30.0	7.1	21.0
December	17	16	-1.0	-1.6	22.5	15.6	18.5	24.4
January	11	23	-1.5	-2.8	23.3	10.1	6.1	26.3
February	8	18	2.6	-1.4	37.5	13.8	20.6	35.5
March	4	7	6.0	2.5	67.3	38.6	15.8	77.4
April	0	1	6.8	7.5	54.7	69.4	19.8	46.6

End of second part
Discharge drought ended 20 February because of a combination of precipitation and some snowmelt. Groundwater drought ended 13 March, but after a few days a new groundwater drought developed (20 March – 25 May). Soil moisture drought ended 21 April. In the summer of 1990 new droughts developed because of a below average precipitation in July and August.

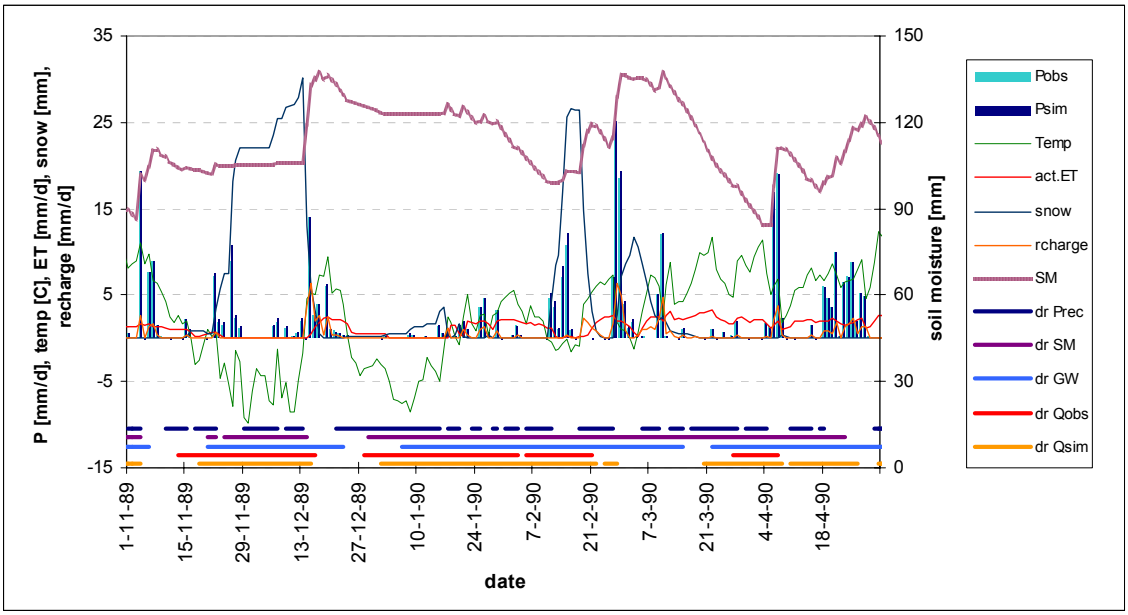

Figure 6.2 Precipitation, temperature, actual evapotranspiration, snow water equivalent, recharge and soil moisture for November 1989 to April 1990. Below the zero-line the drought periods (*dr*) are displayed: a line is visible if the value is below the threshold.

Table 6.4 Droughts in 1989-1990 (only droughts with duration > 10 days between 1-10-1989 and 31-05-1990 are listed)

Drought in	Onset date	End date	Duration	Deficit	Intensity
Psim	15-10-1989	29-10-1989	15	-	-
	10-12-1989	27-01-1990	49	-	-
SM	21-10-1989	2-11-1989	13	-	-
	22-11-1989	12-12-1989	21	-	-
	27-12-1989	21-04-1990	116	-	-
GW	20-10-1989	4-11-1989	16	-	-
	18-11-1989	21-12-1989	34	-	-
	4-01-1990	13-03-1990	69	-	-
	20-03-1990	25-05-1990	67	-	-
Qsim	18-10-1989	2-11-1989	16	0.47	0.03
	16-11-1989	13-12-1989	28	1.93	0.07
	30-12-1989	20-02-1990	53	5.14	0.10
	18-03-1990	6-04-1990	20	3.94	0.20
	8-04-1990	24-04-1990	17	4.02	0.24
	29-04-1990	13-05-1990	15	1.63	0.11
Qobs	10-10-1989	22-10-1989	13	0.38	0.03
	11-11-1989	14-12-1989	34	3.69	0.11
	26-12-1989	1-02-1990	38	6.92	0.18
	3-02-1990	19-02-1990	17	1.33	0.08
	25-03-1990	5-04-1990	12	1.72	0.14

6.3.2 The 2001-2002 drought

A below average December temperature in 2001 (-5.6 °C compared to mean for this month of -1.5 °C) caused an above average snow cover. All days of December were snow days (compared to an average of 16 snow days) (Table 6.6). Almost no recharge occurred in December.

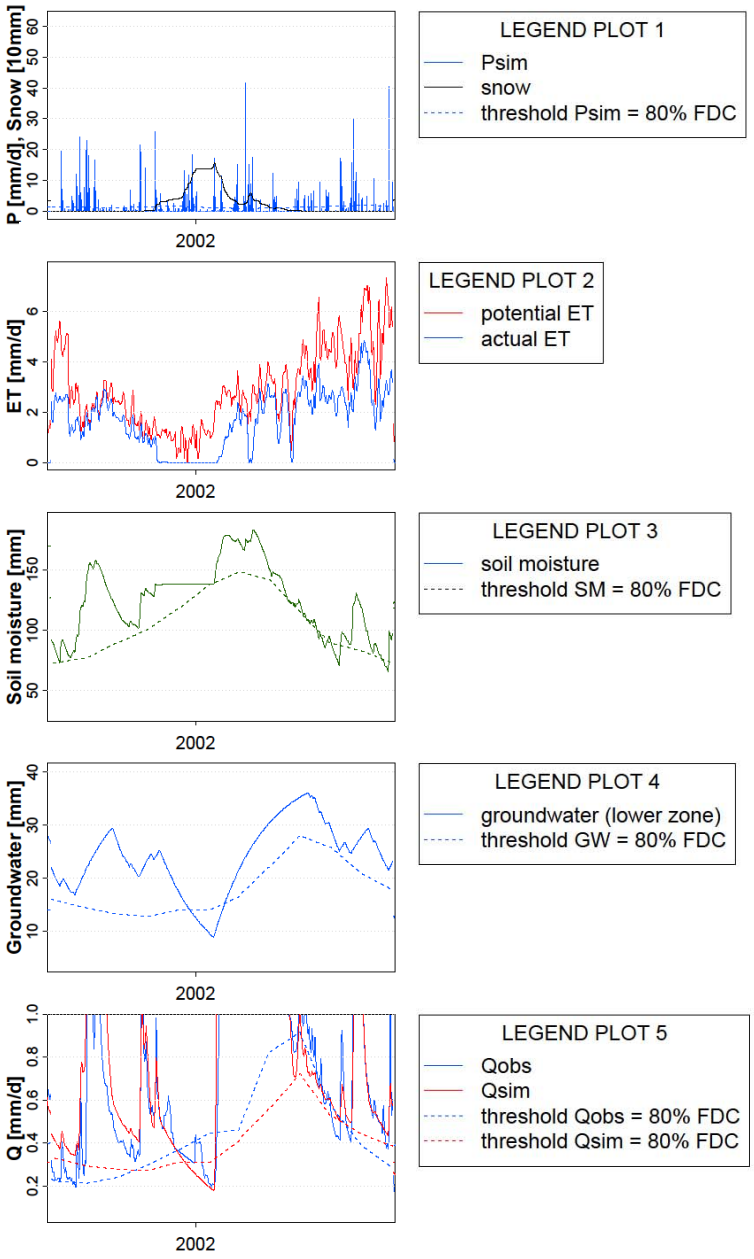

Figure 6.3 The 2001-2002 drought.

Onset of drought

This lack of recharge caused a discharge drought to develop (starting 21 December) (Table 6.5; Figure 6.3 and 6.4). For soil moisture no real drought developed. This is because during the cold period the amount of soil moisture did not change because of the low temperatures (no snowmelt, no evapotranspiration) and because in HBV no flow from soil moisture to groundwater is possible. 26 December a groundwater drought started.

End of drought

The droughts ended January 2002 when temperatures started to rise above zero causing an early snowmelt and above average discharges. The graph shows a sharp increase of discharge, groundwater and soil moisture due to a combination of snowmelt and rain. Discharge drought ended 19 January. 29 January also the groundwater drought ended.

Table 6.5 Droughts in 2001-2002 (only droughts between 1-12-2001 and 28-02-2002 are listed)

	Onset date	End date	No.days	Deficit	Intensity
Psim	6-12-2001	9-12-2001	4	-	-
	11-12-2001	18-12-2001	8	-	-
	3-1-2002	18-1-2002	16	-	-
	22-1-2002	25-01-2002	4	-	-
	29-01-2002	6-02-2002	9	-	-
	14-02-2002	17-02-2002	4	-	-
SM	16-1-2002	18-1-2002	3	-	-
GW	26-12-2001	29-1-2002	35	-	-
Qsim	21-12-2001	19-1-2002	30	2.28	0.08
Qobs	14-12-2001	30-12-2001	17	0.90	0.05
	1-1-2002	21-1-2002	21	3.12	0.15

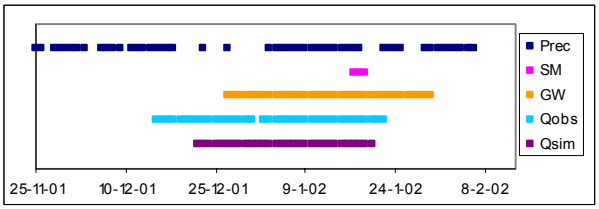

Figure 6.4. The 2001-2002 droughts (line if value is below threshold).

Table 6.6 Actual and mean (1973-2006) observed snow days and mean air temperature [°C] for November 2001 till April 2002

	Snow days		Temperature	
	act.	mean	act.	mean
November	5	5	0.8	2.5
December	31	16	-5.6	-1.5
January	31	23	-2.6	-2.8
February	9	19	2.1	-1.4
March	2	7	4.6	2.5
April	0	1	8.0	7.5

6.3.3 The 2003 drought

With a below average precipitation (680 mm in 2003 against mean annual sum of 870 mm) and a high potential evapotranspiration (1070 mm in 2003 against mean annual sum of 981 mm) 2003 was a year with droughts in all parts of the hydrologic cycle (Table 6.7; Figure 6.7).

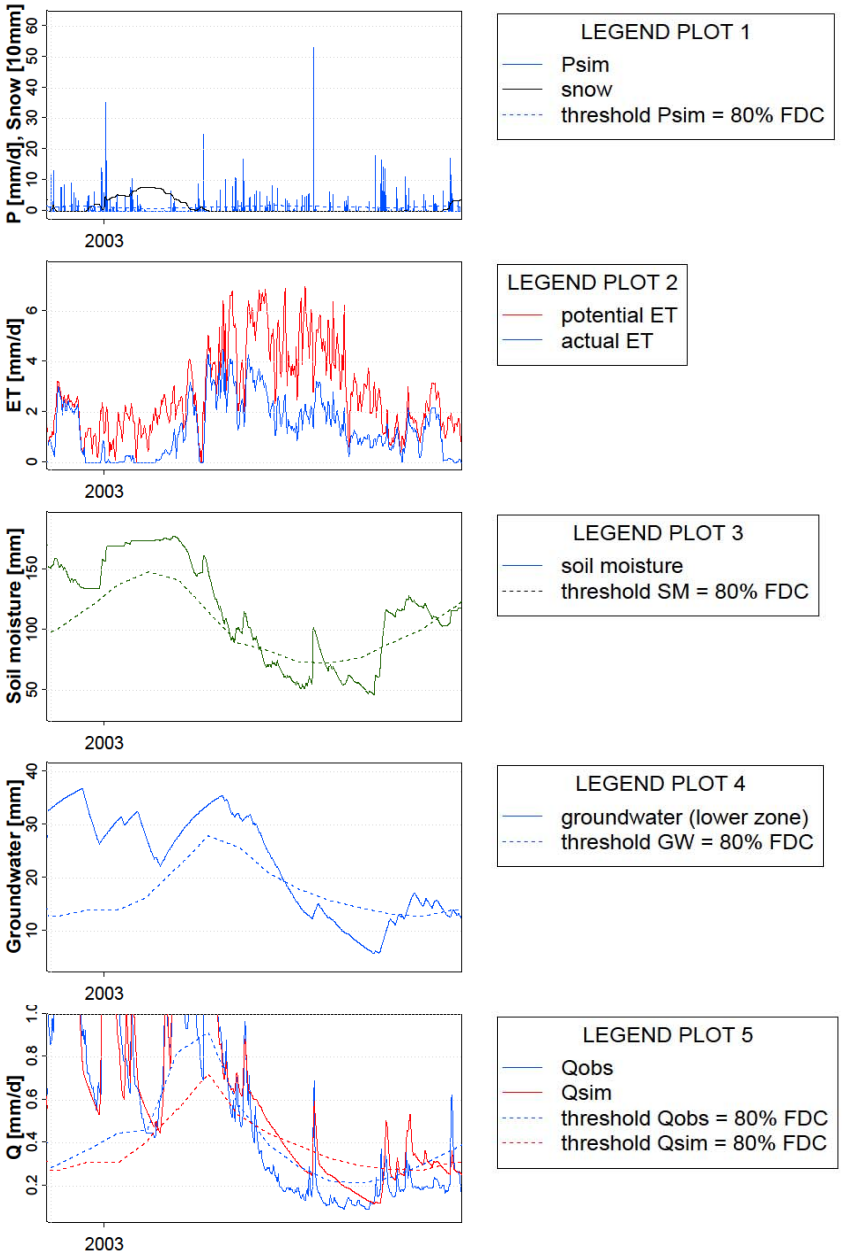

Figure 6.5 The 2003 drought.

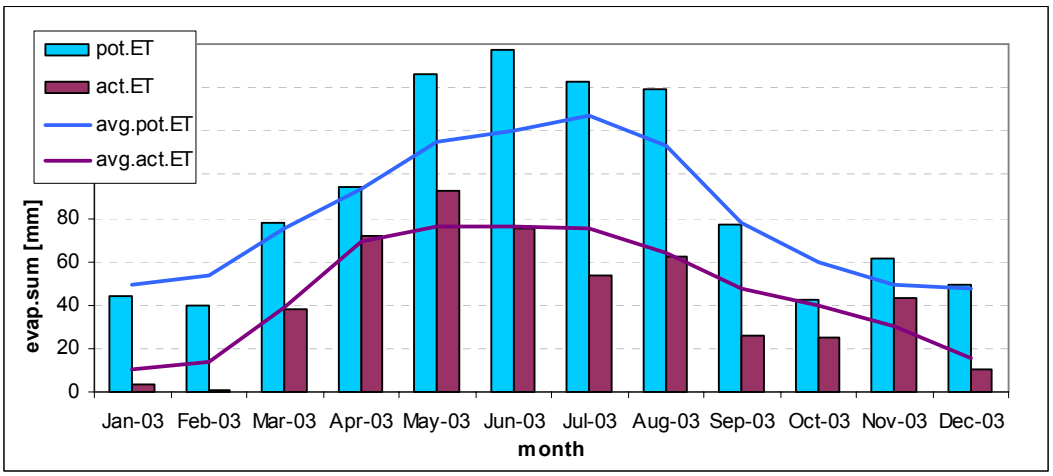

Figure 6.6 Monthly sums for potential and actual evapotranspiration for 2003 compared with the monthly average sums over the period 1974-2006.

Onset of drought

Already in February some low flow due to low precipitation occurred, but because of snowmelt soil moisture and groundwater did not go below the threshold and no extensive drought developed (Figure 6.5). In June droughts in all parts of the hydrological cycle started. The simulated precipitation was below the threshold starting 10 June. 6 June a soil moisture drought developed, followed by a discharge drought (25 June) and a groundwater drought (29 June). From Figure 6.6 it is clear that water availability was not sufficient for actual evapotranspiration to reach its potential value: actual evapotranspiration was already going down starting May, while potential evapotranspiration was still rising (and above average).

At the end of July, a few precipitation events (including a day with 53 mm precipitation) caused soil moisture and discharge to fluctuate around and above the threshold, but shortly after they went below the threshold again for a long period (discharge from 2 August, soil moisture from 9 August).

End of drought

A series of precipitation events at the end of September/beginning of October (October precipitation was above average) ended the soil moisture drought (4 October). Starting from 6 October discharge was above the threshold. The groundwater drought ended 28 October. In November and December 2003 (the new hydrological year) new droughts developed. This droughts were caused by below average precipitation and above average actual evapotranspiration for November.

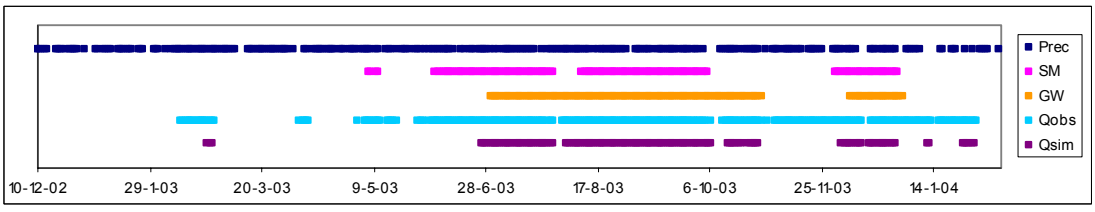

Figure 6.7 The 2003 droughts (line if value is below threshold).

Table 6.7 Droughts in 2003 (only droughts with duration > 10 days are listed)

Drought in	Onset date	End date	Duration	Deficit	Intensity
Psim	11-02-2003	20-03-2003	38	18.55	0.49
	10-06-2003	12-07-2003	33	13.88	0.42
	12-08-2003	18-09-2003	38	20.83	0.55
	12-11-2003	26-11-2003	15	6.77	0.45
SM	6-06-2003	27-07-2003	52	-	-
	9-08-2003	4-10-2003	57	-	-
	30-11-2003	28-12-2003	29	-	-
GW	29-06-2003	28-10-2003	122	-	-
	7-12-2003	30-12-2003	24	-	-
Qsim	25-06-2003	27-07-2003	33	2.31	0.07
	2-08-2003	6-10-2003	66	7.63	0.12
	15-12-2003	27-12-2003	13	0.63	0.05
Qobs	2-06-2003	23-07-2003	52	6.39	0.12
	31-07-2003	28-09-2003	60	5.98	0.10
	3-11-2003	12-12-2003	40	4.84	0.12

6.3.4 Conclusion and discussion

For winter droughts, temperature is an important factor. Below average temperatures can cause a drought to develop, because all precipitation is stored on the surface as snow. No recharge occurs and soil moisture does not change. When temperatures rise in spring, snowmelt starts with above average amounts of water. The high amounts of water stored during the cold period (combined with precipitation in spring) can even cause floods that stop the drought period. On the other hand, above average temperatures in winter cause early snowmelt and less snow. Months, which normally have high discharges because of melting snow from the snowpack, have lower discharges. Additionally, higher temperatures cause above average actual evapotranspiration. Combined with below average precipitation, a drought is likely to develop. Literature mentions below average temperatures or delayed onset of snowmelt as reason for winter drought (Hisdal et al., 2000; Fleig et al., 2006), no literature about winter droughts caused by above average temperatures was found. A winter drought in general ends because of snowmelt. In case of low snow amount, recharge from snowmelt is too low to end the winter drought and the drought continues in summer (and can be enhanced by a precipitation drought in summer). This 'worst-case scenario' is not observed in the time series of the Nedožery catchment.

For summer droughts, the results of this study and literature indicate that both precipitation and evapotranspiration are important factors (Van Lanen et al., 2004). A below average precipitation combined with above average temperatures causes a drought to develop. High evapotranspiration values decrease the soil moisture content. Minor precipitation events can end a soil moisture drought. But, because almost no recharge takes place, the groundwater drought will sustain until a series of precipitation events combined with lower potential evapotranspiration (due to low temperature) takes place.

The importance of both precipitation and temperature in drought development is underlined by literature (Van Lanen et al., 2004). In catchments where precipitation partly falls as snow, deviations from normal temperature determine if a hydrological drought develops. The differences between summer and winter indicated that for the Nedožery catchment summer and winter droughts had to be separated in the analysis. The use of this method is supported by literature (Hisdal et al., 2000; Van Lanen et al., 2004; Fleig et al., 2006).

The difference between observed and simulated discharge makes clear that observed discharge shows more variability and therefore more droughts. The effect of conflicting trends on drought occurrence is not clear and needs more research.

Propagation of drought

Both in winter and summer, droughts caused by below average precipitation and above average evapotranspiration start first in soil moisture, followed by discharge and groundwater. In winter, below average temperatures cause discharge and groundwater drought to start earlier than soil moisture drought.

In case of a winter drought caused by below zero temperatures soil moisture values do not change while the groundwater and discharge go down. However, a soil moisture drought can occur, because soil moisture is expected to rise (the threshold rises: variable threshold). In other cases soil moisture is a component of the hydrological cycle that reacts faster than groundwater. Groundwater droughts start later and persist longer. Because of the high number of minor precipitation droughts it is not easy to link hydrological drought and precipitation drought (which is dependent on *n*-day moving average).

In general the end of drought shows the following pattern: the first drought to end is the soil moisture drought, followed by discharge, and groundwater. Sometimes, the soil moisture drought ends later than the discharge drought (in the 1989-1990 winter drought). Groundwater is anyway the most persistent component of the hydrological cycle. Peters and Van Lanen (2000) confirm the results of this study, stating that in the drought sequence groundwater is the last to react to a drought situation (unless surface water is mainly fed by groundwater) and that groundwater levels recover slowly.

7. Comparison with other hydrological models

At Comenius University in Bratislava, the hydrological models BILAN and FRIER are used to model the Nedožery catchment. This offers the opportunity to intercompare the models and to investigate the conflicting trends in more depth. After a short description of the structure of these two models and the differences with HBV (Section 7.1 and 7.2) the results of all three models are compared (Section 7.3).

7.1 Description of BILAN

The BILAN model is described by Kašpárek and Novický (2004). BILAN simulates the components of the water balance for a catchment. The model is not spatially distributed. Originally, the model was developed with a monthly time step, but currently also a daily time step is possible. Inputs are catchment means for precipitation, air temperature, potential evaporation and relative humidity. It is also possible to let BILAN calculate potential evaporation, for which various methods can be chosen. The model distinguishes between summer and winter conditions. A snow accumulation algorithm (used if $T < 0$) is used in stead of a summer algorithm (used if $T \geq 0$). Total discharge is simulated as the sum of three components: direct runoff, interflow and base flow. Direct runoff is the fast component, which is a result of high intensity rain in summer conditions. It does not affect the soil water balance and is not available for evaporation. This is different in HBV where surface runoff is not included (Section 3.1.2). Interflow results from the water balance as excess water in the unsaturated zone. In winter or snowmelt situations interflow is assumed to include direct runoff. Base flow is the result of outflow from the groundwater storage and is calculated in the same way as in HBV (Section 3.1.2). Evapotranspiration is at its potential level when the amount of precipitation (reduced by direct runoff) is equal to or higher than potential evapotranspiration or if soil moisture storage can supply the deficiency. In winter evapotranspiration is at its potential level if the sum of precipitation and water storage in the snow cover exceeds potential evapotranspiration.
The model has eight parameters. Calibration is done on observed discharge.

Setup
The used evapotranspiration method is the Recomendaci method based on digitized Russian hydro-meteorological tables with input of annual mean temperature, daily temperature and relative humidity (pers. comm. Machlica, 2009). Input data from several stations is used (Table 7.1). Spatial averaging is done using Thiessen polygons.

Table 7.1 Used data in BILAN

	Precipitation	Temperature	Air humidity
Nitrianske Pravno	x		
Chvojnica	x		
Valaská Belá Gápel	x		
Slovenské Pravno	x		
Vrícko	x		
Prievidza	x	x	x

7.2 Description of FRIER

FRIER is a physically based rainfall-runoff model with spatially distributed parameters (Horvát, 2008; pers. comm. Horvát, 2009). Spatial inputs are a digital elevation model, and soil texture and

land use maps of the catchment. Time series of meteorological data can be distributed in space by calculating the mean, using Thiessen polygons, using lapse rate or Kriging.

Meteorological data is needed for the various evaporation calculation methods, which are mainly based on the surface energy balance. Soil texture and land use (including growing season of crops) are also used in the calculation of evapotranspiration. Total actual evapotranspiration is the sum of four parts: evaporation from interception storage, evaporation from depression storage, evapotranspiration from the soil and transpiration from groundwater storage (note that in FRIER flow from groundwater to soil moisture is possible, whereas in HBV and BILAN only downward movement is possible).

Using flow accumulation and a threshold for the starting point of springs, a stream network is generated. Hydraulic parameters of this network are the Manning roughness and the hydraulic radius. Using the digital elevation model, depressions are identified in which infiltration, storage and/or evaporation takes place. The water balance is evaluated at three levels: surface, soil and subsoil. Total discharge (sum of overland flow, interflow and base flow) is the result of the flow response from all grid cells. A degree-day method is used for snow melt and accumulation, but time series of snow cover can also be provided as input.

Outputs of FRIER are time series and spatial maps. The model uses eleven global parameters. Calibration of the model can be done random or step by step. Calibration is done using a quantity comparison with the BIAS model and with a hydrograph using the Nash-Sutcliffe coefficient, in which especially high and low values of discharge are monitored.

Setup
Used evapotranspiration method: Tomlain's method (simplification of Budyko's method) which uses temperature, relative humidity and wind speed.
Method for spatial averaging: Kriging

7.3 Comparison of results

Results from HBV, BILAN, and FRIER were compared for the period 1982-2006. For this comparison HBV was calibrated and ran for the period 1982-2006 (in stead of the period 1974-2006). This resulted in a higher efficiency because of the shorter calibration period. In comparing simulated discharge of the three models with observed discharge, the HBV model simulation has the highest efficiency, both for R_{eff} and $\ln R_{eff}$ (Table 7.2). To see whether BILAN and FRIER show the same trends as HBV discharge and evapotranspiration are discussed in the next sections (Section 7.3.1 and Section 7.3.2).

Table 7.2 Efficiencies for HBV, BILAN and FRIER for the modeling period 1982-2006

	HBV	BILAN	FRIER
R_{eff}	0.7178	0.5265	0.5691
$\ln R_{eff}$	0.7733	0.4911	0.5917

7.3.1 Discharge

Visual inspection of the low flow hydrograph shows flow peaks during recessions are almost not visible in BILAN: recession curves are long and almost without response to precipitation events. Both HBV and FRIER show much more response to precipitation events (Figure 7.1).

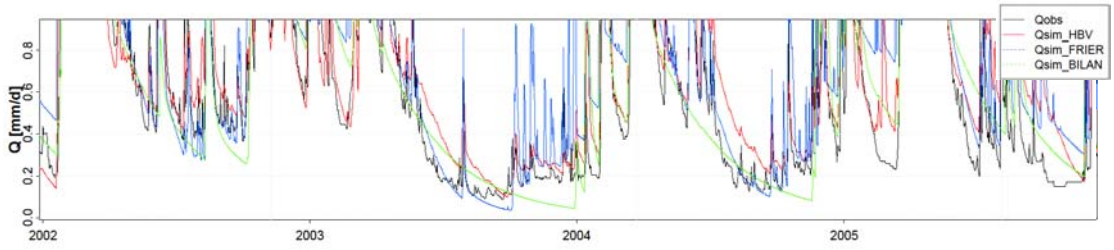

Figure 7.1 Observed and simulated discharge for the three models for the period 2002-2005 (for whole period 1982-2006 see Annex 14).

As in HBV (Section 5.1), FRIER and BILAN are underestimating observed discharge in the first half of the period and overestimating observed discharge in the second half of the period (Figure 7.2). This under- and overestimation can be explained by the occurring tendencies (Annex 15).

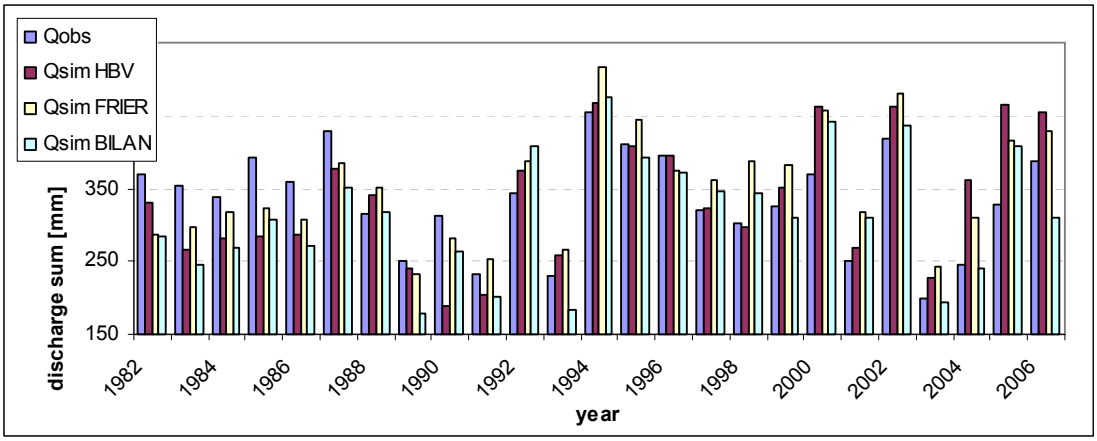

Figure 7.2 Annual discharge sums for three models (HBV, BILAN, FRIER) compared with the observed discharge.

7.3.2 Evapotranspiration

Potential evapotranspiration is much higher in HBV than in the other models. For actual evapotranspiration this is not the case (Annex 15). The difference between HBV and the other models in mean potential evapotranspiration is the result of a higher potential evapotranspiration in winter (Figure 7.3, plot 2).

7.3.3 Drought

The differences between the models have some effect on the simulated droughts (Table 7.3). Observed discharge in BILAN shows less droughts that are longer and have a higher deficit. This difference can not be explained as all models were supposed to have the same input.

The long recession curves with almost no response to precipitation events decrease the number of droughts in the simulated discharge for BILAN, and increase their mean duration and deficit. FRIER has more discharge droughts, which are shorter. This indicates FRIER reacts faster to precipitation events than HBV.

The number of groundwater droughts in HBV is higher than in BILAN and FRIER. This indicates that the groundwater system in BILAN and FRIER reacts slower than that in HBV. For soil moisture, FRIER has the highest number of droughts while HBV and BILAN show similar results.

This indicates that the soil moisture component in FRIER reacts faster than that in the two other models.

Table 7.3 Drought characteristics for the three models (1982-2006)[*1]

		Total number	Mean no.days	Mean deficit
Prec	HBV	112	15.46	6.71
	BILAN	118	14.81	6.12
	FRIER	116	14.57	5.97
SM	HBV	85	20.92	
	BILAN	79	20.85	
	FRIER	118	14.53	
GW	HBV	63	27.62	
	BILAN	41	45.37	
	FRIER	45	38.91	
Qsim	HBV	104	16.75	1.33
	BILAN	53	34.53	2.97
	FRIER	125	13.88	1.20
Qobs	HBV	166	10.38	0.84
	BILAN[*2]	155	11.30	0.95
	FRIER	166	10.38	0.84

[*1] The thresholds are calculated for each model separately.

[*2] Actually, there should be no differences between the models for observed discharge.

The 2003 drought

A closer look at 2003 gives insight in the differences between the models in drought propagation. All three models simulate droughts in this year (Figure 7.3; Table 7.4), but in some parts of the hydrological cycle the occurrence of drought differs.

For soil moisture FRIER is the first model to show a drought, soon followed by BILAN and HBV (Figure 7.3). In BILAN, the soil moisture drought is much longer than in HBV and FRIER. For both groundwater and discharge, BILAN is the first model to develop a drought. HBV is the last model to show a drought in groundwater and discharge. For the end of droughts in soil moisture, discharge and groundwater HBV and FRIER show almost no difference. The droughts in BILAN continue much longer compared to HBV and FRIER.

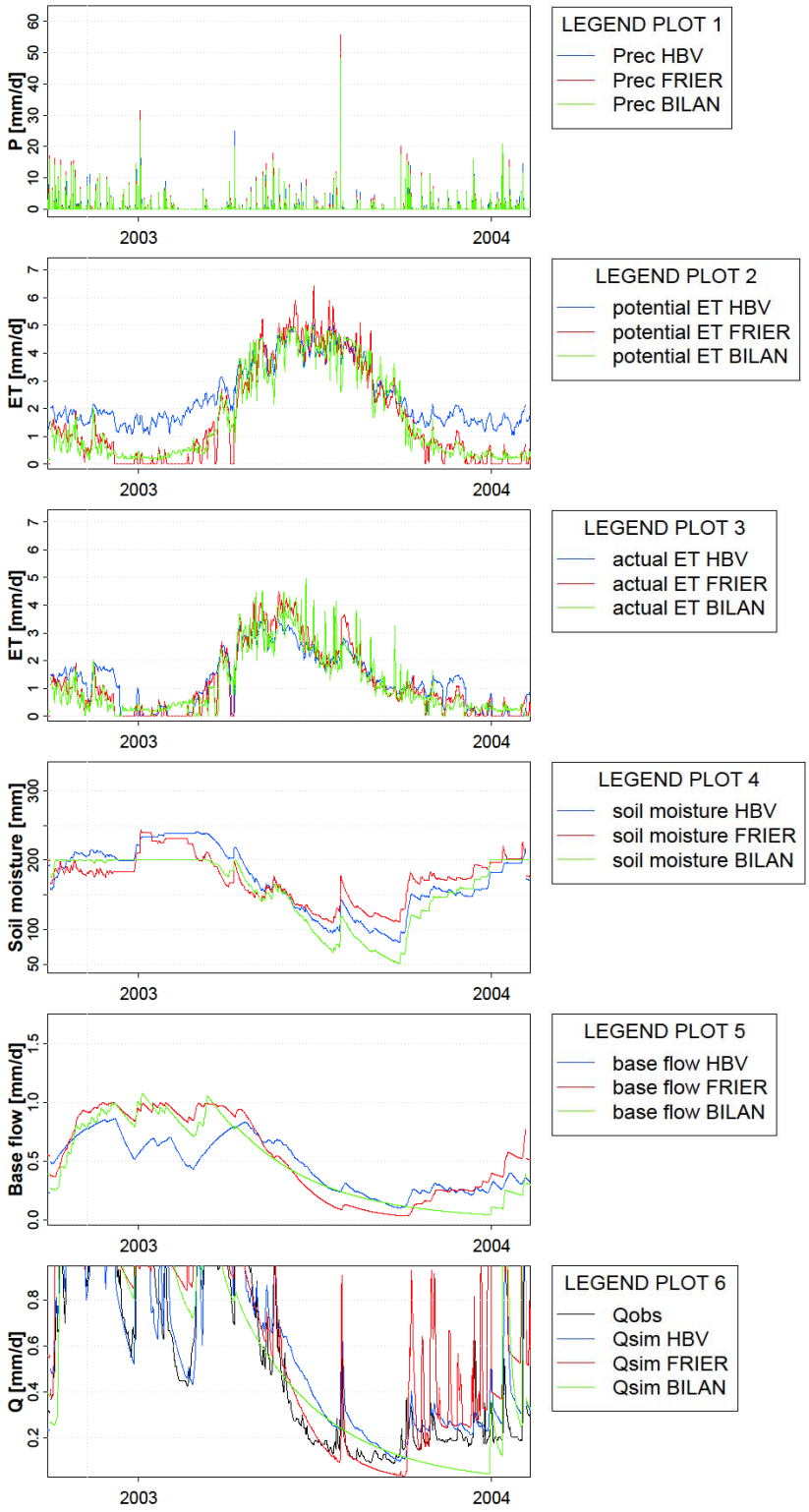

Figure 7.3 The 2003 drought for the three models.

In all parts of the hydrological cycle BILAN shows longer droughts (drought continues into a winter drought) (Figure 7.4). This indicates BILAN is the slowest reacting model.

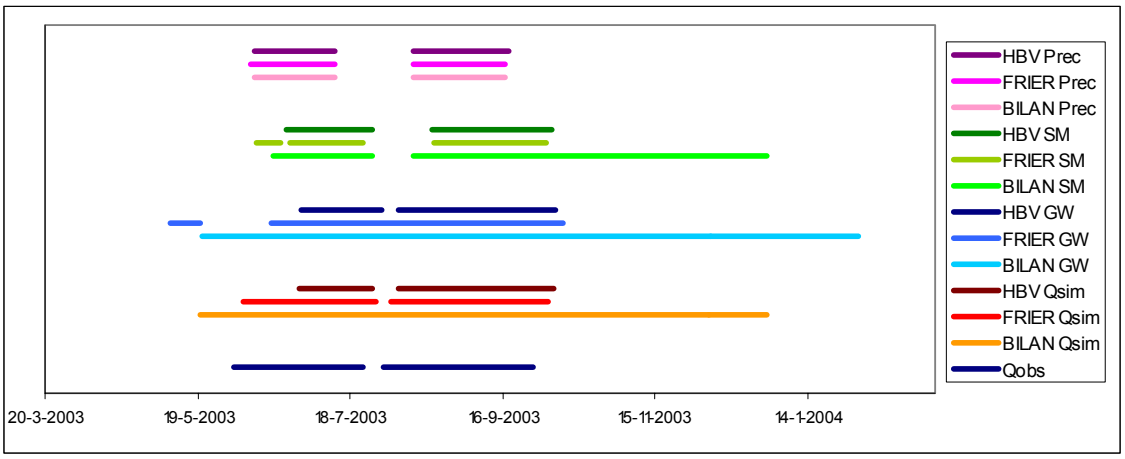

Figure 7.4 The 2003 droughts for the three models (line if value is below threshold).

Table 7.4 Droughts in 2003 (only droughts with duration > 10 days between 01-05-2003 and 31-09-2003 are listed) (based on a monthly 80% threshold for the modeling period 1982-2006)

Drought in	Model	Onset date	End date	Duration	Deficit	Intensity
Prec	HBV	10-06-2003	12-07-2003	33	11.87	0.36
		12-08-2003	18-09-2003	38	15.44	0.41
	FRIER	9-06-2003	12-07-2003	34	15.78	0.46
		12-08-2003	17-09-2003	37	22.09	0.60
	BILAN	10-06-2003	12-07-2003	33	12.72	0.39
		12-08-2003	17-09-2003	37	22.26	0.60
SM	HBV	23-06-2003	27-07-2003	35		
		19-08-2003	5-10-2003	48		
	FRIER	11-06-2003	21-06-2003	11		
		24-06-2003	23-07-2003	30		
		20-08-2003	3-10-2003	45		
	BILAN	18-06-2003	27-07-2003	40		
		12-08-2003	29-12-2003	140		
GW	HBV	29-06-2003	30-07-2003	32		
		6-08-2003	7-10-2003	63		
	FRIER	8-05-2003	20-05-2003	13		
		17-06-2003	10-10-2003	116		
	BILAN	21-05-2003	3-02-2004	259		
Qsim	HBV	28-06-2003	27-07-2003	30	1.76	0.06
		6-08-2003	6-10-2003	62	3.53	0.06
	FRIER	6-06-2003	28-07-2003	53	2.73	0.05
		3-08-2003	4-10-2003	63	2.93	0.05
	BILAN	20-05-2003	29-12-2003	224	10.95	0.05
Qobs		2-06-2003	23-07-2003	52	4.57	0.09
		31-07-2003	28-09-2003	60	5.03	0.08

Drought propagation in 2003

In FRIER, soil moisture and discharge drought start earlier than groundwater drought. The groundwater drought is the most persistent drought. In BILAN, groundwater and discharge drought start before the precipitation drought. Both groundwater and discharge drought are not above the threshold until the end of December (discharge) and the beginning of February (groundwater). The persistence of droughts in BILAN is caused by the slow response the model has to precipitation.

8. Conclusions and discussion

- An underestimation of observed discharge in the first half of the modeling period and an overestimation in the second half are the result of 'conflicting' trends (observed discharge has a downward trend and simulated discharge shows an upward trend) (Section 5.4). Observed precipitation shows an upward trend and the annual number of snow days increases. Potential and actual evapotranspiration show an upward trend (Section 4.3), but this trend is not sufficient to compensate for the increased precipitation. A closer look at separate months shows that upward trends in simulated discharge in the winter months due to snow melt correspond to upward trends in snow cover. Discharge in the summer months shows no clear pattern. FRIER and BILAN are also underestimating discharge in the first half of the modeling period and overestimating discharge in the second half (Section 7.3) thereby supporting the HBV results.

- The use of groundwater data for calibration does improve the modeling efficiency (R_{eff}), but not the modeling of low flows (lnR_{eff}). A drawback of the current HBV light structure is that it is not possible to calibrate on both lnR_{eff} and groundwater (Section 5.1). When calibrating the model against discharge and groundwater simultaneously, Seibert (2000) found the same poor fit for low flows.

- The three different catchment zonation variants (based on land use, soil texture, or geology) did not give different calibration results (Section 5.1.2). This indicates either that land use, soil texture, and geology in the catchment are correlated, or that the percentages of the classes in each elevation zone do not differ that much (only percentages are used, no additional data about characteristics of the soil). It is also possible that zonation in this study has no influence on the modeling at all.

- Some parameters could vary without effects on modeling efficiency. This corresponds with Seibert (1999) who found that "almost equally good simulations can be obtained at very different locations in the parameter space" (equifinality (Beven, 2001)). Parameters that define the lower groundwater box have the most significant effect on modeling efficiency (Section 5.2).

- Not only precipitation, but also temperature is important for the hydrological regime of the Nedožery catchment. Highest discharges occur during snowmelt, lowest discharges occur in late summer/autumn (Section 5.3). This corresponds to a snow affected humid climate (Van Lanen et al., 2004), in which streamflow generation is dependent on both temperature and precipitation. Around zero temperatures in winter cause soil moisture to rise because of incidental snow melt on some days in that period.

- Both this study and the literature (Section 6.3.4) support that it is important to distinguish between winter and summer droughts because of their different characteristics. Hydrological droughts (both winter and summer) in Nedožery develop due to above average temperatures combined with below average precipitation. In winter, this leads to a below average snow cover (resulting in low spring discharges) and the occurrence of relatively high evapotranspiration. In winter hydrological drought can also be caused by below average temperatures, because water is stored on the surface as snow. Such a winter drought will not continue into summer, because it ends by above average snowmelt in spring (Section 6.3).

The differences between a winter drought caused by higher and lower temperatures are also mentioned by Van Lanen et al. (2004), who state that late snowmelt (due to low temperatures) might lead to drought in the period preceding the melt because no recharge occurs.

- In case of a drought caused by below average precipitation and above average evapotranspiration (both in summer and winter), drought in Nedožery starts in soil moisture and discharge with only a few days difference. Groundwater is the slowest component of the hydrological cycle and therefore, a drought in groundwater starts a week or more after the start of discharge drought. In case of a drought caused by below average temperatures in winter, discharge and groundwater drought occur before a soil moisture drought. Precipitation shows a lot of minor droughts, which makes it not easy to link hydrological droughts to precipitation droughts. In general, a drought ends first in soil moisture and discharge. Groundwater droughts are the most persistent droughts (Section 6.3).

- In comparing the models BILAN and FRIER, HBV has the highest modeling efficiency. But visual inspection on the whole time series is not done. BILAN gives long recession curves and shows almost no response to precipitation. Potential evapotranspiration in winter is much higher in HBV than in the other models. For actual evapotranspiration this is not the case. Drought analysis on the outputs of the BILAN model gives less but longer droughts because of the slow reaction of the model in all parts of the hydrological cycle. FRIER outputs show more but shorter droughts which indicates FRIER reacts faster on precipitation than HBV and BILAN (Section 7.3).

9. Recommendations

HBV modeling

- The differences in the Nedožery catchment (Section 2.1.6) indicate that the modeling of the catchment might need more spatial detail. HBV results for the Nedožery catchment give a lumped outcome, but in reality there are differences in drought occurrence between the faster and the slower reacting sub-catchments of the Nedožery catchment. For adequate drought analysis a more detailed study and modeling of the three headwater catchments is needed (which is possible because three sub-catchments are gauged). The spatial distributed hydrological model FRIER can give more insight in the differences in drought occurrence in the sub-catchments.
- Calibration on groundwater data is possible in HBV *light*, but not in combination with calibration on the logarithm of the discharge (Section 5.1.1). A further extension of the model is required.

Data

- Further research on trends in all water balance components is needed (Section 4.3) because no decisive answer was found in literature, at Comenius University or the Slovak Hydro Meteorological Institute. More knowledge is needed about (the influence of) possible, historical land use changes and/or groundwater extractions.
- Further research on the history of the gauging stations is needed, because some of them have moved during the time of measurement and gauging methods have changed.

Drought analysis

- Further research on the effect of conflicting trends on drought occurrence is needed.
- The choice of a threshold value becomes more useful if it is based on needs of the stakeholders in the catchment. This can, for example, be ecological minimum flow or agricultural needs.
- Some kind of pooling is needed to couple dependent droughts and to remove minor droughts and peaks. For example a minimal duration for the inter-event time can be set. The coupling of dependent droughts can also be done by doing drought analysis on the moving average, which smooths the time series and thereby removes minor peaks (Tallaksen et al., 1997; Hisdal et al., 2000).
- The events defined with a variable threshold should not be called a 'drought' but streamflow deficiency or streamflow anomaly, because periods with a relatively low flow during the high flow season or due to a delayed onset of snowmelt are no real 'drought' (Hisdal et al., 2000). In this catchment, a difference can be made between winter/spring (snowmelt) in which high flows are expected and summer in which low flows are expected (Section 5.3; Tallaksen and Van Lanen, 2004a).

Comparison models

- The comparison of the three models is done with thresholds which are calculated for each model separately (Section 7.3). The use of the same set of thresholds (for example from observed discharge, or ecological minimum flow) for each model will change the results and might be a better way of intercomparing.

Literature

ALLEN, R.G., PEREIRA, L.S., RAES, D., SMITH, M., 1998, Crop evapotranspiration, guidelines for computing crop water requirements, *FAO Irrigation and Drainage paper*, no. 56, Rome, pp. 174.

BATES, B.C., KUNDZEWICZ, Z.W., WU, S., PALUTIKOF, J.P. (eds.), 2008, Climate Change and Water, *Technical Paper of the Intergovernmental Panel on Climate Change*, IPCC Secretariat, Geneva, pp. 210.

BERGSTRÖM, S., FORSMAN, A., 1973, Development of a conceptual deterministic rainfall-runoff model, Swedish Meteorological and Hydrological Institute, Stockholm, *Nordic Hydrology*, 4, pp. 147-170.

BEVEN, K.J., 2001, *Rainfall-Runoff Modelling : The Primer*, Wiley, Chichester, England, pp. 234-246.

BLAŠKOVIČOVÁ, L., pers. comm., 2009, Slovak Hydro Meteorological Institute (SHMU)

DAS, T., BÁRDOSSY, A., ZEHE, E., HE, Y., 2008, Comparison of conceptual model performance using different representations of spatial variability, *Journal of Hydrology*, 356, pp. 106-118.

DEMUTH, S., STAHL, K., 2002, Climate variability and drought, *Wasser und Bodem*, 54, 10, pp. 36-40.

DOORENBOS, J., PRUITT, W.O., 1975, Guidelines for predicting crop water requirements, *FAO irrigation and drainage paper*, no. 24, Rome.

FLEIG, A.K., TALLAKSEN, L.M., HISDAL, H., DEMUTH, S., 2006, A global evaluation of streamflow drought characteristics, *Hydrol.Earth Syst. Sci*, 10, pp. 535-552.

Geological Map of Slovakia, 1996, Ministry of the environment of Slovak republic, geological survey of Slovak republic, Bratislava.

HISDAL, H., TALLAKSEN, L.M., STAHL, K., ZAIDMAN, M., DEMUTH, S., GUSTARD, A., 2000, Hydrological drought – streamflow. In: Hisdal, H., Tallaksen, L.M. (eds.), 2000, *Drought event definition*, Assessment of the Regional Impact of Droughts in Europe, ARIDE Technical Report, No. 6, pp. 8-15.

HISDAL, H., STAHL, K., TALLAKSEN, L.M., DEMUTH, S., 2001, Have streamflow droughts in Europe become more severe or frequent?, *Int. J. Climatology*, 21, pp. 317-333.

HISDAL, H., TALLAKSEN, L.M., CLAUSEN, B., PETERS, E., GUSTARD, A., 2004, Hydrological drought characteristics, In: Tallaksen, L.M., Van Lanen, H.A.J. (eds.), 2004a, *Hydrological drought: Processes and Estimation Methods for Streamflow and Groundwater*, Developments in Water Science, 48, Elsevier Science BV, The Netherlands, pp. 139-198.

HOHENRAINER, J., 2008, *Propagation of drought through the hydrological cycle in two different climatic regions*, MSc thesis, Institut für Hydrologie der Albert-Ludwigs-Universität Freiburg, Germany.

HORVÁT, O., 2008, Description of the rainfall-runoff model FRIER, *Podzemná Voda XIV 1.*

HORVÁT, O., pers. comm., 2009, Department of Land and Water Resources Management, Faculty of Civil Engineering, Slovak University of Technology, Bratislava, Slovak Republic.

KABAT, P., SCHULZE, R.E., HELLMUTH, M.E., VERAART, J.A., 2002, *Coping with impact of climate variability and climate change in water management: a scoping paper*, DWC-Report no.

DWCSSO-01(2002), International Secretariat of the Dialogue on Water and Climate, Wageningen, the Netherlands

KAŠPÁREK, L., NOVICKÝ, O., 2004, Background information BILAN, available on CD as attachment to: Tallaksen, L.M., Van Lanen, H.A.J. (eds.), 2004a, *Hydrological drought: Processes and Estimation Methods for Streamflow and Groundwater*, Developments in Water Science, 48, Elsevier Science BV, The Netherlands.

KUNDZEWICZ, Z.W., MATA, L.J., ARNELL, N.W., DÖLL, P., KABAT, P., JIMÉNEZ, B., MILLER, K.A., OKI, T., SEN, Z., SHIKLOMANOV, I.A., 2007, Freshwater resources and their management, *Climate Change 2007: Impacts, Adaptation and Vulnerability. Contribution of Working Group II to the Fourth Assessment Report of the Intergovernmental Panel on Climate Change,* Cambridge University Press, Cambridge, UK, pp. 173-210.

MACHLICA, A., STOJKOVOVÁ, M., 2008, Groundwater drought in different geological conditions, *IOP Conf. Series: Earth and Environmental Science*, 4, pp. 9.

MACHLICA, A., pers. comm., 2009, Department of Hydrogeology, Faculty of Natural Sciences, Comenius University, Bratislava, Slovak Republic.

MEEHL, G.A., STOCKER, T.F., COLLINS, W.D., FRIEDLINGSTEIN, P., GAYE, A.T., GREGORY, J.M., KITOH, A., KNUTTI, R., MURPHY, J.M., NODA, A., RAPER, S.C.B., WATTERSON, I.G., WEAVER, A.J., ZHAO, Z.-C., 2007, Global Climate Projections, *Climate Change 2007: The Physical Science Basis. Contribution of Working Group I to the Fourth Assessment Report of the Intergovernmental Panel on Climate Change*, Cambridge University Press, Cambridge, United Kingdom and New York, NY, USA.

PETERS, L, VAN LANEN, H.A.J., 2000, Hydrological drought – groundwater. In: Hisdal, H., Tallaksen, L.M. (eds.), 2000, *Drought event definition*, Assessment of the Regional Impact of Droughts in Europe, ARIDE Technical Report, No. 6, pp. 15-17.

SEALTHUN, N.R., 1996, *The 'Nordic' HBV model*, Norwegian Water Resources and Energy Administration, Oslo, Norway, pp. 26.

SEIBERT, J., 2000, Multi-criteria calibration of a conceptual runoff model using a genetic algorithm, *Hydrology and Earth System Sciences*, 4, 2, pp. 215-224.

SEIBERT, J., 2005, *HBV light version 2, User's Manual*, Uppsala University, Institute of Earth Sciences, Department of Hydrology, Uppsala, Sweden.

STAHL, K., 2001, *Hydrological drought – a study across Europe*, PhD Thesis, Albert-Ludwigs-Universität Freiburg, Freiburger Schriften zur Hydrologie, 15, pp. 129.

STAHL, K., HISDAL, H., TALLAKSEN, L.M., LANEN, H.A.J. VAN, HANNAFORD, J., SAUQUET, E., 2008, *Trends in low flows and streamflow droughts across Europe*, UNESCO, Paris.

TALLAKSEN, L.M., MADSEN, H., CLAUSEN, B., 1997, On the definition and modelling of streamflow drought duration and deficit volume, *Hydrological Sciences*, 42 (1), pp. 15-33.

TALLAKSEN, L.M., VAN LANEN, H.A.J. (eds.), 2004a, *Hydrological drought: Processes and Estimation Methods for Streamflow and Groundwater*, Developments in Water Science, 48, Elsevier Science BV, The Netherlands.

TALLAKSEN, L.M., VAN LANEN, H.A.J., 2004b, Introduction, In: Tallaksen, L.M., Van Lanen, H.A.J. (eds.), 2004a, *Hydrological drought: Processes and Estimation Methods for Streamflow and Groundwater*, Developments in Water Science, 48, Elsevier Science BV, The Netherlands, pp. 3-17.

UNDP, 2006, *Summary Human Development Report, Beyond scarcity: power, poverty and the global water cycle*, Palgrave Macmillam, New York, USA.

VAN LANEN, H.A.J., FENDEKOVÁ, M., KUPCZYK, E., KASPRZYK, A., POKOJSKI, W., 2004, Flow generating processes. In: Tallaksen, L.M., Van Lanen, H.A.J. (eds.), 2004a, *Hydrological drought: Processes and Estimation Methods for Streamflow and Groundwater*, Developments in Water Science, 48, Elsevier Science BV, The Netherlands, pp. 139-198.

VAN LANEN, H.A.J., 2006, Drought propagation through the hydrological cycle, Climate variability and Science – Hydrological impacts, Proceedings of the Fifth FRIEND World Conference, Havana, Cuba, IAHS Publ. 308.

VAN LOON, A.F., 2008, *Towards a generic model for the propagation of drought through the terrestrial part of the hydrologic cycle*, PhD project proposal, Wageningen University, Department of Environmental Sciences, Hydrology and Quantitative Water Management Group, Wageningen, the Netherlands.

VAN LOON, A.F., pers. comm., 2009, Hydrology and Quantitative Water Management Chair Group, Wageningen University, the Netherlands.

WILHITE, D.A., SVOBODA, M.D., HAYES, M.J., 2007, Understanding the complex impacts of drought: A key to enhancing drought mitigation and preparedness, *Water Resource Management*, 21, pp. 763–774.

YEVJEVICH, V., 1967, An objective approach to definition and investigation of continental hydrologic droughts, *Hydrology Papers 23*, Colarado State University, Fort Collins, USA.

Internet

eu-watch.org, site of the European WATCH project, last visited 30-05-2009.

maps.google.com, site with online maps from the whole world, last visited 30-05-2009.

r-project.org, site of the R project for statistical computing, last visited 30-05-2009.

Annexes

Annex 1 Description of measurements carried out during the fieldtrip

During the fieldtrip in the snowmelt period at the end of March (30-03-2009 to 1-04-2009) some measurements in the different streams were done which reflect the nature of the different sub catchments in the Nedožery catchment (Table 2.1, Figure A.1).

Chvojnica

The Chvojnica river mainly flows through crystalline rocks, with a minor contribution from Mesozoic rocks. A number of tributaries had measured conductivities between 73 and 82 μS/cm indicating the crystalline nature of their catchment. One tributary had a conductivity of 228 μS/cm indicating some influence of Mesozoic rocks. The final value of 190 μS/cm at the gauging station indicates the mainly crystalline nature of the Chvojnica sub catchment (Table A.1).

Tužina

The upper part of Tužina catchment consists of Mesozoic rocks. This is reflected in the conductivity of two tributaries: 351 μS/cm (western stream) and 372 μS/cm (eastern stream). Measurements in a tributary in the crystalline part of the Tužina catchment showed a conductivity of 205 μS/cm. Finally, at the gauging station a value of 283 μS/cm was measured for the Tužina river (Table A.1).

Kl'ačno

The Kl'ačno catchment is situated mainly in Mesozoic rocks, which is reflected in the conductivity. Two springs in the upstream part of Kl'ačno showed high conductivity values (Pramen Nitra: 336 μS/cm; Kamena Dolina: 343 μS/cm). The value at the gauging station was 305 μS/cm. In the upper part of the Kl'ačno catchment there are some northward dipping Mesozoic layers. This means there is a possible loss of water towards the river Rajčanka in the north which flows into the river Váh. Because of the small area concerned and the relatively low contribution of the Kl'ačno sub-catchment to the river flow at Nedožery this loss is assumed to be negligible (Table A.1).

Table A.1 Measured conductivity and temperature at gauging stations during snowmelt (31-03-2009), mean yearly discharge (based on period 1973-2006) and the catchment area

Profile	EC [μS/cm]	T [^{o}C]	Mean discharge [m^3/s]	Catchment area [km^2]
Chvojnica	190	6.4	0.25	17.8
Tužina	283	6.6	0.51	35.6
Kl'ačno	305	5.7	0.20	10.5
Nedožery	273	7.8	2.08	181.6

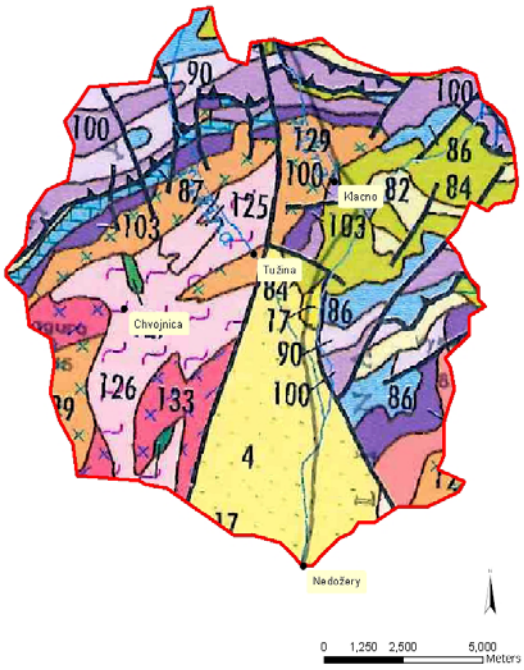

Legend

Neogene
4. Variegated kaolinite clays, sands, gravels, rare lignite seams
17. Siltstones, claystones, sandstones, tuffites, variegated and coal clays, coal, conglomerates
Mesozoic of the Inner Carpathians
82. Sandstones, marlstones, shales: flysch
84. Bedded clayey limestones, marlstones and breccias
86. Sandy and spotted limestones
87. Sandy and crinoidal limestones
90. Variegated shales, sandstones and dolomites
100. Dark limestones and dolomites
103. Quartzites, sandstones and shales
Early Paleozoic – Proterozoic ?
125. Biotite and two-mica plagioclase paragneisses, migmatitic paragneisses
126. Banded gneisses, augengneisses and migmatites
127. Amphibolites, local amphibole gneisses
Magmatic rocks
129. Leucocrate granitic rocks
133. Hybrid granodiorites to tonalites passing locally into migmatites

Figure A.1 Detailed geological map of the Nedožery catchment (derived from the Geological Map of Slovakia, 1996).

Annex 2 Data availability (stations, length time series), altitude and used Thiessen factors

		Station	Altitude m a.s.l.	Length time series	Thiessen factor
Precipitation	mm	Nitrianske Pravno	351	01-01-1981 to 31-12-2007	0.39
		Chvojnica	435	01-01-1981 to 31-12-2007	0.32
		Vricko	603	01-01-1981 to 31-12-2007	0.14
		Valaská Belá - Gapel	490	01-02-1981 to 31-12-2007	0.12
		Slovenské Pravno	500	01-01-1981 to 31-12-2007	0.03
		Prievidza	260	01-07-1972 to 31-12-2007	0
		Bojnice	325	01-01-1961 to 31-12-1972	0
		Kláštor pod Znievom	480	01-11-1961 to 31-10-1998	0
		Nitrianske Rudno	312	01-01-1981 to 31-12-2007	0
		Zliechov	598	01-01-1981 to 31-12-2007	0
Air temperature	°C	Prievidza	260	01-07-1972 to 31-12-2007	0.63
		Turcianske Teplice	510	01-04-1990 to 31-12-2007	0.37
		Banska Bystrica	427	01-01-1984 to 31-12-2002	0
		Banska Stiavnica	575	01-01-1961 to 31-12-2004	0
		Kremnicke Bane	758	01-01-1987 to 31-12-2007	0
		Krizna	1570	01-11-1963 to 31-12-2000	0
		Lom nad Rimavicou	1018	01-06-1961 to 31-12-2002	0
		Topolcany	192	01-01-1961 to 31-12-2007	0
		Trencianske Teplice	306	01-01-1992 to 31-12-2007	0
		Trencin - Biskupice	209	01-01-1961 to 31-03-2006	0
Min Temperature	°C	Trencianske Teplice	306	01-01-1992 to 31-12-2007	0.53
		Krizna	1570	01-11-1963 to 31-12-2002	0.47
		Banska Bystrica	427	01-01-1984 to 31-01-2001	0
		Banska Stiavnica	575	01-01-1961 to 31-12-2004	0
		Lom nad Rimavicou	1018	01-07-1961 to 31-12-2002	0
		Topolcany	192	01-01-1961 to 31-12-2007	0
		Trencin - Biskupice	209	01-01-1961 to 31-03-2006	0
Max temperature	°C	Trencianske Teplice	306	01-01-1992 to 31-12-2007	0.53
		Krizna	1570	01-11-1963 to 31-12-2002	0.47
		Banska Bystrica	427	01-01-1984 to 31-01-2001	0
		Banska Stiavnica	575	01-01-1961 to 31-12-2004	0
		Lom nad Rimavicou	1018	01-06-1961 to 31-12-2002	0
		Topolcany	192	01-01-1961 to 31-12-2007	0
		Trencin - Biskupice	209	01-01-1961 to 31-03-2006	0
Windspeed	m/s	Prievidza	260	01-07-1972 to 31-12-2007	0.63
		Turcianske Teplice	510	01-04-1990 to 31-12-2007	0.37
		Banska Stiavnica	575	01-01-1961 to 31-12-2004	0
		Kremnicke Bane	758	01-01-1987 to 31-12-2007	0
		Krizna	1570	01-04-1980 to 31-12-2007	0
		Trencin - Biskupice	209	01-01-1961 to 31-03-2006	0
Cloudiness	1/10	Prievidza	260	01-07-1972 to 31-12-2007	0.63
		Turcianske Teplice	510	01-01-1990 to 31-12-2007	0.37
		Banska Stiavnica	575	01-01-1961 to 31-12-2004	0
		Kremnicke Bane	758	01-01-1987 to 31-12-2007	0
		Krizna	1570	01-11-1963 to 31-12-2007	0
		Topolcany	192	01-01-1961 to 31-12-2007	0
		Trencin - Biskupice	209	01-01-1961 to 31-03-2006	0
Rel. air humidity	%	Prievidza	260	01-07-1972 to 31-12-2007	0.63
		Turcianske Teplice	510	01-04-1991 to 31-12-2007	0.37
		Banska Stiavnica	575	01-01-1961 to 31-12-2004	0
		Kremnicke Bane	758	01-01-1987 to 31-12-2007	0
		Krizna	1570	01-04-1964 to 31-12-2007	0
		Trencin - Biskupice	209	01-01-1961 to 31-03-2006	0
Snow cover	cm	Prievidza	260	01-07-1972 to 31-12-2007	1.00
Discharge	m³/s	Nedožery	287	01-11-1940 to 31-12-2006	-
		Chvojnica	489	01-11-1974 to 31-12-2006	-
		Tužina	359	01-11-1969 to 31-12-2006	-
		Kľačno	472	01-11-1975 to 31-12-2006	-
Groundwater heads	m a.s.l.	Nedožery	287	05-11-1969 to 29-10-2006	-

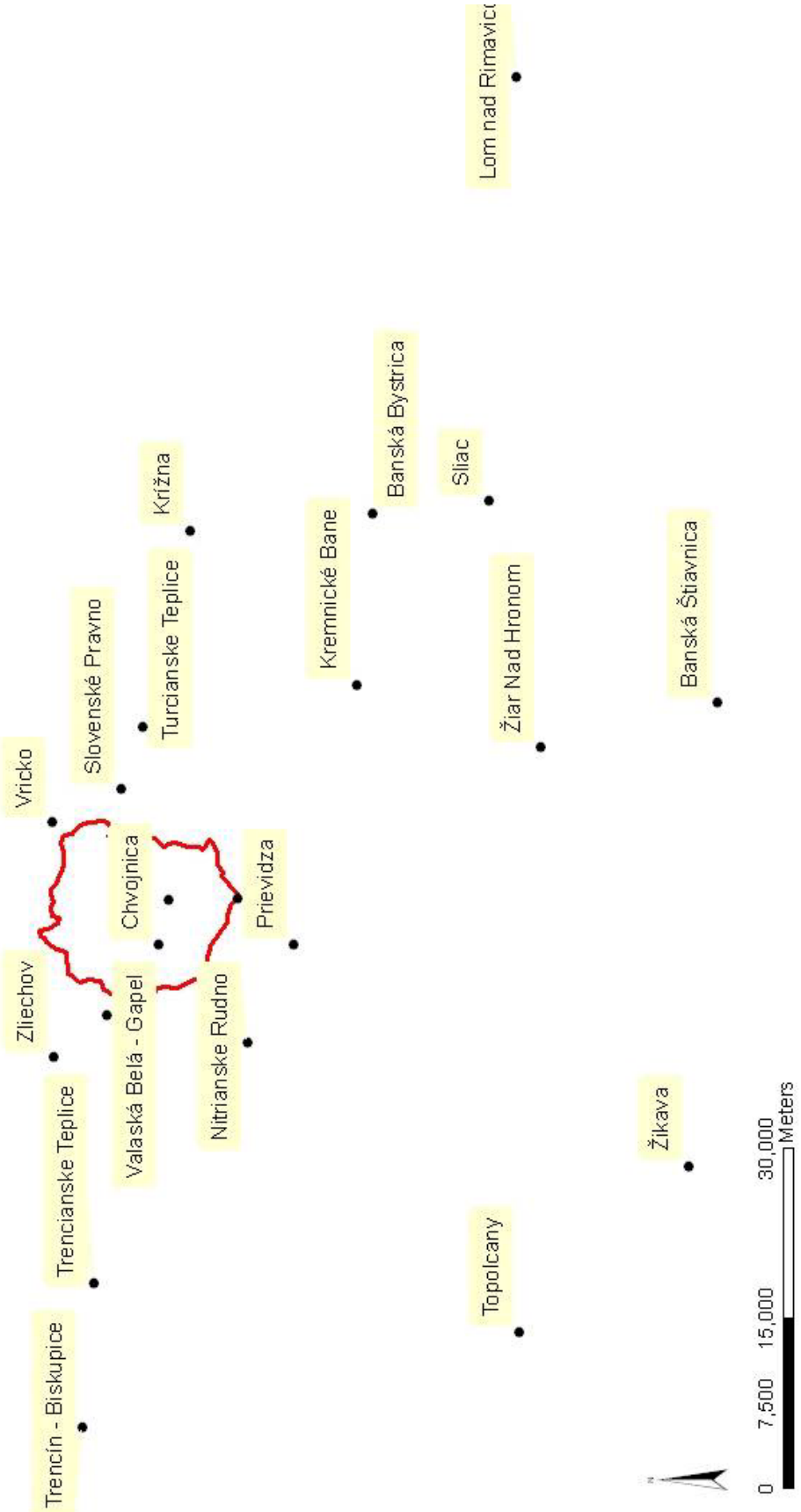

Annex 2a (Meteorological) stations in and around the Nedožery catchment.

Annex 3 Precipitation gradients

Station	Chvojnica	Nitriansk e Pravno	Nitriansk e Rudno	Prievidza	Slovenské Pravno	Valaská Belá - Gapel	Vricko	Zliechov	
Altitude [m a.s.l]	435	351	312	260	500	490	603	598	average
Gradient [mm/100m]									
January	0.0551	0.0430	0.0531	0.0483	0.0480	0.0678	0.0620	0.0610	0.0057
February	0.0534	0.0489	0.0567	0.0422	0.0514	0.0560	0.0594	0.0608	0.0071
March	0.0649	0.0571	0.0544	0.0458	0.0483	0.0658	0.0569	0.0662	0.0071
April	0.0613	0.0592	0.0508	0.0469	0.0534	0.0563	0.0648	0.0626	0.0083
May	0.0715	0.0455	0.0582	0.0506	0.0479	0.0588	0.0707	0.0592	0.0079
June	0.0551	0.0559	0.0556	0.0409	0.0547	0.0597	0.0618	0.0660	0.0063
July	0.0601	0.0493	0.0494	0.0547	0.0515	0.0620	0.0596	0.0600	0.0086
August	0.0546	0.0442	0.0602	0.0459	0.0590	0.0563	0.0593	0.0648	0.0062
September	0.0584	0.0530	0.0520	0.0512	0.0498	0.0605	0.0627	0.0602	0.0088
October	0.0615	0.0599	0.0548	0.0494	0.0476	0.0611	0.0690	0.0611	0.0065
November	0.0518	0.0418	0.0515	0.0470	0.0537	0.0583	0.0651	0.0593	0.0066
December	0.0706	0.0563	0.0484	0.0425	0.0493	0.0637	0.0710	0.0723	0.0059
average	0.0599	0.0512	0.0538	0.0471	0.0512	0.0605	0.0635	0.0628	0.0071
Gradient [%/100m]									
January	10.38	13.31	10.77	11.84	11.92	8.44	9.23	9.37	10.66
February	13.22	14.44	12.44	16.72	13.73	12.59	11.88	11.60	13.33
March	11.01	12.50	13.12	15.59	14.79	10.85	12.54	10.79	12.65
April	13.56	14.05	16.38	17.73	15.58	14.76	12.83	13.29	14.77
May	11.00	17.28	13.51	15.56	16.41	13.38	11.12	13.27	13.94
June	11.49	11.33	11.40	15.48	11.58	10.61	10.25	9.60	11.47
July	14.23	17.34	17.32	15.63	16.60	13.81	14.34	14.25	15.44
August	11.27	13.94	10.22	13.41	10.43	10.95	10.39	9.50	11.26
September	15.15	16.69	17.00	17.27	17.75	14.60	14.09	14.69	15.90
October	10.62	10.91	11.94	13.23	13.74	10.71	9.47	10.69	11.41
November	12.75	15.79	12.81	14.03	12.30	11.32	10.14	11.13	12.53
December	8.32	10.43	12.12	13.81	11.90	9.21	8.26	8.12	10.27
average	11.83	13.84	13.17	15.03	13.83	11.70	11.15	11.28	12.73

Annex 4 Zonation as input for HBV

Annex 4a Land use-elevation zones used as input for HBV

	Forests	Agriculture/ meadow	Artificial
< 300 m a.s.l.	0.0%	0.4%	0.4%
301 - 400 m a.s.l.	3.7%	13.6%	3.4%
401 - 500 m a.s.l.	8.2%	9.1%	0.9%
501 - 600 m a.s.l.	14.5%	1.9%	0.1%
601 - 700 m a.s.l.	17.2%	1.1%	0.0%
701 - 800 m a.s.l.	13.2%	1.4%	0.0%
801 - 900 m a.s.l.	6.8%	0.7%	0.0%
901 - 1000 m a.s.l.	2.0%	0.4%	0.0%
1001 - 1100 m a.s.l.	0.8%	0.1%	0.0%
> 1101 m a.s.l.	0.2%	0.0%	0.0%
Sum	66.6%	28.7%	4.8%

Annex 4b Geology-elevation zones used as input for HBV (Magmatic and Early paleozoic-proterozoic are added up to one class as HBV input)

	Magmatic rocks	Early paleozoic - proterozoic	Mesozoic of the IC	Neogene
< 300 m a.s.l.	0.0%	0.0%	0.0%	0.8%
301 - 400 m a.s.l.	1.2%	0.9%	4.8%	14.0%
401 - 500 m a.s.l.	4.7%	3.4%	9.5%	0.6%
501 - 600 m a.s.l.	4.3%	3.1%	9.0%	0.0%
601 - 700 m a.s.l.	3.8%	3.1%	11.4%	0.0%
701 - 800 m a.s.l.	2.1%	2.0%	10.5%	0.0%
801 - 900 m a.s.l.	1.2%	1.0%	5.3%	0.0%
901 - 1000 m a.s.l.	1.0%	0.3%	1.2%	0.0%
1001 - 1100 m a.s.l.	0.6%	0.0%	0.2%	0.0%
> 1101 m a.s.l.	0.1%	0.0%	0.0%	0.0%
Sum	18.9%	13.9%	51.8%	15.4%

Annex 4c Soil texture-elevation zones used as input for HBV (Loamy sand and sandy loam are added up to one class as HBV input)

	Loamy sand	Sandy loam	Loam	Clay loam
< 300 m a.s.l.	0.0%	0.7%	0.1%	0.0%
301 - 400 m a.s.l.	2.7%	1.3%	14.8%	2.0%
401 - 500 m a.s.l.	0.9%	2.7%	11.0%	3.6%
501 - 600 m a.s.l.	1.8%	4.6%	9.3%	0.7%
601 - 700 m a.s.l.	3.5%	4.8%	9.8%	0.2%
701 - 800 m a.s.l.	3.6%	2.7%	7.7%	0.7%
801 - 900 m a.s.l.	1.0%	1.7%	4.2%	0.5%
901 - 1000 m a.s.l.	0.3%	1.0%	1.2%	0.0%
1001 - 1100 m a.s.l.	0.2%	0.4%	0.2%	0.0%
> 1101 m a.s.l.	0.1%	0.0%	0.0%	0.0%
Sum	14.2%	19.9%	58.2%	7.6%

Annex 5 Monthly threshold values

Annex 5a Monthly 80% thresholds for the drought analysis

Month	t.Qobs	t.Qsim	t.Psim	t.SM	t.GW
1	0.446	0.311	1.147	137.9	14.1
2	0.460	0.413	0.883	148.5	16.6
3	0.823	0.558	1.002	141.7	22.1
4	0.915	0.721	1.364	115.1	28.0
5	0.572	0.527	1.557	89.3	25.8
6	0.389	0.442	1.897	83.0	20.9
7	0.287	0.386	1.717	73.4	17.9
8	0.221	0.326	1.457	73.3	15.7
9	0.212	0.292	1.298	77.2	14.4
10	0.239	0.277	1.069	89.7	13.2
11	0.298	0.271	1.517	100.8	12.8
12	0.368	0.310	1.606	118.0	14.0

Annex 5b Monthly 90% thresholds for the drought analysis

Month	t.Qobs	t.Qsim	t.Psim	t.SM	t.GW
1	0.319	0.244	0.754	124.1	11.7
2	0.373	0.304	0.538	143.6	13.7
3	0.612	0.471	0.661	130.1	19.9
4	0.701	0.574	1.082	104.8	25.1
5	0.492	0.460	1.231	78.4	22.7
6	0.298	0.384	1.506	73.6	18.6
7	0.235	0.313	1.394	65.1	15.1
8	0.175	0.267	0.990	58.9	13.3
9	0.184	0.190	0.877	63.8	9.4
10	0.203	0.229	0.571	80.6	11.0
11	0.236	0.232	1.141	86.6	11.4
12	0.288	0.239	1.271	106.7	11.2

Annex 6 Overview trends

Annex 6a Annual precipitation sums [mm] for the different stations

Station	Chvojnica	Nitrianske Pravno	Nitrianske Rudno	Prievidza	Slovenské Pravno	Valaská Belá - Gapel	Vricko	Zliechov
altitude [m a.s.l.]	435	351	312	260	500	490	603	598
1973	NA	NA	NA	441	NA	NA	NA	NA
1974	NA	NA	NA	875	NA	NA	NA	NA
1975	NA	NA	NA	644	NA	NA	NA	NA
1976	NA	NA	NA	703	NA	NA	NA	NA
1977	NA	NA	NA	694	NA	NA	NA	NA
1978	NA	NA	NA	470	NA	NA	NA	NA
1979	NA	NA	NA	690	NA	NA	NA	NA
1980	NA	NA	NA	664	NA	NA	NA	NA
1981	971	762	805	642	945	780	1170	725
1982	688	612	636	545	810	676	889	536
1983	680	560	568	509	686	623	858	544
1984	945	821	737	641	798	912	993	593
1985	879	771	753	649	883	902	1036	465
1986	1005	846	843	696	857	908	1006	864
1987	826	682	691	547	763	888	1018	994
1988	926	770	764	750	837	988	1005	949
1989	690	601	545	503	636	760	814	684
1990	924	787	729	596	840	872	887	918
1991	802	647	637	523	572	797	889	746
1992	868	683	770	629	628	906	963	855
1993	809	624	512	583	657	773	949	834
1994	1096	917	953	923	944	1036	1231	1147
1995	1041	735	850	699	765	1005	1148	1034
1996	1056	804	907	644	794	1017	1151	1079
1997	931	755	744	633	695	927	1220	1077
1998	961	746	762	677	849	914	1143	978
1999	882	779	799	643	857	878	1039	987
2000	959	767	791	625	902	911	1232	988
2001	916	741	742	615	998	946	1201	1004
2002	1061	916	915	804	897	1089	1261	1011
2003	647	500	525	491	600	683	819	669
2004	871	727	833	706	769	886	1087	840
2005	1099	895	988	800	974	1181	1235	1110
2006	821	636	803	566	761	793	1056	916
Mean	898	734	754	640	797	886	1050	867
Slope	3.97	1.77	5.67	3.25	1.43	6.64	8.20	14.91
Slope%	0.44%	0.24%	0.75%	0.19%	0.18%	0.75%	0.78%	1.72%
P-value	0.355	0.724	0.064	0.836	0.659	0.086	0.017	0.006

Annex 6b Values and trends for annual mean air temperature, maximum and minimum temperature for the period 1973-2006

	Station	Altitude [m a.s.l.]	Mean [°C]	Slope [°C/y]
Air temperature	Topolcany	192	10.01	0.015
	Trencin - Biskupice	209	9.14	0.033
	Prievidza	260	9.14	0.027
	Trencianske Teplice	306	9.25	0.016
	Banska Bystrica	427	8.47	0.079
	Turcianske Teplice	510	7.66	0.037
	Banska Stiavnica	575	7.89	0.025
	Kremnicke Bane	758	6.38	0.031
	Lom nad Rimavicou	1018	5.45	0.048
	Krizna	1570	1.91	0.041
Maximum air temperature	Topolcany	192	15.12	0.036
	Trencin - Biskupice	209	14.14	0.027
	Trencianske Teplice	306	14.44	-0.043
	Banska Bystrica	427	13.44	0.084
	Banska Stiavnica	575	12.74	0.027
	Lom nad Rimavicou	1018	9.34	0.065
	Krizna	1570	4.89	0.028
Minimum air temperature	Topolcany	192	5.24	0.006
	Trencin - Biskupice	209	4.35	0.041
	Trencianske Teplice	306	4.80	-0.013
	Banska Bystrica	427	3.95	0.092
	Banska Stiavnica	575	3.67	0.020
	Lom nad Rimavicou	1018	1.92	0.071
	Krizna	1570	-1.39	0.055

Annex 7 Observed and simulated discharge (with and without calibration on groundwater)

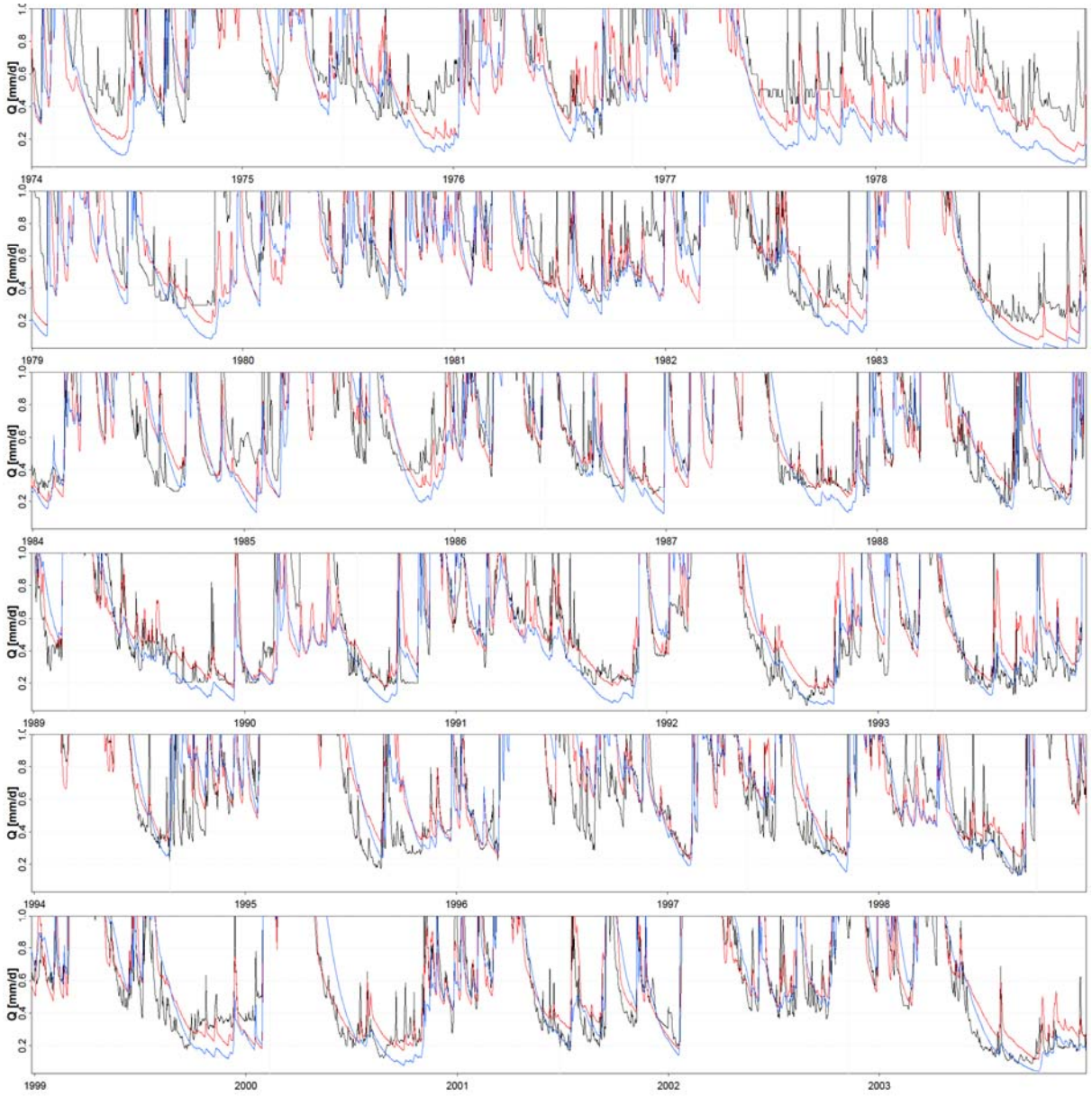

Legend

- Observed discharge
- Simulated discharge; based on calibration on R_{eff} (ln Q)
- Simulated discharge; based on calibration on Reff and r^2 (GW)

Annex 8 Observed and simulated groundwater heads

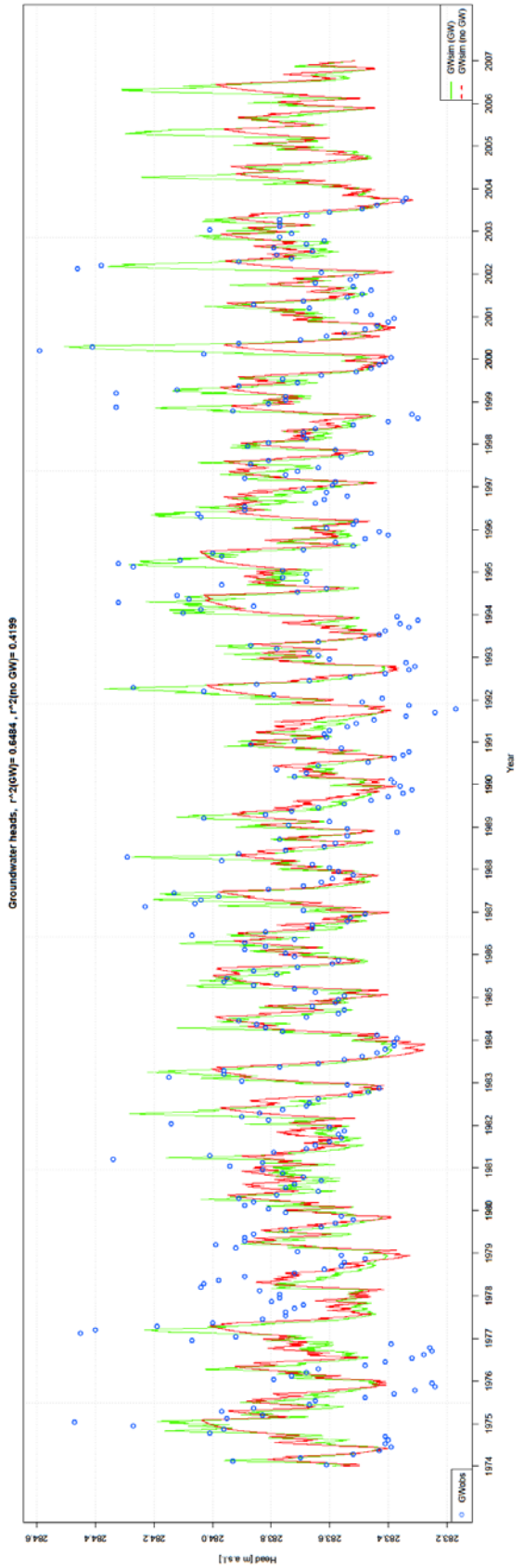

Legend

o Observed groundwater heads [m a.s.l.]

— Simulated groundwater heads; based on calibration on R_{eff} (ln Q)

— Simulated groundwater heads; based on calibration on Reff and r^2 (GW)

Annex 9 Statistics of the parameter values

Parameter	Mean	Standard Deviation	Minimum	Maximum
TT 1	-0.17	1.00	-1.35	1.10
TT 2	0.04	0.74	-0.88	0.93
TT 3	0.36	1.76	-1.50	2.30
CFMAX 1	3.89	1.72	1.71	7.52
CFMAX 2	3.72	0.94	2.76	5.59
CFMAX 3	6.18	3.08	2.40	10.00
SFCF 1	1.20	0.00	1.20	1.20
SFCF 2	1.20	0.00	1.20	1.20
SFCF 3	1.20	0.00	1.19	1.20
CFR 1	0.0004	0.0008	0.0000	0.0023
CFR 2	0.0034	0.0091	0.0000	0.0259
CFR 3	0.0232	0.0215	0.0002	0.0652
CWH 1	0.0009	0.0022	0.0000	0.0064
CWH 2	0.0001	0.0002	0.0000	0.0005
CWH 3	0.0421	0.0798	0.0000	0.1999
FC 1	181.2	22.2	143.4	204.0
FC 2	210.2	15.3	187.8	224.5
FC 3	231.0	38.3	193.5	302.2
LP 1	0.87	0.13	0.60	1.00
LP 2	0.72	0.09	0.59	0.87
LP 3	0.59	0.20	0.30	0.79
BETA 1	3.20	1.68	1.66	6.00
BETA 2	2.71	0.86	1.11	3.82
BETA 3	5.04	1.88	1.00	6.00
PERC	1.05	0.14	0.82	1.32
UZL	17.4	2.2	14.9	21.2
K0	0.22	0.05	0.17	0.31
K1	0.11	0.02	0.09	0.14
K2	0.02	0.00	0.02	0.03
MAXBAS	2.19	0.07	2.07	2.32

Annex 10 Detailed HBV results

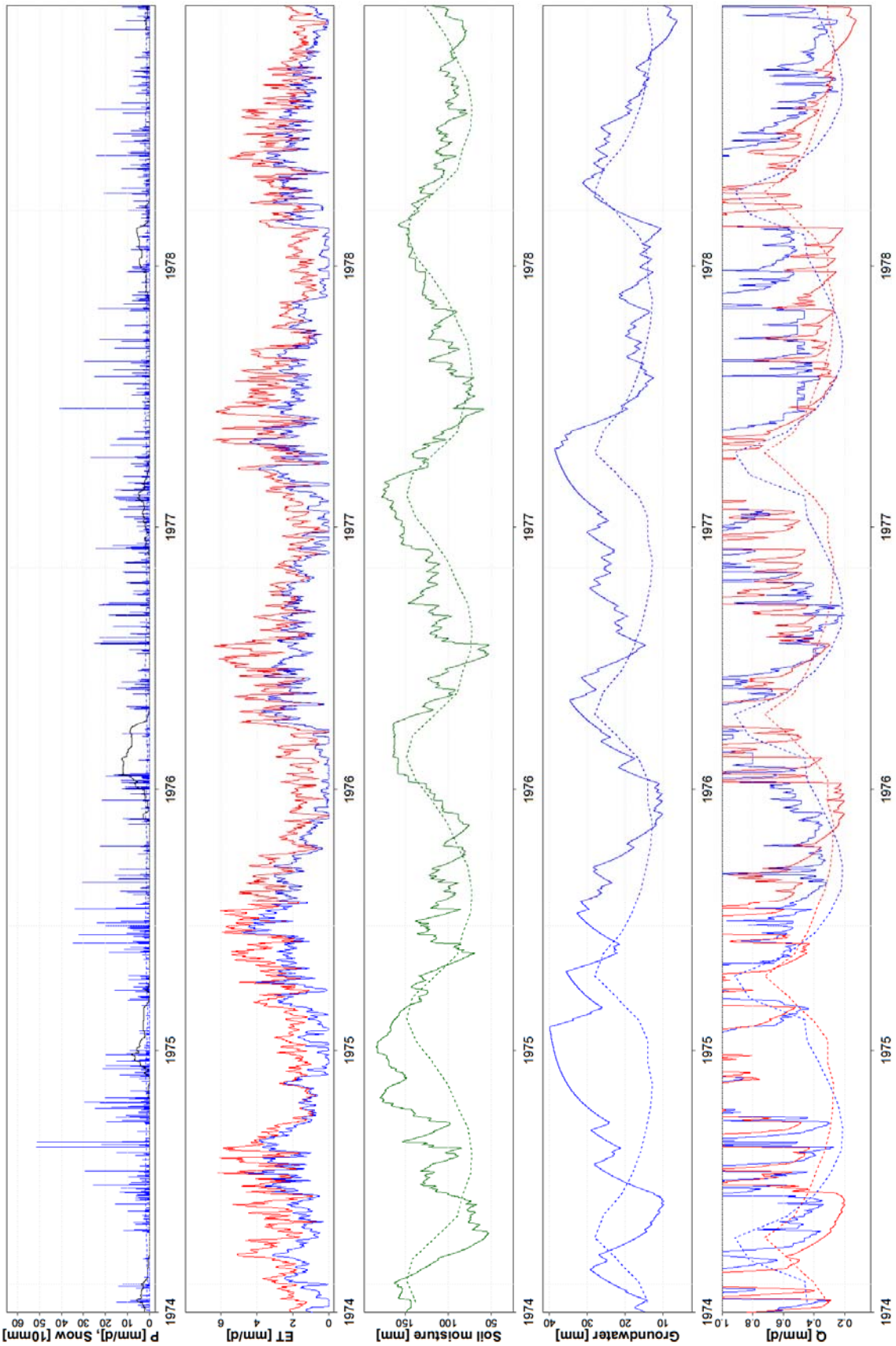

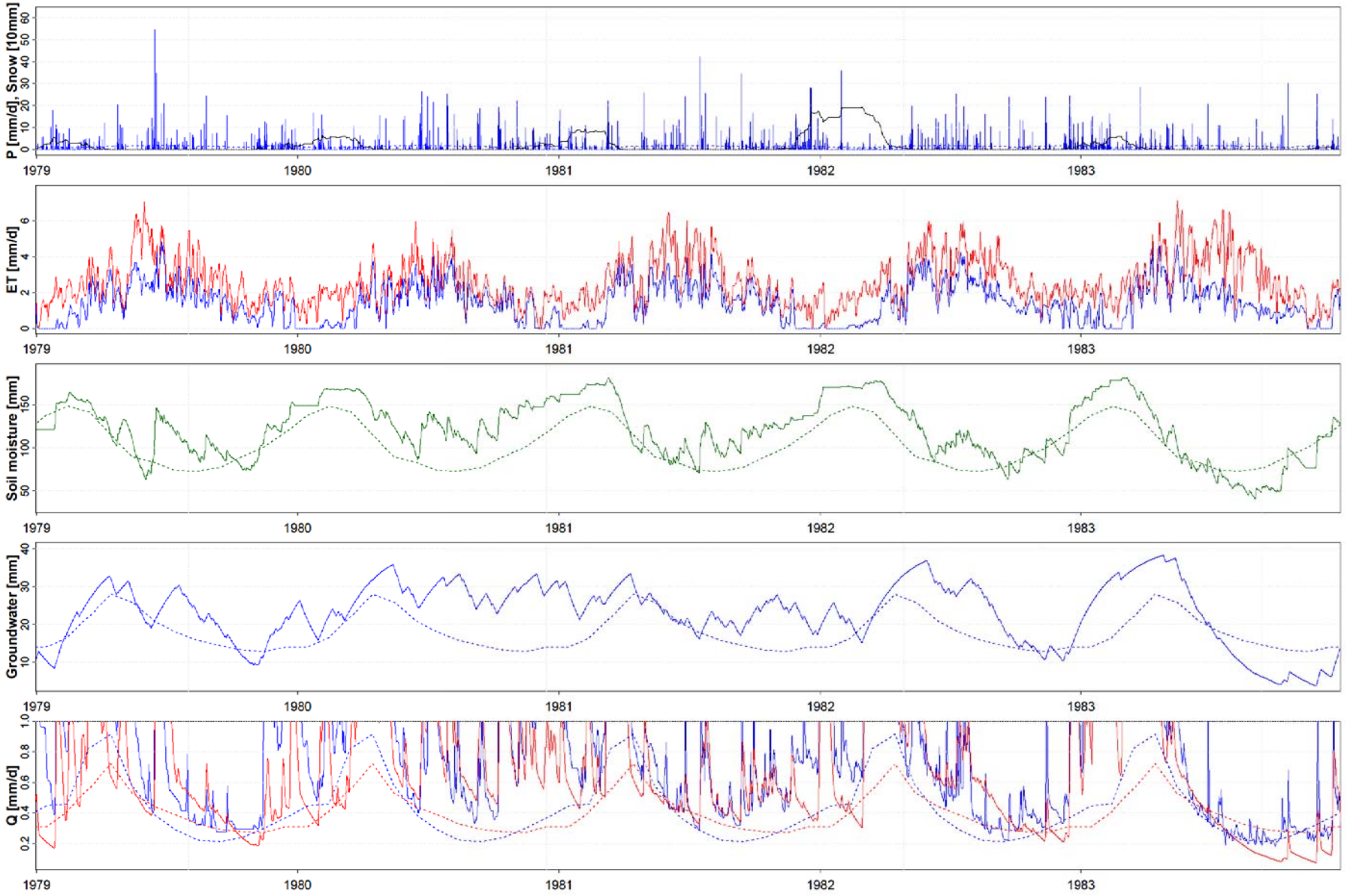
P [mm/d], Snow [10mm]
0
10
20
30
40
50
60
1979
1980
1981
1982
1983
ET [mm/d]
0
2
4
6
1979
1980
1981
1982
1983
Soil moisture [mm]
50
100
150
1979
1980
1981
1982
1983
Groundwater [mm]
10
20
30
40
1979
1980
1981
1982
1983
Q [mm/d]
0.2
0.4
0.6
0.8
1.0
1979
1980
1981
1982
1983

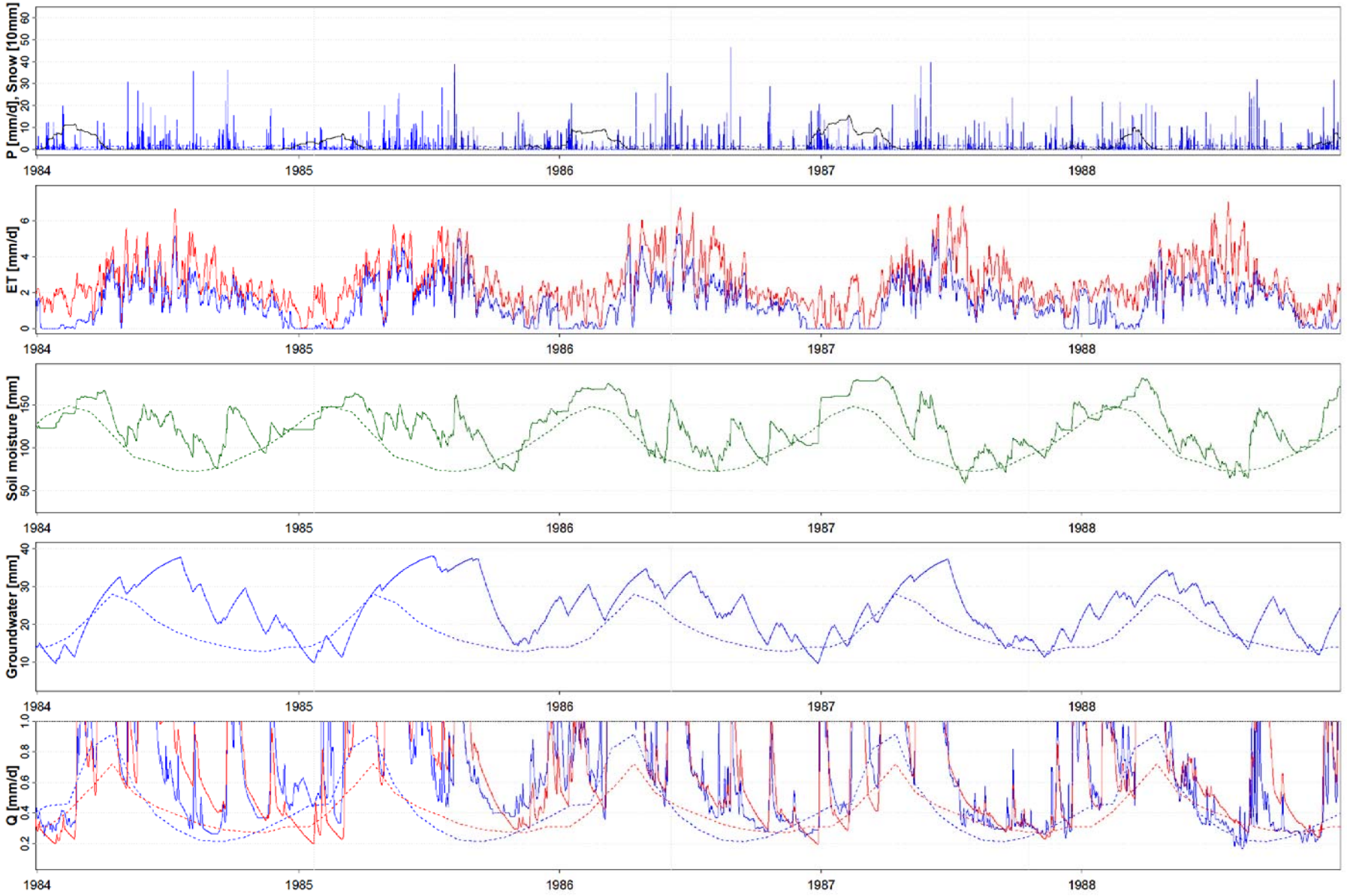
P [mm/d], Snow [10mm]
0
10
20
30
40
50
60
1984
1985
1986
1987
1988
ET [mm/d]
0
2
4
6
1984
1985
1986
1987
1988
Soil moisture [mm]
50
100
150
1984
1985
1986
1987
1988
Groundwater [mm]
10
20
30
40
1984
1985
1986
1987
1988
Q [mm/d]
0.2
0.4
0.6
0.8
1.0
1984
1985
1986
1987
1988

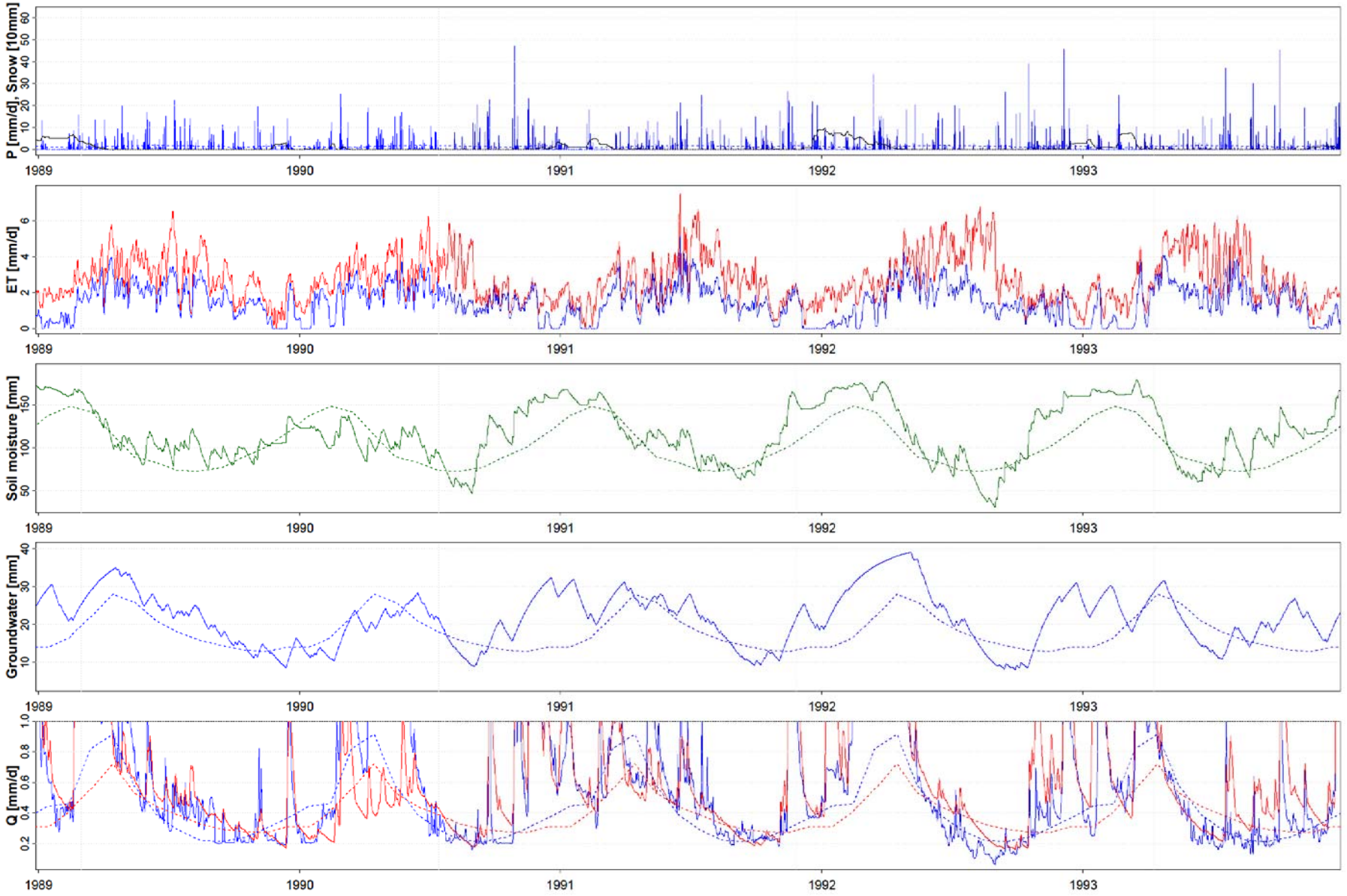
P [mm/d], Snow [10mm]
0
10
20
30
40
50
60
1989
1990
1991
1992
1993
ET [mm/d]
0
2
4
6
1989
1990
1991
1992
1993
Soil moisture [mm]
50
100
150
1989
1990
1991
1992
1993
Groundwater [mm]
10
20
30
40
1989
1990
1991
1992
1993
Q [mm/d]
0.2
0.4
0.6
0.8
1.0
1989
1990
1991
1992
1993

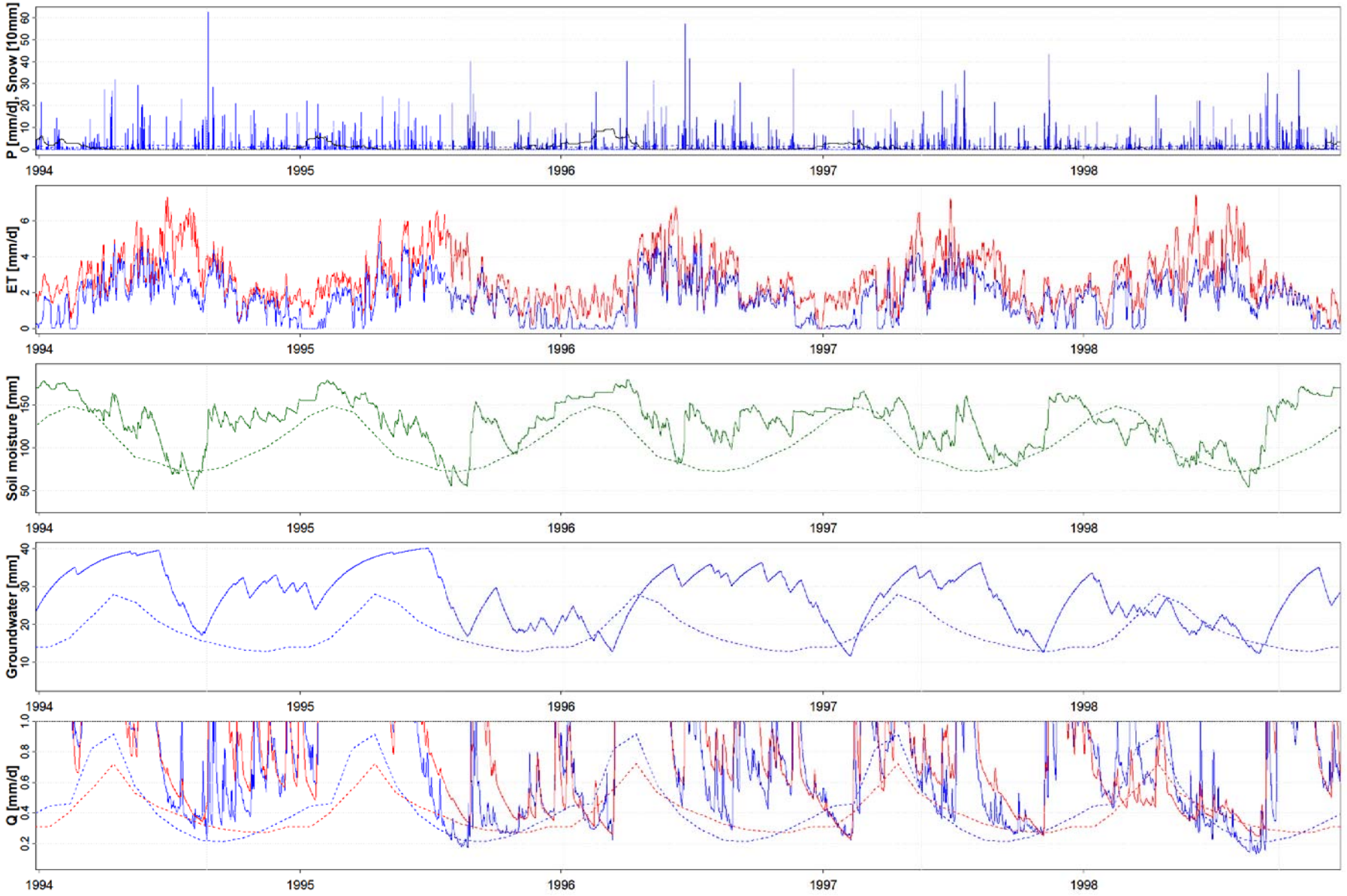
P [mm/d], Snow [10mm]
0
10
20
30
40
50
60
1994
1995
1996
1997
1998
ET [mm/d]
0
2
4
6
1994
1995
1996
1997
1998
Soil moisture [mm]
50
100
150
1994
1995
1996
1997
1998
Groundwater [mm]
10
20
30
40
1994
1995
1996
1997
1998
Q [mm/d]
0.2
0.4
0.6
0.8
1.0
1994
1995
1996
1997
1998

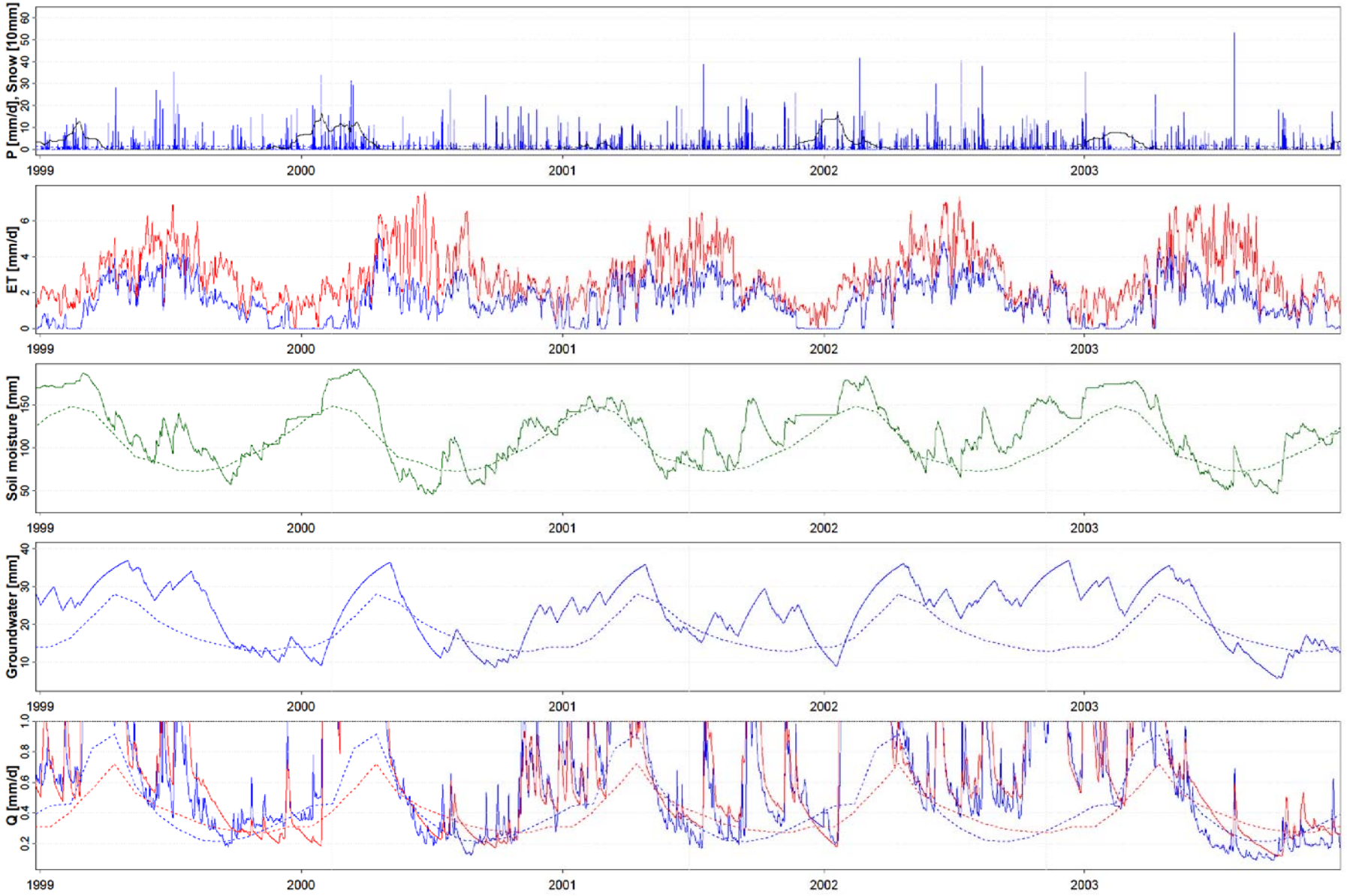
P [mm/d], Snow [10mm]
0
10
20
30
40
50
60
1999
2000
2001
2002
2003
ET [mm/d]
0
2
4
6
1999
2000
2001
2002
2003
Soil moisture [mm]
50
100
150
1999
2000
2001
2002
2003
Groundwater [mm]
10
20
30
40
1999
2000
2001
2002
2003
Q [mm/d]
0.2
0.4
0.6
0.8
1.0
1999
2000
2001
2002
2003

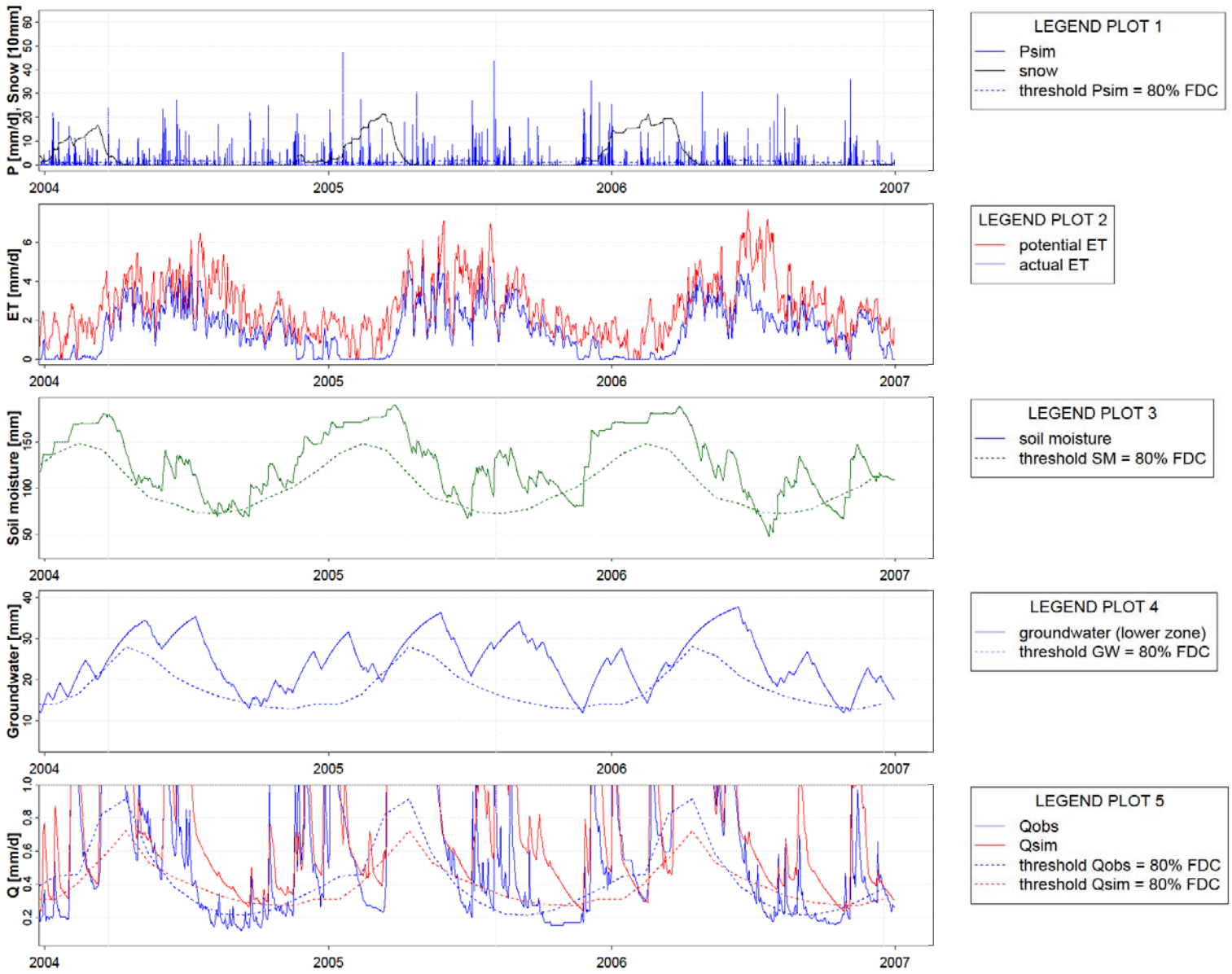
P [mm/d], Snow [10mm]
0
10
20
30
40
50
60
2004
2005
2006
2007
LEGEND PLOT 1
Psim
snow
threshold Psim = 80% FDC
ET [mm/d]
0
2
4
6
2004
2005
2006
2007
LEGEND PLOT 2
potential ET
actual ET
Soil moisture [mm]
50
100
150
2004
2005
2006
2007
LEGEND PLOT 3
soil moisture
threshold SM = 80% FDC
Groundwater [mm]
10
20
30
40
2004
2005
2006
2007
LEGEND PLOT 4
groundwater (lower zone)
threshold GW = 80% FDC
Q [mm/d]
0.2
0.4
0.6
0.8
1.0
2004
2005
2006
2007
LEGEND PLOT 5
Qobs
Qsim
threshold Qobs = 80% FDC
threshold Qsim = 80% FDC

Annex 11 Trends in the monthly sums of the outflow from the two groundwater boxes

Annex 11a Tendencies in the monthly sums of Q_k0 (discharge from the upper groundwater box above the threshold)

	Mean [mm]	Slope [mm/y]	Slope [%/y]	P-value
January	1.61	0.07	4.46%	0.5921
February	4.68	0.24	5.10%	0.1027
March	15.12	0.95	6.30%	0.0299
April	10.94	0.69	6.33%	0.0837
May	0.70	0.00	0.14%	0.6104
June	0.35	-0.01	-3.29%	0.4388
July	0.48	0.04	7.67%	0.1893
August	0.43	-0.04	-8.53%	0.7624
September	0.49	0.04	7.62%	0.5711
October	1.36	-0.12	-8.92%	0.7624
November	0.92	0.04	4.51%	0.9006
December	0.66	-0.01	-1.29%	0.7811

Annex 11b Tendencies in the monthly sums of Q_k1 (discharge from the upper groundwater box)

	Mean [mm]	Slope [mm/y]	Slope [%/y]	P-value
January	10.34	0.02	0.22%	0.9136
February	14.12	0.23	1.66%	0.8162
March	31.54	0.72	2.29%	0.0365
April	26.39	0.84	3.19%	0.0424
May	7.05	0.13	1.91%	0.9506
June	7.09	-0.08	-1.17%	0.4477
July	5.50	0.09	1.55%	0.8768
August	3.88	0.03	0.89%	0.5452
September	6.18	0.10	1.68%	0.7803
October	6.14	-0.08	-1.28%	0.9259
November	7.14	0.27	3.85%	0.1496
December	7.80	0.00	0.01%	0.9506

Annex 11c Tendencies in the monthly sums of Q_k2 (discharge from the lower groundwater box)

	Mean [mm]	Slope [mm/y]	Slope [%/y]	P-value
January	13.67	0.05	0.39%	0.3139
February	12.87	-0.01	-0.08%	0.8404
March	16.27	-0.01	-0.05%	0.9629
April	18.63	0.05	0.25%	0.5876
May	18.67	0.11	0.59%	0.1777
June	16.18	0.07	0.43%	0.3606
July	15.27	-0.02	-0.14%	0.8647
August	13.53	-0.01	-0.07%	0.7216
September	12.08	-0.02	-0.15%	0.7216
October	12.11	0.00	-0.03%	0.6091
November	11.80	0.05	0.39%	0.5052
December	12.97	0.06	0.46%	0.4477

Annex 12 Trends in the monthly and yearly sums of actual evapotranspiration

	Mean [mm]	Slope [mm/y]	Slope [%/y]	P-value
January	10.1	0.0	-0.17%	0.8162
February	13.8	-0.1	-0.55%	0.4384
March	38.6	-0.4	-1.00%	0.2713
April	69.4	0.9	1.26%	**0.0010**
May	75.8	0.5	0.66%	0.0567
June	76.4	0.3	0.38%	0.1328
July	75.1	0.4	0.48%	0.0699
August	64.3	0.2	0.24%	0.6757
September	47.9	-0.1	-0.19%	0.4294
October	39.8	0.1	0.25%	0.6091
November	30.0	0.3	1.01%	0.2850
December	15.6	0.1	0.61%	0.7332
Year	556.7	2.1	0.38%	**0.0178**

Annex 13 Observed (Prievidza) and simulated (HBV elev. zone 1) snow

snow water equivalent [mm] and snow depth [cm]

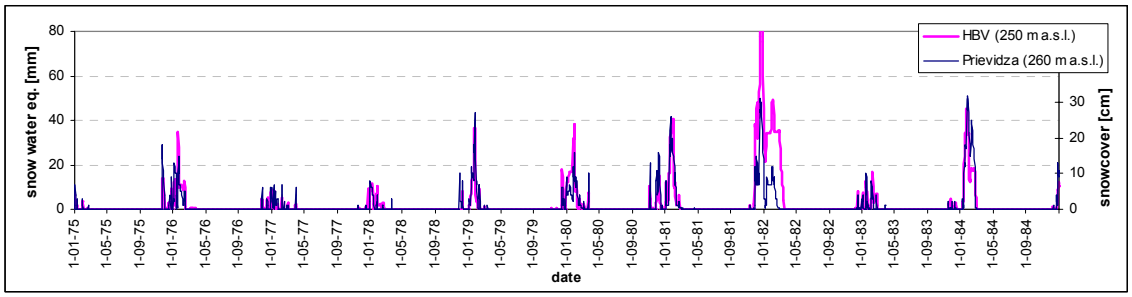

Annex 13a Simulated snow water equivalent (HBV elevation zone 1) and observed snow cover (Prievidza) from 01-01-1975 till 31-12-1984.

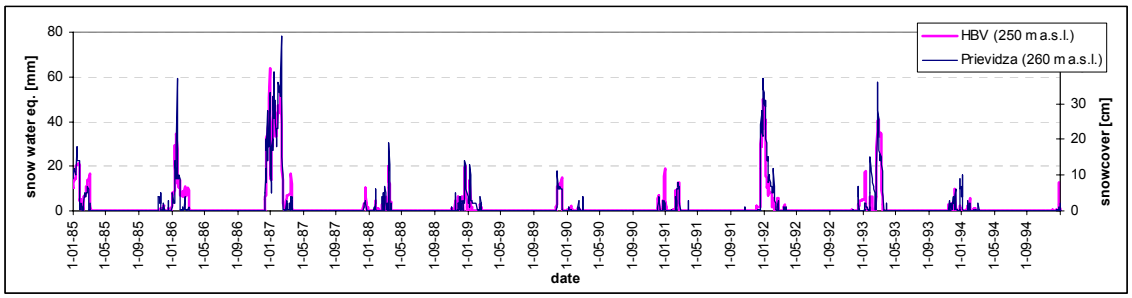

Annex 13b Simulated snow water equivalent (HBV elevation zone 1) and observed snow cover (Prievidza) from 01-01-1985 till 31-12-1994.

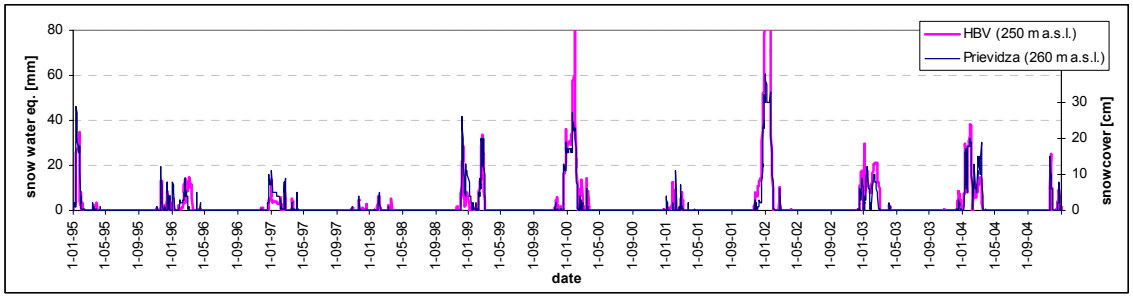

Annex 13c Simulated snow water equivalent (HBV elevation zone 1) and observed snow cover (Prievidza) from 01-01-1995 till 31-12-2004.

Annex 14 Results for hydrological models HBV, FRIER and BILAN

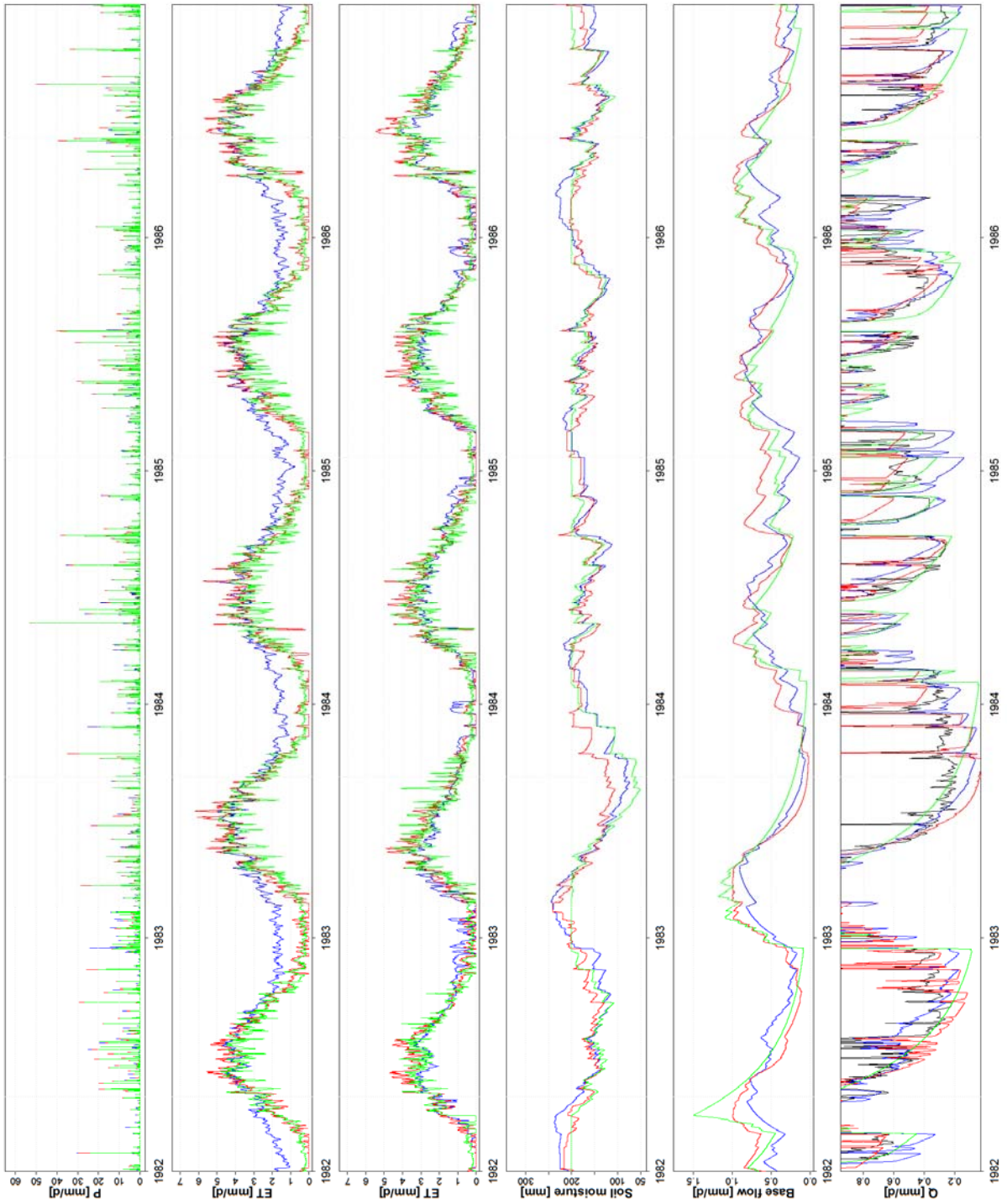

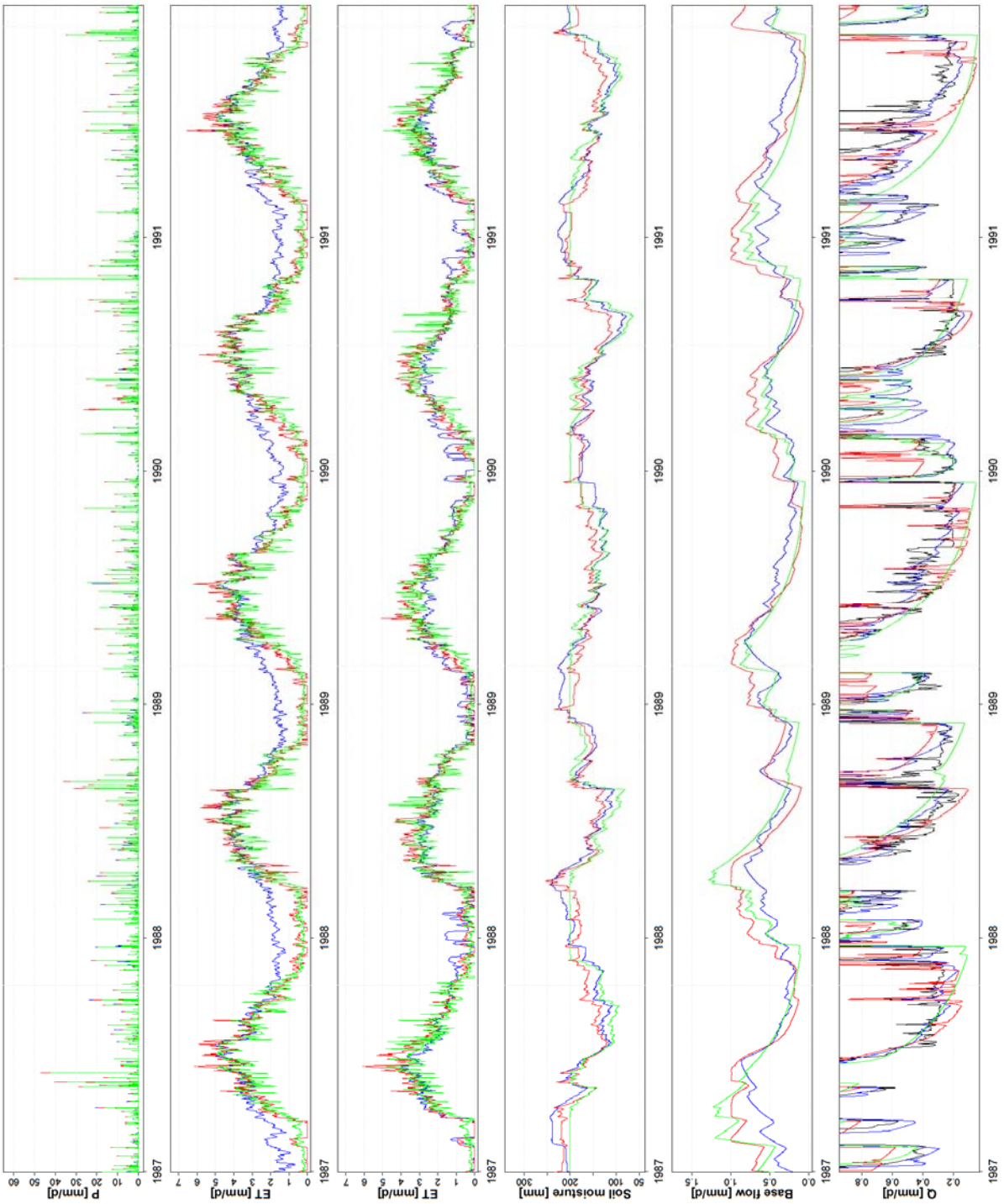
P [mm/d]
ET [mm/d]
ET [mm/d]
Soil moisture [mm]
Base flow [mm/d]
Q [mm/d]
1987
1988
1989
1990
1991

P [mm/d]
ET [mm/d]
ET [mm/d]
Soil moisture [mm]
Base flow [mm/d]
Q [mm/d]
1992
1993
1994
1995
1996

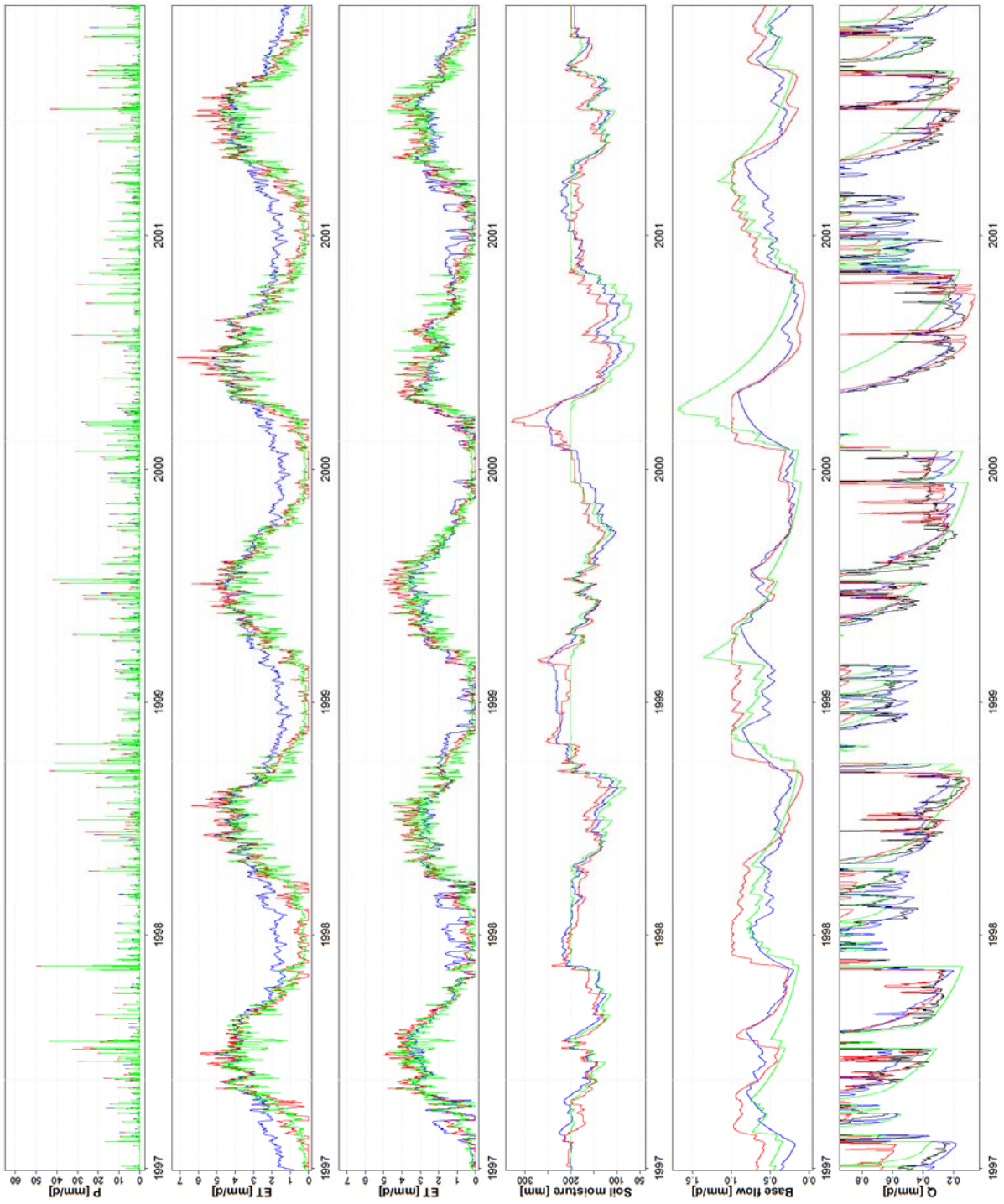
P [mm/d]
ET [mm/d]
ET [mm/d]
Soil moisture [mm]
Base flow [mm/d]
Q [mm/d]
1997
1998
1999
2000
2001

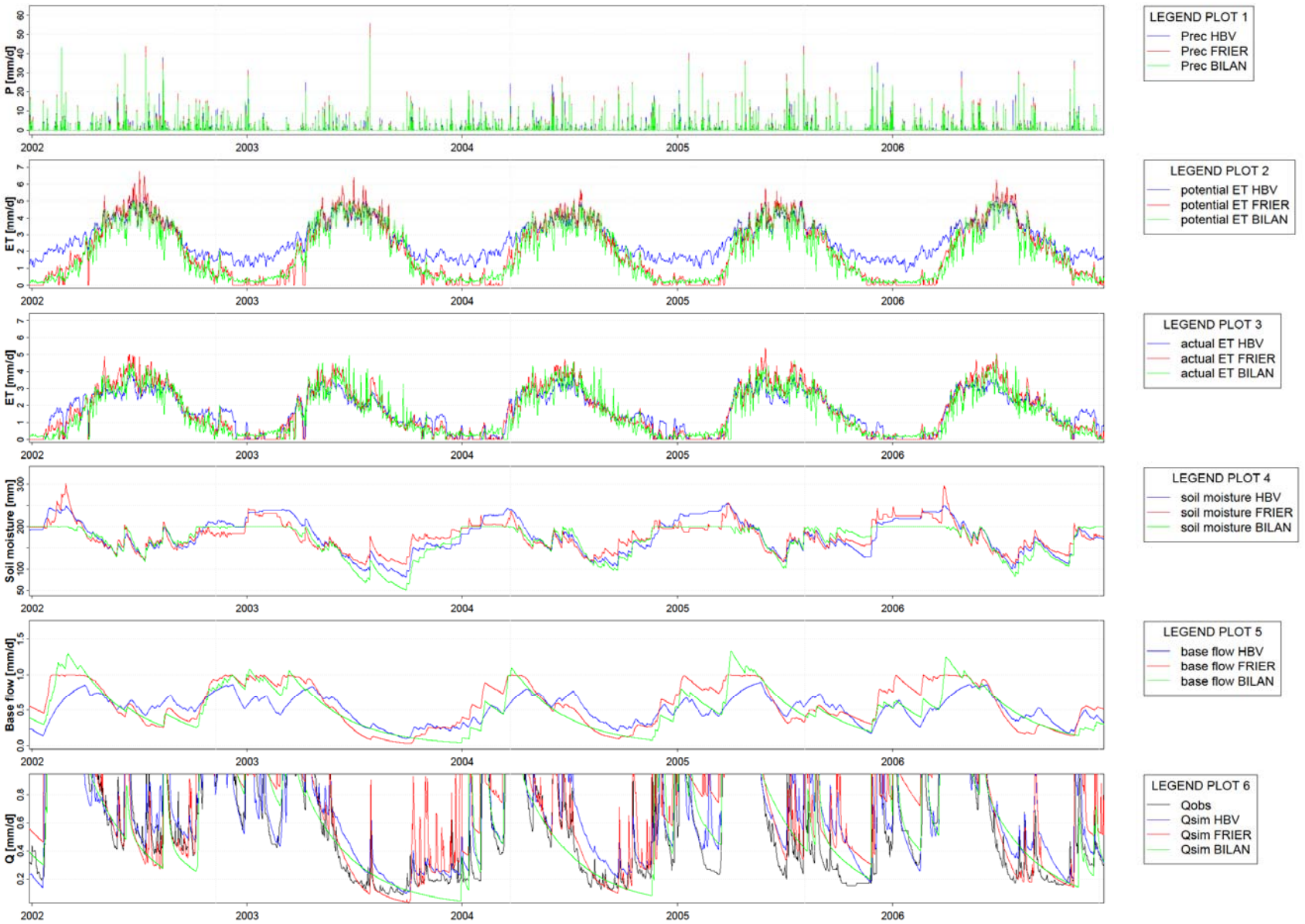
P [mm/d]
ET [mm/d]
ET [mm/d]
Soil moisture [mm]
Base flow [mm/d]
Q [mm/d]
2002
2003
2004
2005
2006
LEGEND PLOT 1
Prec HBV
Prec FRIER
Prec BILAN
LEGEND PLOT 2
potential ET HBV
potential ET FRIER
potential ET BILAN
LEGEND PLOT 3
actual ET HBV
actual ET FRIER
actual ET BILAN
LEGEND PLOT 4
soil moisture HBV
soil moisture FRIER
soil moisture BILAN
LEGEND PLOT 5
base flow HBV
base flow FRIER
base flow BILAN
LEGEND PLOT 6
Qobs
Qsim HBV
Qsim FRIER
Qsim BILAN

Annex 15 Trends in the annual sums for the three models (1982-2006)

	Sum [mm]	Slope [mm/y]	Slope [%/y]	P-value
Qobs	333	-1.75	-0.52%	0.388
Qsim HBV	335	5.30	1.58%	0.053
Qsim FRIER	352	4.18	1.19%	0.047
Qsim BILAN	314	3.16	1.00%	0.293
Prec HBV	893	6.86	0.77%	0.027
Prec FRIER	876	5.44	0.62%	0.072
Prec BILAN	849	4.86	0.57%	0.199
pot ET HBV	985	1.31	0.13%	**0.024**
pot ET FRIER	739	1.55	0.21%	0.080
pot ET BILAN	687	1.11	0.16%	0.691
act ET HBV	592	1.54	0.26%	0.441
act ET FRIER	608	1.25	0.21%	0.591
act ET BILAN	545	0.94	0.17%	0.498